

**BIOLOGICAL MECHANISMS OF URANIUM TRANSFORMATION CATALYZED BY  
*GEOBACTER* BACTERIA**

By

Dena L. Cologgi

A DISSERTATION

Submitted to  
Michigan State University  
in partial fulfillment of the requirements  
for the degree of

DOCTOR OF PHILOSOPHY

Microbiology and Molecular Genetics

2012

## ABSTRACT

### BIOLOGICAL MECHANISMS OF URANIUM TRANSFORMATION CATALYZED BY *GEOBACTER* BACTERIA

By

Dena L. Cologgi

An insufficient knowledge of the biological mechanisms of contaminant transformation often limits the performance of in situ subsurface bioremediation and long-term stewardship strategies. The in situ stimulation of Fe(III) oxide reduction by *Geobacter* bacteria leads to the concomitant precipitation of U(VI) from groundwater. However, the biological mechanism behind this reaction has remained elusive. Because Fe(III) oxide reduction requires the expression of conductive pili in *Geobacter*, we also evaluated their contribution to uranium reduction. In chapter 2 of my dissertation I demonstrate a previously unrecognized role for *Geobacter* pili in the extracellular reduction of uranium and its essential function as a catalytic and protective cellular mechanism.

The expression of pili by *Geobacter* also promotes cell aggregation and biofilm formation. Recent work has shown that *Geobacter* cells transition from planktonic to biofilm physiologies during the active phase of U reduction in the subsurface. Despite these findings, the contribution of *Geobacter* biofilms to uranium removal and reduction has not been investigated. In chapter 3 of my dissertation I demonstrate that multilayer biofilms are able to reduce and tolerate substantially more U than planktonic cells for prolonged periods of time, making them an attractive option for the development of permeable biobarriers for U bioremediation. I also demonstrate the role of pili as a primary U reductase in the biofilm.

To gain further insight into how biofilms transform U, in chapter 4 of my dissertation I screened a library of transposon-insertion mutants and identified mutants with biofilm defects. This study confirmed the role of *Geobacter* pili in biofilm formation, and identified other genes encoding cell envelope and electron transport components that had not previously been implicated in biofilm development. These molecular markers can be used to predict and monitor the physiological state of *Geobacter* bacteria during the *in situ* bioremediation of U.

Previous work, including the prior chapters of my dissertation, has highlighted the importance of the cell envelope and its components for the survival of *Geobacter* in the subsurface. However, little is known regarding the regulation of the cell envelope. Thus, I investigated the role of the *Geobacter's* ECF sigma factor, RpoE. In the last chapter of my dissertation, I show that RpoE is required for response to cell envelope stress, as well as the regulation of *Geobacter's* extracellular electron transfer pathways. This highlights the functional specialization that RpoE has undergone to control the adaptive responses that enable *Geobacter* bacteria to survive in the environment, and links my findings to the physiology of *Geobacter* in the subsurface.

## **DEDICATION**

This dissertation is dedicated to my family. Thank you for staying rational when I wasn't, and believing in me when I didn't. I am so fortunate to have you in so many ways. I am incredibly thankful that being in Michigan has given me the opportunity to know my family in New York and become a part of their lives, especially during this past year. Thank you for all of your love, guidance and support.

## ACKNOWLEDGEMENTS

I would first like to acknowledge my mentor, Dr. Gemma Reguera, who has been there for me throughout this process and taught me more than I can describe. Thank you for taking a tremendous risk and entrusting your first lab to two very enthusiastic (but even more inexperienced and naive!) first-year rotation students. I am proud to have been a part of that beginning. I also need to extend a huge thank you to Allison Speers who has been with me since day one when we started the transposon mutagenesis together during our rotation. I don't think I would have survived grad school without you, Allison – literally! I will always owe you for accompanying me to Argonne and ensuring I didn't do something horrible (hitting the big red button, locking myself in the hutch, blowing up the synchrotron...) during those late-night sample changes performed in a nearly non-functional, sleep-deprived state.

I would also like to thank the other individuals who contributed directly to the work presented in my dissertation. Blair Bullard worked side-by-side with me on many of the biofilm experiments, and was instrumental in obtaining anything and everything needed for my research! Two amazing undergrad students, Annie Otwell and John Rotondo worked with me on the transposon mutagenesis project. Annie and John, you made my first experiences mentoring both easy and fun; I was very lucky to have you. No one else in the world would have so calmly tolerated my ups and downs, or endured so well the endless colony picking, plate transfers, and rarely-successful sequencing attempts. I would also like to acknowledge Sanela Lampa-Pastirk, who developed the pili isolation protocol used in chapter 2. Sanela welcomed

me into her family and provided significant support for me, both emotionally as well as scientifically, throughout this process.

I would like to thank our collaborator, Shelly Kelly (EXAFS analysis) not only for her scientific contributions, but also for taking the time to train (and in general put up with) Allison and me so we could play a more active role in our trips to Argonne. And special thanks for being such a wonderful hostess and humoring us in our non-scientific adventures including the search for albino deer, the tricycle rides, and the hunt for the coffee cart! I'd also like to acknowledge the rest of the Sector 20 staff at Argonne National Lab for all of their help and patience

Acknowledgement must also go to the other members of the Reguera Lab who may not have been directly involved in my research, but have had a huge impact nonetheless. First, to my long-term lab-mates Jenna Young, Becky Steidl, and Mike Manzella, along with Allison and Sanela -- what can I say? I can't imagine a lab without you. You have truly been like family. Thank you so much for your humor, support and loyalty. I would never have survived without you. I would also like to thank Bryan Schindler, Jihwan Hwang, Ana Lara, and Catherine Silva. Though they were in our lab only a short time, I am very thankful for both their scientific input and conversations about life. I have to especially thank Ana for keeping me company during those depressing late night battles with the KPA! I would also like to acknowledge our dishwashers and media-makers (Marvin, Max, Derek, Mike2, Mellissa, Karl, Katie, Alex and Eric). Without them our lab couldn't function. The last in this category is Kwi Kim, who has relentlessly kept me on track and made sure that I didn't forget what's important in life.

Other people who have been integral to the success of my grad school career include my committee members, Dr. Rob Britton, Dr. Terry Marsh, and Dr. Lee Kroos, who have been

very patient and supportive throughout this process. I would also like to acknowledge several individuals who assisted with some of the technical aspects of my research including Matthew Marshall (PNNL), Evgenya Shelobolina (University of Wisconsin-Madison) and Kazem Kashefi, who provided some of the protocols crucial to my work, as well as Weimin Chen (and Sanela and Igor) who helped me master the KPA. I would also like to extend a huge thank you to the amazing people at the Center for Advanced Microscopy (Alicia Pastor, XouDong Fan, Melinda Frame, Carole and Stanley Flegler) who have gone out of their way to be helpful, and were always understanding when I was running very late! As Alicia (who I also need to thank for being such a great friend and neighbor!) once so eloquently put it, “this is the Center for Advanced Microscopy, where all your dreams come true!”

I have been fortunate enough to have been funded throughout my Ph.D. by agencies such as the National Institute of Environmental Health Science’s Superfund program (R01 ES017052-03), the Office of Science (BER), U.S. Department of Energy (DOE) (DE-SC0000795), the College of Natural Science at Michigan State University (Hensley fellowship), and the Biogeochemistry Environmental Research Initiative at Michigan State University (research fellowship). PNC/XSD facilities and research at the APS are supported by the US DOE-BES, a Major Resources Support grant from NSERC, the University of Washington, Simon Fraser University and the APS. The APS is an Office of Science User Facility operated for the U.S. DOE’s Office of Science by Argonne National Laboratory and supported by the U.S. DOE under contract No. DE-AC02-06CH11357.

I, of course, also have to acknowledge the other MMG grad students who have been with me over the years. I am incredibly grateful for your camaraderie, companionship, support and scientific advice, and I wish you all the best.

Lastly, I would like to thank my family, to whom this dissertation is dedicated.

## TABLE OF CONTENTS

LIST OF TABLES .....	xii
LIST OF FIGURES .....	xiii
KEY TO SYMBOLS AND ABBREVIATIONS.....	xvi
<b>CHAPTER 1</b>	
<b>INTRODUCTION .....</b>	<b>1</b>
<b>URANIUM CONTAMINATION AND ITS IMPACT ON PUBLIC HEALTH .....</b>	<b>2</b>
<b>REMEDICATION STRATEGIES.....</b>	<b>3</b>
<b>MICROBIAL U(VI) REDUCTION.....</b>	<b>4</b>
<b>THE SEARCH FOR U(VI) REDUCTASES.....</b>	<b>6</b>
<b>PILUS NANOWIRES .....</b>	<b>7</b>
<b>BIOFILMS IN THE SUBSURFACE .....</b>	<b>9</b>
<b>BIOFILM DEVELOPMENT .....</b>	<b>11</b>
<b>REGULATION OF CELL ENVELOPE COMPONENTS AND ELECTRON TRANSFER     PROCESSES.....</b>	<b>12</b>
<b>REFERENCES.....</b>	<b>13</b>
<b>CHAPTER 2</b>	
<b>EXTRACELLULAR REDUCTION OF URANIUM VIA <i>GEOBACTER</i> CONDUCTIVE PILI AS A PROTECTIVE CELLULAR MECHANISM .....</b>	<b>21</b>
<b>ABSTRACT .....</b>	<b>22</b>
<b>INTRODUCTION .....</b>	<b>23</b>
<b>MATERIALS AND METHODS.....</b>	<b>25</b>
Strains and culture conditions .....	25
Pili induction at suboptimal growth temperatures .....	26
U(VI) resting cell suspension assays .....	26
Gene expression analyses by qRT-PCR .....	27
TEM and Energy Dispersive Spectroscopy (EDS) analyses.....	28
Pili purification, quantification, and biochemical characterization.....	28
Transmission Electron Microscopy (TEM) and Confocal Laser Scanning Microscopy (CLSM) analyses of purified pili .....	31
SDS-PAGE and staining of outer membrane, heme-containing proteins.	31
X-ray Adsorption Spectroscopy (XAS) analyses .....	32
Vitality and viability assays .....	33
<b>RESULTS .....</b>	<b>34</b>
Expression of pili promotes the extracellular reduction of U(VI).....	34
X-ray absorption fine structure (EXAFS) analyses demonstrate the reduction of U(VI) to mononuclear U(IV) .....	41
U reduction via pili as a cellular protective mechanism.....	45

<b>DISCUSSION .....</b>	<b>47</b>
Physiological relevance of the extracellular reduction of U by <i>Geobacter's</i> pili.....	47
Reduction of U to mononuclear U(IV) phases .....	48
Model for the reduction of U(VI) by <i>Geobacter</i> bacteria .....	50
Implications for the <i>in situ</i> bioremediation of U .....	52
<b>REFERENCES .....</b>	<b>53</b>

### CHAPTER 3

#### URANIUM TRANSFORMATIONS DURING BIOFILM DEVELOPMENT IN *GEOBACTER*

<b><i>SULFURREDUCTENS</i> .....</b>	<b>61</b>
<b>ABSTRACT .....</b>	<b>62</b>
<b>INTRODUCTION .....</b>	<b>63</b>
<b>MATERIALS AND METHODS .....</b>	<b>64</b>
Strains and culture conditions .....	64
U(VI) resting cell suspension and biofilm assays .....	66
Vitality fluorescent assays .....	66
Microscopy .....	67
X-ray Absorption Spectroscopy (XAS) analyses .....	68
SDS-PAGE and heme-stain of proteins of the biofilm EPS matrix.....	69
<b>RESULTS AND DISCUSSION .....</b>	<b>70</b>
Enhanced U(VI) immobilization and tolerance by biofilms .....	70
Extracellular reduction of U by biofilms .....	71
Role of conductive pili and c-cytochromes of the biofilm matrix in U reduction .....	76
XAS analyses .....	78
Implications for bioremediation .....	81
<b>APPENDIX .....</b>	<b>82</b>
<b>REFERENCES .....</b>	<b>88</b>

### CHAPTER 4

#### GENETIC ANALYSIS OF BIOFILM FORMATION IN *GEOBACTER SULFURREDUCTENS* .....

<b>ABSTRACT .....</b>	<b>94</b>
<b>INTRODUCTION .....</b>	<b>95</b>
<b>MATERIALS AND METHODS .....</b>	<b>98</b>
Strains and culture conditions .....	98
Biofilm assays.....	98
Confocal Laser Scanning Microscopy (CLSM) .....	99
Transposon mutagenesis .....	99
High-throughput biofilm screening .....	100
Identification of transposon-insertion sites .....	101
Rescue cloning .....	101
Arbitrary PCR.....	102
Mutant confirmation .....	103

SDS-PAGE and heme-stain of proteins in biofilm EPS matrix .....	104
U(VI) resting cell suspension biofilm assays .....	104
<b>RESULTS AND DISCUSSION .....</b>	<b>105</b>
Development of an assay to characterize biofilm developmental stages .....	105
Identification of Tn5-insertion mutants with biofilm defects .....	108
Description of mutant groups.....	109
Cell envelope.....	110
Electron transfer .....	111
Role of pili in biofilm development and uranium immobilization .....	114
Conclusions .....	117
<b>APPENDIX .....</b>	<b>118</b>
<b>REFERENCES.....</b>	<b>127</b>
<b>CHAPTER 5</b>	
<b>IDENTIFICATION AND CHARACTERIZATION OF THE RPOE SIGMA FACTOR OF <i>GEOBACTER SULFURREDUCTENS</i>.....</b>	<b>134</b>
<b>ABSTRACT .....</b>	<b>135</b>
<b>INTRODUCTION.....</b>	<b>136</b>
<b>MATERIALS AND METHODS .....</b>	<b>138</b>
Bacterial strains and culture conditions .....	138
Complementation .....	138
Transcriptional analysis of the <i>rpoE</i> gene and the gene region by RT-PCR.....	139
Stress tolerance assays .....	140
Biofilm assays.....	141
Transmission Electron Microscopy (TEM) .....	141
Fe(III) reduction assays .....	142
<b>RESULTS AND DISCUSSION .....</b>	<b>142</b>
Genetic organization of the <i>rpoE</i> region.....	142
RpoE is not essential for growth, but regulates cell envelope integrity during growth transition.....	144
RpoE is required for stress tolerance.....	149
RpoE regulates electron transfer at the cell envelope .....	154
Implications.....	156
<b>REFERENCES.....</b>	<b>158</b>
<b>CHAPTER 6</b>	
<b>CONCLUSIONS AND FUTURE DIRECTIONS.....</b>	<b>166</b>
<b>REFERENCES.....</b>	<b>171</b>

## LIST OF TABLES

<b>TABLE 2.1</b>	EXAFS modeling results for $R$ and $\sigma^{2*}$ .....	44
<b>TABLE 2.2</b>	EXAFS modeling results for coordination numbers .....	44
<b>TABLE 3.1</b>	COMSTAT analysis.....	75
<b>TABLE 3.A.1</b>	EXAFS modeling results for $R$ and $\sigma^{2**}$ .....	87
<b>TABLE 3.A.2</b>	EXAFS modeling results for coordination numbers .....	87
<b>TABLE 4.1</b>	Primers .....	102
<b>TABLE 4.A.1</b>	Plates, coatings, growth media, and solvents assessed for their use in the biofilm assay.....	119
<b>TABLE 4.A.2</b>	Transposon-insertion mutants displaying deficient or enhanced biofilm phenotypes.....	122

## LIST OF FIGURES

<b>FIGURE 2.1</b>	Reduction and subcellular localization of U.....	35
<b>FIGURE 2.2</b>	Fold change expression of <i>pilA</i> relative to <i>recA</i> in resting cell suspensions of the WT <sub>p+</sub> and WT <sub>p-</sub> strains after 6 h of incubation with 1 mM U(VI) acetate.....	36
<b>FIGURE 2.3</b>	Micrographs of purified pilus fibers.....	37
<b>FIGURE 2.4</b>	Energy dispersive X-ray spectrum of the pili-associated electron-dense deposits imaged by TEM .....	38
<b>FIGURE 2.5</b>	Subcellular localization of uranium deposits by TEM analyses of thin sections of pili-expressing (WT <sub>p+</sub> and pRG5:: <i>pilA</i> ) and non-expressing (WT <sub>p-</sub> and PilA <sup>-</sup> ) cells.....	39
<b>FIGURE 2.6</b>	SDS-PAGE profiling of mechanically detached outer membrane proteins .....	40
<b>FIGURE 2.7</b>	U L <sub>III</sub> -edge EXAFS spectra and models .....	42
<b>FIGURE 2.8</b>	Effect of U(VI) exposure on cell vitality and viability .....	46
<b>FIGURE 2.9</b>	Model for the extracellular reduction of U(VI) to U(IV).....	50
<b>FIGURE 3.1</b>	Biofilms maintain vital activities through 24 h of U exposure .....	70
<b>FIGURE 3.2</b>	SEM micrographs of 48 h biofilms .....	72
<b>FIGURE 3.3</b>	U(VI) immobilization/reduction, and cytochrome profile of the WT, PilA <sup>-</sup> , and pRG5:: <i>pilA</i> strains .....	73
<b>FIGURE 3.4</b>	CLSM micrographs showing side view projections of (A) WT (24, 48 and 72h), (B) PilA <sup>-</sup> (48 h), and (C) pRG5:: <i>pilA</i> (48 h) biofilms stained with the BacLight viability kit (green, live cells; red, dead cells).....	74
<b>FIGURE 3.5</b>	U L <sub>III</sub> -edge XAFS spectra. EXAFS spectra and model.....	79
<b>FIGURE 3.A.1</b>	SEM micrograph and EDS analysis of U precipitates .....	83

<b>FIGURE 3.A.2</b>	CLSM micrographs showing top view projections of 24, 48, and 72 h WT (A), 48 h $PilA^-$ (B) and 48 h pRG5:: <i>pilA</i> biofilms stained with BacLight viability kit (green, live cells; red, dead cells) .....	84
<b>FIGURE 3.A.3</b>	Correlation of biofilm age and biofilm biomass (A), thickness (B), surface area (C), surface coverage (D), and surface:volume ratio (E) .....	85
<b>FIGURE 3.A.4</b>	Linear correlation between the total protein content of biofilms and biofilm age ( $R^2=0.94$ ) (A) and between piliation (planktonic cells grown under pili-inducing conditions at 25°C) and U reduction by 48 h biofilms of the WT, $PilA^-$ and pRG5:: <i>pilA</i> strains ( $R^2 = 0.999$ ) (B) .....	86
<b>FIGURE 4.1</b>	Comparison of the effect of growth medium type and electron donor (acetate) concentrations on biofilm formation (A). CLSM images of wild-type biofilms grown in FW 30A/40F (B) (24 (top), 48 (middle), and 72 (bottom) h growth), FW 15A/40F (72 h growth) (C), and DB 30A/40F (72 h growth) (D). Bar, 20 $\mu$ M .....	107
<b>FIGURE 4.2</b>	Crystal violet staining of representative Tn5-insertion mutants .....	109
<b>FIGURE 4.3</b>	Phenotypic characterization of selected mutants .....	116
<b>FIGURE 4.A.1</b>	A selection of 96-well plates investigated for their ability to maximize <i>G. sulfurreducens</i> 72-hour biofilm growth at 30°C .....	120
<b>FIGURE 4.A.2</b>	Selection of a solvent for de-staining of crystal violet biofilms .....	121
<b>FIGURE 4.A.3</b>	Southern blot to confirm a single Tn5 insertion event .....	126
<b>FIGURE 5.1:</b>	Genetic arrangement of the <i>rpoE</i> region.....	142
<b>FIGURE 5.2:</b>	$RpoE^-$ demonstrates impaired growth in NBAF medium compared to WT.....	145
<b>FIGURE 5.3:</b>	Regulation of biofilm formation by $RpoE^-$ .....	148
<b>FIGURE 5.4:</b>	The effect of environmental stressors on the growth of the wild-type (solid symbols) and the $RpoE^-$ mutant (open symbols) strains .....	151
<b>FIGURE 5.5:</b>	Reverse transcriptase (RT)-PCR of <i>rpoE</i> and <i>recA</i> transcripts.....	153

**FIGURE 5.6:** Fe(III) reductase activity of resting cell suspensions..... 154

## KEY TO SYMBOLS AND ABBREVIATIONS

CLSM.....	Confocal Laser Scanning Microscopy
DB (30A/40F) .....	minimal medium with 30 mM acetate and 40 mM fumarate
EPS.....	exopolysaccharide
EXAFS.....	Extended X-Ray Absorption Fine Structure
Fe(II), Fe(III).....	iron in the +2 and +3 oxidation states, respectively
FWAF or FW (15A/40F) .....	fresh water medium with 15 mM acetate and 40 mM fumarate
FW (30A/40F) .....	fresh water medium with 30 mM acetate and 40 mM fumarate
L.....	liter
ml.....	milliliter
mM.....	millimolar
mol.....	moles
NBAF.....	nutrient broth with 15 mM acetate and 40 mM fumarate
nm.....	nanometer
OD <sub>580</sub> .....	optical density at 580nm
OD <sub>600</sub> .....	optical density at 600nm
PCR.....	polymerase chain reaction
PilA <sup>-</sup> .....	pilin-deficient mutant
SEM.....	Scanning Electron Microscopy
TEM.....	Transmission Electron Microscopy
U.....	uranium

U(IV), U(VI)..... uranium in the +4 (insoluble) and +6 (soluble) oxidation state, respectively

μg..... microgram

μl..... microliter

XANES..... X-ray absorption near edge structure

# **CHAPTER 1**

## **INTRODUCTION**

## URANIUM CONTAMINATION AND ITS IMPACT ON PUBLIC HEALTH

Uranium (U) is a naturally occurring metal that is nearly ubiquitous at low levels in soil and rocks (1). U is an extremely dense metal, which serves as an excellent large-scale and emission-free power source (25). Thus, it is frequently used for both civilian (nuclear reactors) and military (nuclear submarine reactor cores, nuclear weapons, radiation shielding, missile projectiles) applications (1, 34). From the 1940s on, particularly during the Cold War era, U has been extensively mined for its use in the production of the items listed above, leaving behind large amounts of radionuclide waste as a result. Other sources of nuclear waste and contamination include weapons testing, fuel reprocessing, as well as nuclear accidents such as Chernobyl (25). The largest volume of waste, however, is the result of U mining and milling processes (25).

Although many believe the primary health risk from U lies in its radioactivity, in general it is the chemical toxicity that is more hazardous (34). Toxicity can occur via inhalation, ingestion, or through direct contact with the skin. Following a significant acute or chronic exposure event, serious health effects can occur. The most commonly affected organs are the kidneys, but in some cases the respiratory, neurological, and reproductive system can also be affected (1). For this reason, the U.S. Environmental Protection Agency (EPA) has established a maximum allowable level of 30 µg/L in drinking water (1), and the Superfund program has set a preliminary remediation goal of 2.22 µg/L (34).

## REMEDICATION STRATEGIES

The mobility of U in the subsurface is dependent on a variety of factors including pH, redox potential, and other materials present (coatings, sediments, organic and inorganic compounds) (1, 34, 69). Under oxidizing conditions (i.e. surface or groundwater) U is present in its soluble form as a uranyl ion (U(VI) or  $\text{UO}_2^{2+}$ ) or in carbonate complexes. When reduced by biotic or abiotic factors U is instead present in the insoluble uranous (U(IV)) state (34, 69). It is soluble U that poses a greater public health threat as it can migrate in groundwater and contaminate larger areas, as well as drinking water supplies. For this reason, many bioremediation schemes seek to reduce U(VI) to U(IV), thereby immobilizing it and preventing its migration.

Since radionuclides such as U cannot be degraded, and have a lengthy half-life, removal or sequestration of the contaminant is the only available remediation strategy. This can be accomplished using physical or chemical processes (i.e. containment, excavation, chemical extraction, chelation), although these methods are often costly, non-specific, and can produce large amounts of waste which require safe disposal (4, 19, 37, 69). Biological methods, however, are often a safer, more cost-effective option for either *in situ* or *ex situ* remediation, and in some cases can be used as a complement to physical and chemical methods (19). *In situ* remediation is especially advantageous as it requires little excavation of the affected site, and a smaller risk of exposing the public and/or remediation team to the contaminant (19). Biological mechanisms of bioremediation include phytoremediation (the sequestration of the contaminant by plants), or the stimulation of natural microbial communities to convert the contaminant either to a less toxic, or less soluble form. As described below, microbial

bioremediation is a promising strategy. However, a lack of knowledge regarding the mechanism of U reduction by subsurface bacteria has impaired the success of these techniques.

### **MICROBIAL U(VI) REDUCTION**

Although the reduction of U(VI) in anaerobic environments has long been recognized, it was initially presumed that the observed U reduction was due to an indirect and abiotic association with the microorganisms (29). It was believed that microbes acted as passive attachment surfaces for abiotic reduction, or provided reduced metabolic byproducts (such as H<sub>2</sub>S) that in turn were responsible for the observed U reduction (29, 38). This premise was later challenged with the discovery that dissimilatory metal reducers such as GS-15 (later renamed *Geobacter metallireducens*) and *Alteromonas putrefaciens* (later renamed *Shewanella putrefaciens*) were capable of using U as an energy source, and could carry out U reduction more quickly than was observed for abiotic processes. This demonstration of the direct role of bacteria in U reduction led the researchers to hypothesize that this phenomenon could be harnessed for bioremediation purposes (38).

Following these investigations, experiments were carried out under more environmentally relevant conditions, specifically within sediment microcosms in the laboratory. These studies demonstrated that microbial reduction of U followed the consumption of acetate, but also noted the concomitant reduction of Fe(III) (17, 18). This lends support to the idea that U reduction is carried out by dissimilatory metal-reducing bacteria, and it was hypothesized that the Fe(III) in the environment was providing the energy for bacterial growth during *in situ* stimulation. This is likely because Fe(III) was present in significantly higher

quantities (mmol/kg sediment) than the U ( $\mu\text{mol/kg}$  sediment) (17). Consistent with the observed Fe(III) and U(VI) reduction, 16S ribosomal DNA sequences obtained from acetate-amended sediments demonstrated an increase (40% of sequences compared to 5% in untreated sediments) in the *Geobacteraceae*, a family which includes dissimilatory metal-reducers such as the organisms described above (17, 18). These laboratory-scale microcosm studies yielded promising results, indicating that microbial U reduction could have potential as an effective bioremediation tool. Following the same experimental scheme as the laboratory sediment studies, field experiments were performed. This first *in situ* study was performed at the Old Rife site in Colorado, where acetate was injected into the groundwater, and the levels of Fe(III) and U(VI), as well as the microbial community were monitored (3). This field study (3), as well as later experiments at the Oak Ridge FRC site in Tennessee (28, 47), reproduced results of the lab-based experiments, showing the consumption of acetate concurrent with the reduction of U(VI)/Fe(III), and the stimulation of the *Geobacteraceae*.

More direct evidence specifically linking the metabolic activity of members of the *Geobacteraceae* with U reduction was explored with the use of BioSep beads incorporating  $^{13}\text{C}$ -labeled acetate. Using stable isotope probing, the researchers were able to demonstrate that the *Geobacteraceae* took up the labeled acetate, and dominated the microbial community in the areas close to the injection site, indicating that they are in fact metabolically active during *in situ* bioremediation (8). Further evidence of metabolic activity was obtained by monitoring the expression of a *Geobacteraceae*-specific citrate synthase gene (24). This gene is eukaryotic-like and phylogenetically distinct from that of other prokaryotes, but also a key component of *Geobacteraceae* metabolism, making it an ideal candidate for monitoring the metabolic activity

of this family of organisms (24). When tested in lab and field experiments, the transcript levels of the citrate synthase gene correlated well with the level of acetate, indicating that with the addition of an electron donor, the *Geobacteraceae* were metabolically active (2, 24). Thus, they are able to reduce U under conditions that are conducive to growth.

### THE SEARCH FOR U(VI) REDUCTASES

Although U is not known to be an essential component for any enzyme or biological structure (69), it has been shown that U can support the growth of *Anaeromyxobacter dehalogenans* and *Geobacter* spp. (38, 62). When provided as an electron acceptor, however, lower-than-expected growth yields were observed, potentially due to toxicity of the U (62). U is known to be toxic to cells upon entering the cell envelope so it has been proposed that U reduction takes place mainly outside of the cell (69). This is in agreement with observations that precipitated U is often found to be localized outside of the cell, or in the periplasm (9, 21, 35, 41, 63, 69). It has therefore been suggested that the best candidates for U reductases are likely to be located in the periplasm or outer membrane (35, 69).

As genome sequences became available, representatives of the *Geobacteraceae* were found to have an unusually large number of genes coding for electron transfer proteins termed cytochromes (45). Multi-heme *c*-type cytochromes are electron transfer proteins that are responsible for passing electrons from the quinone/quinol pool to other cytochromes within the cell membrane, or to exogenous electron acceptors (i.e. fumarate, Fe(III), U(VI)) (64). The genome of the model organism for this family, *Geobacter sulfurreducens*, contains a total of 111 predicted *c*-type cytochromes (45). This unprecedented number may be an indication of

the versatility of electron acceptors that can be used by this organism, as well as the extreme importance of the electron transfer process (45). The search for U reductases therefore focused mainly on cytochromes present in the periplasm or outer membrane.

With the establishment of a genetic system in *G. sulfurreducens* (10) it became possible to investigate the metabolic role and localization of individual cytochromes. In recent years numerous studies in *G. sulfurreducens* have demonstrated the role of cytochromes in the transfer of electron to electrodes, and the reduction of metals, including U(VI) (5, 26, 31, 33, 44, 54, 60, 63).

Studies to date have implicated periplasmic (36, 52, 63) as well as outer membrane (41, 63) cytochromes. U(VI) reduction was not completely eliminated by mutating the genes encoding these cytochromes, however, and extensive periplasmic mineralization was observed in all studies, suggesting that additional reductases remained active in the periplasm. These putative periplasmic reductases are unlikely to be relevant to U reduction under environmental conditions because, as discussed above, this situation is unlikely to be environmentally relevant as it would be to the cell's disadvantage to reduce U intracellularly.

## **PILUS NANOWIRES**

It is important to note that these previous studies were carried out at temperatures that prevent the expression of pilus nanowires (9), which are conductive extracellular appendages required for the transfer of electrons to insoluble electron acceptors in the environment (57). The *G. sulfurreducens* type IV pilus apparatus is very similar to those of other organisms in that it utilizes the same set of core proteins including PilA (pilin subunit), PilD (prepilin peptidase),

PilC (inner membrane protein), PilB (assembly ATPase), PilT (retraction ATPase) and PilQ (outer membrane secretin) (40, 42, 45). The PilA protein of *G. sulfurreducens* also possesses a structure common to type IV pilins with a highly conserved N-terminal alpha-helical region, and a more variable C-terminal region (42, 51, 65). Despite this conservation, the *Geobacter* pilin is evolutionarily distinct from other pilins, and forms an independent line of descent (57). What distinguishes the *Geobacter* pilin from that of other organisms is that it lacks the C-terminus globular head domain commonly found in other pilins. For this reason, it has been predicted that *Geobacter* pili may have adapted to perform a function distinct from that of other organisms (57). This was confirmed by the observation that *G. sulfurreducens* pili were not required for common functions such as adhesion to surfaces and twitching motility, but instead were essential for the reduction of insoluble Fe(III) oxides (57). Conductivity measurements performed with atomic force microscopy (AFM) demonstrated the high conductivity of the pilus filaments, and implicated them as “pilus nanowires” which serve as the electrical conduit between the cell and insoluble electron acceptors such as Fe(III) oxides (57).

As discussed above, *Geobacter* obtain most of their energy for growth during *in situ* U bioremediation from Fe(III) oxides. As reduction of Fe(III) oxides requires the expression of the pilus nanowires (57), we can infer that nanowires are also expressed during *in situ* bioremediation of U. This hypothesis, coupled with the lack of a definitive extracellular U reductase, led us to evaluate the contribution of the pilus nanowires to U(VI) reduction. Chapter 2 of my dissertation describes a previously unrecognized role for *Geobacter* pili in the extracellular reduction of U and their essential function as a catalytic and protective cellular mechanism.

## BIOFILMS IN THE SUBSURFACE

In addition to their role in electron transfer, the expression of pilus nanowires by *G. sulfurreducens* also promotes cell-cell aggregation and biofilm formation (58). Biofilms are defined as “matrix-enclosed bacterial populations adherent to each other and/or to surfaces or interfaces” (12), and have long been observed in the environment, with the first reports dating back to the 1930s and 40s when it was noted by several groups that “solid surfaces are beneficial to bacteria” (72). It was not until many years later that this phenomenon was given a name, and demonstrated to be both ubiquitous and the predominate mode of bacterial growth in the environment (12-15, 20).

Upon encountering a surface for adhesion, bacteria undergo a variety of phenotypic changes allowing them to attach to the surface, and develop a three-dimensional biofilm. These phenotypic alterations can include the abundant production of exopolysaccharide (EPS), as well as an increased resistance to heavy metals and other antibiotics (12, 23), with one study demonstrating heavy metal resistance of the biofilm at levels up to 600-fold greater than that of planktonic cells (66). Furthermore, it appeared that metal immobilization and toxicity was localized to the exterior of the biofilm while the interior cells remained viable, potentially because EPS is able to prevent the toxin from diffusing into the center of the biofilm (66).

This increased resistance of biofilms to toxic compounds led researchers to investigate the potential for their use in bioremediation schemes. For example, biofilms of *Pseudomonas extremaustralis* display higher growth and hydrocarbon degradation capabilities than planktonic cells (68), and preliminary studies with yeast have shown promise in utilizing biofilms

as trickling filter for the degradation of diesel oil (7). Similarly, biofilm carriers were shown to be an effective method of removing pharmaceutical substances (diclofenac, ketoprofen, gemfibrozil, clofibrac acid and mefenamic acid) from wastewater (16). In addition, it has been hypothesized that U reduced by biofilms could be protected from reoxidation and remobilization. While the U at the surface of the biofilm may become reoxidized as a result of the oxygen intrusions common to the subsurface environment, it is possible that reducing conditions will be maintained in the inner layers of the biofilm, thereby preventing reoxidation of U (6). This is in contrast to cultures of planktonic cells from which bound U is readily oxidized (6). Additionally, recent work has shown that following the addition of acetate to contaminated groundwater *Geobacter* cells transition from growing predominately as planktonic cells to dominating the metabolically active, sediment-associated biofilm community (30).

Despite these findings, the contribution of *Geobacter* biofilms to uranium removal and reduction has not been investigated. Previous studies in planktonic cells have demonstrated the role of the pilus nanowires, a cell envelope component essential to biofilm development, in U immobilization and reduction (9). Thus, we sought to determine the role of pili in biofilm development, as well as U reduction.

In chapter 3 of this dissertation I demonstrate that multilayer biofilms are able to reduce and tolerate substantially more U than planktonic cells for prolonged periods of time (up to 24 h), making them an attractive option for the development of permeable biobarriers for U bioremediation. I also demonstrate the role of pili as a U reductase in the biofilms.

## BIOFILM DEVELOPMENT

The development of a biofilm progresses in several stages beginning with an approach to the surface and initial attachment, colonization and microcolony development, and finally growth into a mature biofilm (15, 48). The transition to each stage requires the expression of a unique set of cellular components, many of them extracellular structures (22). For example, motility proteins such as pili and flagella are often important for initial attachment and colonization, while the EPS matrix facilitates the development of a mature biofilm (22, 70). This is not representative of every organism, however, as some non-motile bacteria, such as *Staphylococcus epidermidis*, utilize protein and/or polysaccharides as adhesins (22, 61).

The work presented in chapter 3 highlights the distinct role of each biofilm developmental stage to the immobilization and reduction of U, leading us to examine the cellular components characteristic of each stage. Previous studies have utilized random transposon mutagenesis coupled with a high-throughput screening for biofilm-deficient phenotypes to identify genes involved in the developmental process (39, 49, 50, 53, 56, 59, 67). Thus, to gain further insight into how biofilms transform U I developed and screened a library of transposon-insertion mutants and identified mutants with biofilm defects. This study confirmed the role of *Geobacter* pili in biofilm formation, and identified other cell envelope components involved in biofilm formation and electron transport that may be relevant to U transformations in the subsurface.

## REGULATION OF CELL ENVELOPE COMPONENTS AND ELECTRON TRANSFER PROCESSES

The work described in the previous chapters of my dissertation has highlighted the importance of the cell envelope and its components for the development of biofilms, as well as the survival of *Geobacter* in the subsurface. However, little is known regarding the regulation of the cell envelope. Thus, I investigated the role of the *Geobacter*'s extracytoplasmic function (ECF) sigma factor, RpoE.

Sigma factors ( $\sigma$ ) such as RpoE are able to respond to environmental signals and direct the bacterial RNA polymerase to specific promoters (71), allowing the cell to reprogram gene expression in order to adapt to the given environment (27).

The ECF sigma factors, in particular, are responsible for coordinating the expression of genes in response to environmental stressors, specifically those that cause imbalanced synthesis of outer membrane components (43, 46). This can occur as a result of generalized stressors such as temperature and ethanol (55), or more specific cues such as the transition from exponential to stationary phase, or response to nutritional stress (11), as well as increased sensitivity to adverse environmental conditions such as antibiotics, reactive oxygen species, and changes in osmolarity (32).

In the last chapter of my dissertation, I show that RpoE is required for response to cell envelope stress caused by oxygen, high pH, and low temperature, as well as the regulation of *Geobacter*'s extracellular electron transfer pathways. This highlights the functional specialization that RpoE has undergone to control the adaptive responses that enable *Geobacter* bacteria to survive in the subsurface, and links my findings to *Geobacter*'s physiology in the subsurface.

## REFERENCES

## REFERENCES

1. **Agency for Toxic Substances and Disease Registry, A. S. T. D. R.** 2011. Toxicological profile for uranium. *In* P. H. S. Department of Health and Human Services (ed.), Atlanta, GA.
2. **Akob, D. M., H. J. Mills, T. M. Gihring, L. Kerkhof, J. W. Stucki, A. S. Anastacio, K. J. Chin, K. Kusel, A. V. Palumbo, D. B. Watson, and J. E. Kostka.** 2008. Functional diversity and electron donor dependence of microbial populations capable of U(VI) reduction in radionuclide-contaminated subsurface sediments. *Appl Environ Microbiol* **74**:3159-3170.
3. **Anderson, R. T., H. A. Vrionis, I. Ortiz-Bernad, C. T. Resch, P. E. Long, R. Dayvault, K. Karp, S. Marutzky, D. R. Metzler, A. Peacock, D. C. White, M. Lowe, and D. R. Lovley.** 2003. Stimulating the in situ activity of *Geobacter* species to remove uranium from the groundwater of a uranium-contaminated aquifer. *Appl. Environ. Microbiol.* **69**:5884-5891.
4. **Barkay, T., and J. Schaefer.** 2001. Metal and radionuclide bioremediation: issues, considerations and potentials. *Curr. Opin. Microbiol.* **4**:318-323.
5. **Butler, J. E., F. Kaufmann, M. V. Coppi, C. Nunez, and D. R. Lovley.** 2004. MacA, a diheme *c*-type cytochrome involved in Fe(III) reduction by *Geobacter sulfurreducens*. *J. Bacteriol.* **186**:4042-4045.
6. **Cao, B., B. Ahmed, and H. Beyenal.** 2010. Immobilization of uranium in groundwater using biofilms, p. 1-37. *In* V. Shah (ed.), *Emerging Environmental Technologies*. Springer Science+Business Media.
7. **Chandran, P., and N. Das.** 2011. Degradation of diesel oil by immobilized *Candida tropicalis* and biofilm formed on gravels. *Biodegradation* **22**:1181-1189.
8. **Chang, Y. J., P. E. Long, R. Geyer, A. D. Peacock, C. T. Resch, K. Sublette, S. Pfiffner, A. Smithgall, R. T. Anderson, H. A. Vrionis, J. R. Stephen, R. Dayvault, I. Ortiz-Bernad, D. R. Lovley, and D. C. White.** 2005. Microbial incorporation of <sup>13</sup>C-labeled acetate at the field scale: detection of microbes responsible for reduction of U(VI). *Environ. Sci. Technol.* **39**:9039-9048.
9. **Cologgi, D. L., S. Lampa-Pastirk, A. M. Speers, S. D. Kelly, and G. Reguera.** 2011. Extracellular reduction of uranium via *Geobacter* conductive pili as a protective cellular mechanism. *Proc Natl Acad Sci U S A* **108**:15248-15252.
10. **Coppi, M. V., C. Leang, S. J. Sandler, and D. R. Lovley.** 2001. Development of a genetic system for *Geobacter sulfurreducens*. *Appl. Environ. Microbiol.* **67**:3180-3187.

11. **Costanzo, A., and S. E. Ades.** 2006. Growth phase-dependent regulation of the extracytoplasmic stress factor, sigmaE, by guanosine 3',5'-bispyrophosphate (ppGpp). *J. Bacteriol.* **188**:4627-4634.
12. **Costerton, J. W.** 1995. Overview of microbial biofilms. *J Ind Microbiol* **15**:137-140.
13. **Costerton, J. W., K. J. Cheng, G. G. Geesey, T. I. Ladd, J. C. Nickel, M. Dasgupta, and T. J. Marrie.** 1987. Bacterial biofilms in nature and disease. *Annu. Rev. Microbiol.* **41**:435-464.
14. **Costerton, J. W., G. G. Geesey, and K. J. Cheng.** 1978. How bacteria stick. *Scientific American* **238**:86-95.
15. **Costerton, J. W., Z. Lewandowski, D. E. Caldwell, D. R. Korber, and H. M. Lappin-Scott.** 1995. Microbial biofilms. *Annu Rev Microbiol* **49**:711-745.
16. **Falas, P., A. Baillon-Dhumez, H. R. Andersen, A. Ledin, and J. la Cour Jansen.** 2012. Suspended biofilm carrier and activated sludge removal of acidic pharmaceuticals. *Water research* **46**:1167-1175.
17. **Finneran, K. T., R. T. Anderson, K. P. Nevin, and D. R. Lovley.** 2002. Potential for Bioremediation of uranium-contaminated aquifers with microbial U(VI) reduction. *Soil & Sediment Contamination* **11**:339-357.
18. **Finneran, K. T., M. E. Housewright, and D. R. Lovley.** 2002. Multiple influences of nitrate on uranium solubility during bioremediation of uranium-contaminated subsurface sediments. *Environ. Microbiol.* **4**:510-516.
19. **Gavrilescu, M., L. V. Pavel, and I. Cretescu.** 2009. Characterization and remediation of soils contaminated with uranium. *Journal of hazardous materials* **163**:475-510.
20. **Geesey, G. G., R. Mutch, and J. Costerton.** 1978. Sessile bacteria: An important component of the microbial population in small mountain streams. *Limnol. Oceanogr.* **23**:1214-1223.
21. **Gorby, Y., and D. Lovley.** 1992. Enzymatic uranium precipitation. *Environmental science & technology* **26**:205-207.
22. **Hall-Stoodley, L., and P. Stoodley.** 2002. Developmental regulation of microbial biofilms. *Current opinion in biotechnology* **13**:228-233.
23. **Harrison, J. J., H. Ceri, and R. J. Turner.** 2007. Multimetal resistance and tolerance in microbial biofilms. *Nat. Rev. Microbiol.* **5**:928-938.
24. **Holmes, D. E., K. P. Nevin, R. A. O'Neil, J. E. Ward, L. A. Adams, T. L. Woodard, H. A. Vrionis, and D. R. Lovley.** 2005. Potential for quantifying expression of the

- Geobacteraceae* citrate synthase gene to assess the activity of *Geobacteraceae* in the subsurface and on current-harvesting electrodes. *Appl. Environ. Microbiol.* **71**:6870-6877.
25. **Hu, Q. H., J. Q. Weng, and J. S. Wang.** 2010. Sources of anthropogenic radionuclides in the environment: a review. *Journal of environmental radioactivity* **101**:426-437.
  26. **Inoue, K., X. Qian, L. Morgado, B. C. Kim, T. Mester, M. Izallalen, C. A. Salgueiro, and D. R. Lovley.** 2010. Purification and characterization of OmcZ, an outer-surface, octaheme c-type cytochrome essential for optimal current production by *Geobacter sulfurreducens*. *Appl Environ Microbiol* **76**:3999-4007.
  27. **Ishihama, A.** 2000. Functional modulation of *Escherichia coli* RNA polymerase. *Annu. Rev. Microbiol.* **54**:499-518.
  28. **Istok, J. D., J. M. Senko, L. R. Krumholz, D. Watson, M. A. Bogle, A. Peacock, Y. J. Chang, and D. C. White.** 2004. *In situ* bioreduction of technetium and uranium in a nitrate-contaminated aquifer. *Environ. Sci. Technol.* **38**:468-475.
  29. **Kauffman, J. W., W. C. Laughlin, and R. A. Baldwin.** 1986. Microbiological treatment of uranium mine waters. *Environmental science & technology* **20**:243-248.
  30. **Kerkhof, L. J., K. H. Williams, P. E. Long, and L. R. McGuinness.** 2011. Phase Preference by Active, Acetate-Utilizing Bacteria at the Rifle, CO Integrated Field Research Challenge Site. *Environmental science & technology* **Epub ahead of print**.
  31. **Kim, B. C., and D. R. Lovley.** 2008. Investigation of direct vs. indirect involvement of the c-type cytochrome MacA in Fe(III) reduction by *Geobacter sulfurreducens*. *FEMS Microbiol Lett* **286**:39-44.
  32. **Korbsrisate, S., M. Vanaporn, P. Kerdsuk, W. Kespichayawattana, P. Vattanaviboon, P. Kiatpapan, and G. Lertmemongkolchai.** 2005. The *Burkholderia pseudomallei* RpoE (AlgU) operon is involved in environmental stress tolerance and biofilm formation. *FEMS Microbiol. Lett.* **252**:243-249.
  33. **Leang, C., M. V. Coppi, and D. R. Lovley.** 2003. OmcB, a c-type polyheme cytochrome, involved in Fe(III) reduction in *Geobacter sulfurreducens*. *J. Bacteriol.* **185**:2096-2103.
  34. **Littleton, B.** 2006. Depleted uranium technical brief, vol. EPA 402-R-06-011. U.S. Environmental Protection Agency Office of Radiation and Indoor Air Radiation Protection Division, Washington, DC 20460.
  35. **Lloyd, J. R., and J. Chesnes.** 2002. Reduction of actinides and fission products by Fe(III)-reducing bacteria. *Geomicrobiol J* **19**:103-120.

36. **Lloyd, J. R., C. Leang, A. L. Hodges Myerson, M. V. Coppi, S. Cuifo, B. Methe, S. J. Sandler, and D. R. Lovley.** 2003. Biochemical and genetic characterization of PpcA, a periplasmic *c*-type cytochrome in *Geobacter sulfurreducens*. *Biochem. J.* **369**:153-161.
37. **Lloyd, J. R., and D. R. Lovley.** 2001. Microbial detoxification of metals and radionuclides. *Curr. Opin. Biotechnol.* **12**:248-253.
38. **Lovley, D. R., E. J. P. Phillips, Y. A. Gorby, and E. R. Landa.** 1991. Microbial reduction of uranium. *Nature* **350**:413-416.
39. **Mack, D., M. Nedelmann, A. Krokotsch, A. Schwarzkopf, J. Heesemann, and R. Laufs.** 1994. Characterization of transposon mutants of biofilm-producing *Staphylococcus epidermidis* impaired in the accumulative phase of biofilm production: genetic identification of a hexosamine-containing polysaccharide intercellular adhesin. *Infect. Immun.* **62**:3244-3253.
40. **Mangan, M. W., and W. G. Meijer.** 2001. Random insertion mutagenesis of the intracellular pathogen *Rhodococcus equi* using transposomes. *FEMS Microbiol Lett* **205**:243-246.
41. **Marshall, M. J., A. S. Beliaev, A. C. Dohnalkova, D. W. Kennedy, L. Shi, Z. Wang, M. I. Boyanov, B. Lai, K. M. Kemner, J. S. McLean, S. B. Reed, D. E. Culley, V. L. Bailey, C. J. Simonson, D. A. Saffarini, M. F. Romine, J. M. Zachara, and J. K. Fredrickson.** 2006. *c*-Type cytochrome-dependent formation of U(IV) nanoparticles by *Shewanella oneidensis*. *PLoS Biol.* **4**:e268.
42. **Mattick, J. S.** 2002. Type IV pili and twitching motility. *Annu. Rev. Microbiol.* **56**:289-314.
43. **Mecas, J., P. E. Rouviere, J. W. Erickson, T. J. Donohue, and C. A. Gross.** 1993. The activity of sigma E, an *Escherichia coli* heat-inducible sigma-factor, is modulated by expression of outer membrane proteins. *Genes Dev.* **7**:2618-2628.
44. **Mehta, T., M. V. Coppi, S. E. Childers, and D. R. Lovley.** 2005. Outer membrane *c*-type cytochromes required for Fe(III) and Mn(IV) oxide reduction in *Geobacter sulfurreducens*. *Appl. Environ. Microbiol.* **71**:8634-8641.
45. **Methé, B. A., K. E. Nelson, J. A. Eisen, I. T. Paulsen, W. Nelson, J. F. Heidelberg, D. Wu, M. Wu, N. Ward, M. J. Beanan, R. J. Dodson, R. Madupu, L. M. Brinkac, S. C. Daugherty, R. T. DeBoy, A. S. Durkin, M. Gwinn, J. F. Kolonay, S. A. Sullivan, D. H. Haft, J. Selengut, T. M. Davidsen, N. Zafar, O. White, B. Tran, C. Romero, H. A. Forberger, J. Weidman, H. Khouri, T. V. Feldblyum, T. R. Utterback, S. E. Van Aken, D. R. Lovley, and C. M. Fraser.** 2003. Genome of *Geobacter sulfurreducens*: metal reduction in subsurface environments. *Science* **302**:1967-1969.
46. **Missiakas, D., and S. Raina.** 1998. The extracytoplasmic function sigma factors: role and regulation. *Mol. Microbiol.* **28**:1059-1066.

47. **North, N. N., S. L. Dollhopf, L. Petrie, J. D. Istok, D. L. Balkwill, and J. E. Kostka.** 2004. Change in bacterial community structure during in situ biostimulation of subsurface sediment cocontaminated with uranium and nitrate. *Appl. Environ. Microbiol.* **70**:4911-4920.
48. **O'Toole, G., H. B. Kaplan, and R. Kolter.** 2000. Biofilm formation as microbial development. *Annu. Rev. Microbiol.* **54**:49-79.
49. **O'Toole, G. A., and R. Kolter.** 1998. Flagellar and twitching motility are necessary for *Pseudomonas aeruginosa* biofilm development. *Mol. Microbiol.* **30**:295-304.
50. **O'Toole, G. A., and R. Kolter.** 1998. Initiation of biofilm formation in *Pseudomonas fluorescens* WCS365 proceeds via multiple, convergent signalling pathways: a genetic analysis. *Mol. Microbiol.* **28**:449-461.
51. **Parge, H. E., K. T. Forest, M. J. Hickey, D. A. Christensen, E. D. Getzoff, and J. A. Tainer.** 1995. Structure of the fibre-forming protein pilin at 2.6 Å resolution. *Nature* **378**:32-38.
52. **Payne, R. B., D. M. Gentry, B. J. Rapp-Giles, L. Casalot, and J. D. Wall.** 2002. Uranium reduction by *Desulfovibrio desulfuricans* strain G20 and a cytochrome *c3* mutant. *Appl. Environ. Microbiol.* **68**:3129-3132.
53. **Pratt, L. A., and R. Kolter.** 1998. Genetic analysis of *Escherichia coli* biofilm formation: roles of flagella, motility, chemotaxis and type I pili. *Mol. Microbiol.* **30**:285-293.
54. **Qian, X., T. Mester, L. Morgado, T. Arakawa, M. L. Sharma, K. Inoue, C. Joseph, C. A. Salgueiro, M. J. Maroney, and D. R. Lovley.** 2011. Biochemical characterization of purified OmcS, a c-type cytochrome required for insoluble Fe(III) reduction in *Geobacter sulfurreducens*. *Biochimica et biophysica acta* **1807**:404-412.
55. **Raivio, T. L., and T. J. Silhavy.** 2001. Periplasmic stress and ECF sigma factors. *Annu. Rev. Microbiol.* **55**:591-624.
56. **Reguera, G., and R. Kolter.** 2005. Virulence and the environment: a novel role for *Vibrio cholerae* toxin-coregulated pili in biofilm formation on chitin. *J. Bacteriol.* **187**:3551-3555.
57. **Reguera, G., K. D. McCarthy, T. Mehta, J. S. Nicoll, M. T. Tuominen, and D. R. Lovley.** 2005. Extracellular electron transfer via microbial nanowires. *Nature* **435**:1098-1101.
58. **Reguera, G., R. B. Pollina, J. S. Nicoll, and D. R. Lovley.** 2007. Possible Nonconductive Role of *Geobacter sulfurreducens* Pilus Nanowires in Biofilm Formation. *J. Bacteriol.* **189**:2125-2127.

59. **Rollefson, J. B., C. E. Levar, and D. R. Bond.** 2009. Identification of genes involved in biofilm formation and respiration via mini-Himar transposon mutagenesis of *Geobacter sulfurreducens*. *J Bacteriol* **191**:4207-4217.
60. **Rollefson, J. B., C. S. Stephen, M. Tien, and D. R. Bond.** 2011. Identification of an extracellular polysaccharide network essential for cytochrome anchoring and biofilm formation in *Geobacter sulfurreducens*. *J Bacteriol* **193**:1023-1033.
61. **Rupp, M. E., J. S. Ulphani, P. D. Fey, and D. Mack.** 1999. Characterization of *Staphylococcus epidermidis* polysaccharide intercellular adhesin/hemagglutinin in the pathogenesis of intravascular catheter-associated infection in a rat model. *Infect Immun* **67**:2656-2659.
62. **Sanford, R. A., Q. Wu, Y. Sung, S. H. Thomas, B. K. Amos, E. K. Prince, and F. E. Loffler.** 2007. Hexavalent uranium supports growth of *Anaeromyxobacter dehalogenans* and *Geobacter* spp. with lower than predicted biomass yields. *Environmental microbiology* **9**:2885-2893.
63. **Shelobolina, E. S., M. V. Coppi, A. A. Korenevsky, L. N. DiDonato, S. A. Sullivan, H. Konishi, H. Xu, C. Leang, J. E. Butler, B. C. Kim, and D. R. Lovley.** 2007. Importance of *c*-Type cytochromes for U(VI) reduction by *Geobacter sulfurreducens*. *BMC Microbiol.* **7**:16.
64. **Shi, L., D. J. Richardson, Z. Wang, S. N. Kerisit, K. M. Rosso, J. M. Zachara, and J. K. Fredrickson.** 2009. The role of outer membrane cytochromes of *Shewanella* and *Geobacter* in extracellular electron transfer. *Environ Microbiol Reports* **1**:220-227.
65. **Strom, M. S., and S. Lory.** 1993. Structure-function and biogenesis of the type IV pili. *Annu. Rev. Microbiol.* **47**:565-596.
66. **Teitzel, G. M., and M. R. Parsek.** 2003. Heavy metal resistance of biofilm and planktonic *Pseudomonas aeruginosa*. *Appl Environ Microbiol* **69**:2313-2320.
67. **Thormann, K. M., R. M. Saviile, S. Shukla, D. A. Pelletier, and A. M. Spormann.** 2004. Initial Phases of biofilm formation in *Shewanella oneidensis* MR-1. *J. Bacteriol.* **186**:8096-8104.
68. **Tribelli, P. M., C. Di Martino, N. I. Lopez, and L. J. Raiger lustman.** 2012. Biofilm lifestyle enhances diesel bioremediation and biosurfactant production in the Antarctic polyhydroxyalkanoate producer *Pseudomonas extremaustralis*. *Biodegradation* **Epub ahead of print.**
69. **Wall, J. D., and L. R. Krumholz.** 2006. Uranium reduction. *Annu. Rev. Microbiol.* **60**:149-166.

70. **Watnick, P. I., and R. Kolter.** 1999. Steps in the development of a *Vibrio cholerae* El Tor biofilm. *Mol. Microbiol.* **34**:586-595.
71. **Wosten, M. M. S. M.** 1998. Eubacterial sigma-factors. *FEMS Microbiol. Rev.* **22**:127-150.
72. **Zobell, C. E.** 1943. The Effect of Solid Surfaces upon Bacterial Activity. *J Bacteriol* **46**:39-56.

## CHAPTER 2

### EXTRACELLULAR REDUCTION OF URANIUM VIA *GEOBACTER* CONDUCTIVE PILI AS A PROTECTIVE CELLULAR MECHANISM

The material presented in Chapter 2 has been adapted from the following publication:

**Cologgi, D. L., S. Lampa-Pastirk, A. M. Speers, S. D. Kelly, and G. Reguera. 2011.**

Extracellular reduction of uranium via *Geobacter* conductive pili as a protective cellular mechanism. *Proc Natl Acad Sci U S A* **108**:15248-15252.

## ABSTRACT

The *in situ* stimulation of Fe(III) oxide reduction by *Geobacter* bacteria leads to the concomitant precipitation of U(VI) from groundwater. Despite its promise for the bioremediation of uranium contaminants, the biological mechanism behind this reaction has remained elusive. Because Fe(III) oxide reduction requires the expression of *Geobacter's* conductive pili, we evaluated their contribution to uranium reduction in *Geobacter sulfurreducens* grown under pili-inducing or non-inducing conditions. A pilin-deficient mutant and a genetically complemented strain with reduced outer membrane *c*-cytochrome content were used as controls. Pili expression significantly enhanced the rate and extent of uranium immobilization per cell and prevented periplasmic mineralization. As a result, pili expression also preserved the vital respiratory activities of the cell envelope and the cell's viability. Uranium preferentially precipitated along the pili and, to a lesser extent, on outer membrane redox-active foci. In contrast, the pilus-defective strains had different degrees of periplasmic mineralization matching well with their outer membrane *c*-cytochrome content. X-ray absorption spectroscopy analyses demonstrated the extracellular reduction of U(VI) by the pili to mononuclear U(IV) complexed by carbon containing ligands, consistent with a biological reduction mechanism. In contrast, the U(IV) in the pilin-deficient mutant cells also required an additional phosphorous ligand, in agreement with the predominantly periplasmic mineralization of uranium observed in this strain. These results demonstrate a previously unrecognized role for *Geobacter* conductive pili in the extracellular reduction of uranium and highlight its essential function as a catalytic and protective cellular mechanism that is of interest for the bioremediation of uranium-contaminated groundwater.

## INTRODUCTION

Dissimilatory metal-reducing microorganisms gain energy for growth by coupling the oxidation of organic acids or H<sub>2</sub> to the reduction of metals. Some can also use U as an electron acceptor (42, 58), a process that could be harnessed for the bioremediation of the contaminated aquifers and sediments left by the intensive U mining practices of the Cold War era (39). Interestingly, stimulating the activity of metal-reducing microorganisms *in situ* resulted in the concomitant removal of soluble U (U(VI)) from the contaminated groundwater and detection of its sparingly soluble, less mobile form, U(IV) in sediments (1, 9, 25, 51, 73). This suggests that stimulating metal reduction in the subsurface results in the biological reduction of U(VI) to U(IV), thereby preventing plume migration and eliminating the potential for contaminant exposure.

The removal of U(VI) from groundwater following the *in situ* stimulation of metal reduction is often concomitant with substantial increases in the growth and activity of dissimilarity metal-reducing microorganisms in the family *Geobacteraceae* (1, 9, 51, 72). Despite extensive efforts to understand the mechanisms and pathways used by these bacteria to reduce U(VI), the nature of its U reductase has remained elusive. Early studies with *Geobacter metallireducens* GS15 suggested that U was reduced extracellularly to uraninite under conditions conducive to cell growth (17, 42). The development of genetic tools in *Geobacter sulfurreducens* (12) motivated molecular studies to elucidate the biological mechanism behind this reaction. Because *c*-cytochromes are abundant in the cell envelope of *Geobacter* bacteria, studies focused on identifying extracytoplasmic *c*-cytochromes that could function as dedicated U reductases (38, 63). However, mutations were often pleiotropic (31-33) and either showed no

defect or only partial defects in the cell's ability to remove U(VI) (38, 63). Interpretation was also difficult due to inconsistencies in the reported mutant phenotypes, with some mutations reportedly abolishing U(VI) removal activities yet mutant cells showing extensive mineralization (63). Furthermore, these studies consistently showed that the U precipitated inside the cell envelope. U is not known to be essential for the synthesis of any cell component or for any cellular biological reaction yet can be reduced and precipitated nonspecifically by the abundant low potential electron donors of the cell envelope of Gram-negative bacteria (71). This is predicted to compromise the integrity of the cell envelope and its vital functions (64). Because of this, the environmental relevance of these early studies in *G. sulfurreducens* is questionable.

The energy to support the growth of *Geobacter* bacteria after *in situ* stimulation results from the reduction of the abundant Fe(III) oxides, a process that requires the expression of their conductive pili (55). In contrast to the lack of conservation of *c*-cytochrome sequences (8), the genes encoding the *Geobacteraceae* pilus subunits or pilins are highly conserved and form an independent line of descent (55). This is consistent with the pili's specialized function as electrical conduits. The pilus apparatus is anchored in the cell envelope of Gram-negative cells (49, 67, 70) and could potentially accept electrons from cell envelope *c*-cytochromes or the menaquinone pool in the inner membrane. Pili also protrude outside the cell envelope and can reach  $\mu\text{m}$  lengths, thereby enhancing the cell's reactive surface. Thus, we hypothesized that the pili could catalyze the reduction of U(VI) 'at a distance' to maximize the cell's catalytic surface while minimizing exposure to U. Here we show that the conductive pili of *G. sulfurreducens* catalyze the extracellular reduction of U(VI) to a mononuclear U(IV) phase and prevent its periplasmic mineralization, thereby preserving the functioning and integrity of the cell envelope

and the cell's viability. These results identify *pili* as the primary U reductase of *Geobacter* bacteria and demonstrate that their catalytic function also serves as a cellular protective mechanism. This suggests that their expression confers on *Geobacter* bacteria an adaptive ecological advantage in the contaminated subsurface of potential interest for the optimization of *in situ* bioremediation.

## MATERIALS AND METHODS

**Strains and culture conditions.** Wild-type (WT) *Geobacter sulfurreducens* PCA (ATCC 51573), a pilin-deficient mutant (*PilA*<sup>-</sup>) (55), and its genetically complemented strain (*pRG5::pila*) (55) were routinely revived from frozen stocks in NB medium (12) supplemented with 15mM acetate and 40mM fumarate (NBAF) and incubated at 30°C. The cultures were transferred to fresh water (FW) medium (41), prepared with the modifications described below, and supplemented with 15mM acetate and 40mM fumarate (FWAF). The electron donor and acceptor were prepared as autoclaved concentrated stocks (0.75 M sodium acetate and 1 M sodium fumarate at pH 7, respectively). FW medium was prepared from a concentrated (10x) basal FW medium stock containing NaHCO<sub>3</sub> (25 g/L), NaH<sub>2</sub>PO<sub>4</sub>·H<sub>2</sub>O (0.6g/L), NH<sub>4</sub>Cl (2.5 g/L), and KCl (1.0 g/L). Vitamins were prepared as separate solutions as previously described (3). Trace minerals were prepared as previously described (40), except that ZnSO<sub>4</sub> was replaced with ZnCl<sub>2</sub> (0.13 g/L), and Na<sub>2</sub>WO<sub>4</sub>·2H<sub>2</sub>O (0.025 g/L) was added. FWAF medium contained FW stock (96 ml/L), 0.75 M sodium acetate (20 ml/L), 1 M sodium fumarate (40 ml/L), vitamin

solution (10 ml/L), mineral solution (10 ml/L). The medium was dispensed in pressure tubes or serum bottles, sparged with N<sub>2</sub>:CO<sub>2</sub> (80:20) to remove dissolved oxygen and sealed with butyl rubber stoppers and aluminum tear off seals (Wheaton) prior to autoclaving. Unless otherwise indicated, all cultures were incubated at 30°C.

**Pili induction at suboptimal growth temperatures.** WT controls expressing pili (WT<sub>p+</sub>) were obtained by growing WT cells at suboptimal growth temperatures (25°C). Bacterial pili expression is often thermoregulated (16), an adaptive mechanism that enables bacteria to rapidly assemble the pili in environments where pili functions are advantageous (65). As in other bacteria (57), pili production in *Geobacter* is induced at suboptimal growth temperatures (25°C) mimicking the suboptimal growth conditions that the cells encountered during the reduction of Fe(III) oxides (55). In contrast, growth at 30°C prevented pili assembly and produced a pili-deficient strain WT<sub>p-</sub>.

**U(VI) resting cell suspension assays.** Resting cell suspensions were prepared as described elsewhere (63), except that cells were harvested from mid-*log* phase cultures (OD<sub>600</sub>, 0.3-0.5) and resuspended in 100 ml reaction buffer with 20 mM sodium acetate to a final OD<sub>600</sub> of 0.1. Heat-killed controls were prepared by autoclaving the cultures for 30 min. Suspensions were incubated for 6 h at 30°C with 1 mM uranyl acetate (Electron Microscopy Sciences), as previously described (63). After incubation, 500 µl samples were withdrawn, filtered (0.22-µm Millex-GS filter, Millipore) to separate the cells, acidified in 2% nitric acid (500 µl), and stored at

-20°C. All procedures were performed anaerobically inside a vinyl glove bag (Coy Labs) containing a H<sub>2</sub>:CO<sub>2</sub>:N<sub>2</sub> (7:10:83) atmosphere. The initial and final concentration of U(VI) in the acidified samples was measured using a Platform Inductively Coupled Plasma Mass Spectrometer (ICP-MS) (Micromass, Thermo Scientific) to calculate the amount of U(VI) removed from solution.

**Gene expression analyses by qRT-PCR.** Quantitative reverse-transcriptase PCR (qRT-PCR) was used to quantify *pilA* and *recA* transcripts in RNA extracted from resting cells of the WT<sub>p+</sub> and WT<sub>p-</sub> strains before and after incubation with uranyl acetate for 6 h. WT<sub>p+</sub> controls incubated in the same reaction buffer without uranyl acetate also were included. RNA was extracted using the TRIzol reagent (Invitrogen, Carlsbad, CA), and treated with RQ1 RNase-free DNase (Promega, Madison, WI) according to the manufacturer's instructions. Reverse transcription was performed using Superscript III Reverse Transcriptase (Invitrogen, Carlsbad, CA) following manufacturer's recommendations. Primer pairs RT\_ORF02545\_F and RT\_ORF02545\_R were used for *pilA* (13) and *recA660f* and *recA737r* were used for *recA* (20). For qRT-PCR, the cDNA generated after reverse transcription was diluted 1:1000 in a 25 µl reaction that contained each primer (5 µM) and SYBR Green MasterMix (Applied Biosystems, Foster City, CA), according to the manufacturer's instructions. Samples were amplified using a Bio-Rad (Hercules, CA) iCycler (iQ5 Multicolor Real-Time PCR Detection System). The comparative C<sub>T</sub> method (61) was used to calculate the relative expression of the *pilA* gene using the *recA* constitutive expression as internal control. Briefly, the  $\Delta C_T$  value ( $C_T(pilA) - C_T(recA)$ )

was calculated for triplicate biological replicates before (0 h) and after (6 h) incubation with U(VI) acetate. The average of the difference between the 6 h and 0 h  $C_T$  values was used to calculate the  $\Delta\Delta C_T$ . The relative fold change in *pilA* expression versus the *recA* internal control was calculated with the formula  $2^{-\Delta\Delta C_T}$ .

**TEM and Energy Dispersive Spectroscopy (EDS) analyses.** After U exposure, resting cells were adsorbed onto 300-mesh carbon-coated copper grids (Ted Pella), fixed with 1% glutaraldehyde for 5 min, and washed 3 times with ddH<sub>2</sub>O for 2 min. Unstained cells were directly imaged with a JEOL100CX electron microscope (Japan Electron Optic Laboratory) operated at a 100 kV accelerating voltage. Imaging and elemental analysis of the extracellular uranium precipitates was performed with a JEOL 2200FS operated at 200 kV and an Energy Dispersive Spectroscopy (EDS) detector.

For thin sections, cells were harvested by centrifugation (1,200 x *g*, 30 min, room temperature) and prepared as previously described (43), except that a Power Tome XL (RMC Products, Boeckler Instruments, Tucson, AZ) was used for sample sectioning. Thin sections were imaged with a JEOL100CX operated at 80 kV. Approximately 400-500 cells from randomly taken, thin-sectioned fields were also examined for periplasmic mineralization. A cell was considered to have a mineralized periplasm when it contained both a fully mineralized outer membrane and generalized mineralization in the periplasm and/or inner membrane.

**Pili purification, quantification, and biochemical characterization.** Pili were purified as detergent-insoluble fractions from cells first lysed by sonication and treated with RNase, DNase

and lysozyme enzymes (11). Three biological replicates were used for each strain. Cell membranes and proteins in the extracts were solubilized with sodium dodecyl sulfate (SDS, 1% final concentration) and separated by preparative 12% polyacrylamide gel electrophoresis (5% stacking gel, 40 mA for 5 h) using a Prep Cell 491 apparatus (Bio-Rad). The detergent-insoluble fraction, which did not enter the stacking gel, was recovered by aspiration, washed in ddH<sub>2</sub>O, extracted once with 95% ethanol (Decon Laboratories), and dried in a SpeedVac system (Savant Instruments Inc.) at room temperature for 20 min. The dry sample was resuspended in 1 ml of ddH<sub>2</sub>O and vortexed for 60 seconds to break up large clumps before extracting poorly bound, soluble protein with 0.2 M glycine (pH 1.5, adjusted with HCl; Invitrogen) at 100°C for 10 min. The insoluble fraction was recovered by centrifugation (16,000 x *g*, 25 min, 4°C), washed five times with ddH<sub>2</sub>O, and dried in a SpeedVac at room temperature prior to storage at -20°C. The amount of pili protein was measured after resuspending the dry samples in 10 mM CHES buffer (pH 9.5), incubating at 4°C overnight, and mixing 1:1 with the working reagent solution of the Pierce Microplate BCA protein assay kit (reducing agent compatible, Thermo). The samples were incubated at 60°C for 1h before spectrophotometric measurements. BSA was used as a standard.

For PAGE analyses, dried preparations of purified pili were resuspended in 5 µl of ddH<sub>2</sub>O containing 10% (w/v) Octyl-β-D-Glucopyranoside (OG) (Sigma, 98%) and incubated at room temperature for 2 h. The samples were diluted with 5 volumes of ddH<sub>2</sub>O to reduce the OG

concentration to 2% (v/v) and incubated for an additional 24 h period at room temperature. The OG-treated sample was boiled in SDS-PAGE sample buffer (59) and subjected to electrophoresis through a 10-20% Tris/Tricine ReadyGel (Bio-rad) using a Mini Protean Tetra Cell apparatus (Bio-Rad). After electrophoresis, the gels were silver stained using the Pierce<sup>®</sup> Silver Stain for Mass Spectrometry kit (Thermo Scientific), following the instructions supplied by manufacturer, and scanned. The migration of the molecular mass standards in the gradient gel was estimated and fitted a polynomial distribution ( $R^2 = 0.95523$ ), which was used to calculate the molecular mass of unknown bands. Duplicate gels were also electrophoretically transferred to a PVDF membrane (HyBond LFP, Amersham GE Healthcare) at 25 V for 150 min using a Mini Protean Tetra Cell apparatus (Bio-rad). The Amersham ECL Plex Western blotting kit was used for the electrophoretic transfer and membrane blocking, following manufacturer's recommendations. After blocking, the membrane was incubated in 10 mL antibody diluent solution (90 min, room temperature, gentle agitation) containing a 1:5,000 dilution of the primary antibody (rabbit  $\alpha$ -PilA polyclonal antibodies raised against the 42 C-t amino acids of *G. sulfurreducens* PilA protein) and a 1:2,500 dilution of goat  $\alpha$ -rabbit IgG antibodies conjugated to the Cytm 5 fluorescence dye (ECL<sup>™</sup> Plex, Amersham GE Healthcare). The membrane was washed 4 x 5 minutes in wash buffer (TBS-T, pH 7.4, 0.1% Tween 20) and rinsed three times in wash buffer without Tween 20. The protein bands that hybridized with the primary antibodies were visualized after scanning the membrane blot with a Typhoon imager operated in fluorescence mode (excitation at 633 nm, 670 BP 30 filter, and PMT setting at 600 V). SDS-PAGE and western blotting experiments were performed by Dr. Sanela Lampa-Pastirk.

**Transmission Electron Microscopy (TEM) and Confocal Laser Scanning Microscopy (CLSM) analyses of purified pili.** Detergent-insoluble fractions were examined by TEM and CLSM. For TEM, an aqueous solution of purified pili was adsorbed on a carbon-copper grid (300 Mesh, Electron Microscopy Sciences), negatively stained with 1% (w/v) uranyl acetate in distilled water, and examined with a JEOL 100 CX electron microscope operated at 100 kV. For CLSM, detergent-insoluble fractions were dissolved in phosphate buffer saline (PBS, pH 7), adsorbed onto glass coverslips for 30 min, washed with PBS and fixed with 3.7% paraformaldehyde in PBS. The samples were then incubated for 30 min in PBS-1% BSA, before overnight incubation at 4°C with a 1:100 dilution anti-PilA primary antibody in PBS-1% BSA. After three washes in PBS-1% BSA, the samples were incubated with a 1:1,000 dilution of anti-rabbit antibodies conjugated to the Alexa fluor 488 dye (Molecular Probes, Invitrogen) for 1 h. The coverslips were then washed 3 times with PBS and examined with a Zeiss LSM Pascal confocal microscope equipped with a Plan-Neofluar 63x oil objective (excitation, 488 nm; emission, 505-535 nm). Visualization and antibody detection of purified nanowires was performed by Dr. Sanela Lampa-Pastirk.

**SDS-PAGE and staining of outer membrane, heme-containing proteins.** Outer membrane *c*-cytochromes were mechanically detached from all the strains and isolated as previously described (47). A mutant deficient in the outer membrane *c*-cytochrome OmcS (47) and grown at 25°C was included as a control. Proteins (2.5 µg) in the supernatant fluids were separated by Tris-Glycine denaturing polyacrylamide gel electrophoresis (2) using a 12% Mini-Protean TGX gel (Bio-Rad). The Novex Sharp molecular weight markers (Invitrogen) were used

as standards. Reducing agents were omitted from the SDS-sample buffer and the samples were loaded onto the gel without boiling to prevent the loss of heme groups (68). C-type cytochromes were detected as heme-stained bands using *N,N,N',N'*-tetramethylbenzidine, as previously described (68). After heme-staining, the gels were photographed, destained with 70 mM sodium sulphite (68), and silver-stained for total protein with the Pierce silver stain for Mass Spectrometry (Thermo).

**X-ray Adsorption Spectroscopy (XAS) analyses.** Resting cells incubated with U for 6 h were harvested by centrifugation (13,000 $g$ , 10 min, 4°C) and loaded into custom-made plastic holders, triply packaged in Kapton film and sealed with Kapton tape (DuPont), under anaerobic conditions. Samples were stored at -80°C and kept frozen during XAS measurements, which were performed with a multielement Ge detector in fluorescence mode, using the PNC-CAT beamline 20-BM at the Advanced Photon Source (Argonne National Laboratory) and standard beamline parameters, as described elsewhere (29). XANES measurements were used to calculate the relative amount of U(VI) to U(IV) by linear combination fitting of the spectrum with U(VI) and U(IV) standards. The spectra were energy aligned by simultaneously measured uranyl nitrate standard. The uranium EXAFS spectra were processed using the methods (48) in Athena (54) and were modeled using FEFFIT (66) with theoretically generated models from FEFF 7.02 (74), as described elsewhere (29). Multiple scattering paths from distant C3 and Odist atoms were also included in the model, yet did not have a significant contribution. The coordination number for U-Oax (Noax values) obtained from EXAFS measurements of 3 to 4 biological replicates from at least two independent experiments also was used to estimate the

amount of U(VI) reduced to U(IV) in each sample. For example, a Noax value of 0.3 was obtained for one of the biological replicates of the WT<sub>p+</sub> (as given in Table 2.2). 100% of U(VI) would have a U-Oax coordination number of 2.0. Therefore the amount of U(IV) that corresponds to the WT<sub>p+</sub> Noax is  $0.3/2.0 = 0.15$ . This indicates that there is 15% U(VI) and 85% U(IV) in this sample. Analysis of all data generated through XANES and EXAFS analyses was performed by Dr. Shelly Kelly.

**Vitality and viability assays.** The RedoxSensor Green reagent (Molecular Probes) was used to measure the cell's vitality (broadly defined as the levels of activity of cell's vital reactions) after U exposure. This reagent yields green fluorescence when modified by the bacterial reductases, which are mostly located in the electron transport system of the cell envelope (19, 26). Resting cells were harvested in a microcentrifuge (12,000xg), washed, and resuspended in a 100 µl Tris-Buffered Saline (TBS) before mixing it with an equal volume of a working concentration of the dye. Fluorescence was measured in two biological replicates, with two technical replicates each, using a SpectraMax M5 plate reader (Molecular Devices) with an excitation of 490nm and emission of 520nm. Cell viability after U exposure in comparison to controls without U was assayed by recovering the resting cells in NBAF medium and measuring the length of the *lag* phase, as described before (36). Prior to inoculation, resting cell suspensions were gassed for 15 min with filtered-sterilized air to reoxidize the U deposits (63) without compromising *G. sulfurreducens* viability (36). Cells were harvested by centrifugation (1,200 x g, 5 min), resuspended in 1 ml of wash buffer (final OD<sub>600</sub> of 0.4), and mixed with 10

ml of NBAF in pressure tubes. The cultures were incubated at 25°C and growth was periodically monitored as OD<sub>600</sub>.

## RESULTS

**Expression of pili promotes the extracellular reduction of U(VI).** The correspondence between pili expression and U immobilization was examined by monitoring the removal of U(VI) acetate from solution by resting wild-type cells incubated at 25°C (WT<sub>p+</sub>) or 30°C (WT<sub>p-</sub>) to induce or prevent pili assembly, respectively. Controls with a pilin-deficient mutant (PilA<sup>-</sup>) and its genetically complemented strain (pRG5::*pilA*) were also included. The pilated strains WT<sub>p+</sub> and pRG5::*pilA* removed substantially more U(VI) from solution than the nonpilated strains WT<sub>p-</sub> and PilA<sup>-</sup> (Fig. 2.1, top).

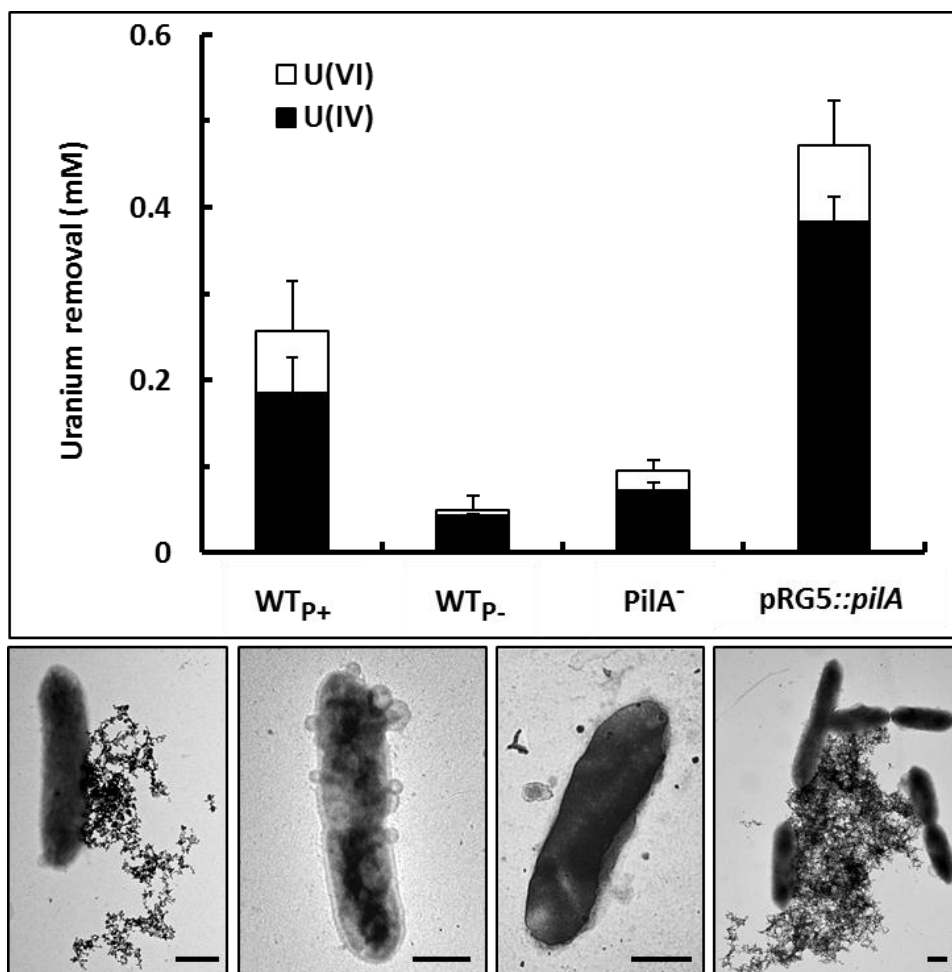


**FIGURE 2.1: Reduction and subcellular localization of U.** Reduction of U(VI) to U(IV) (top) and TEM images (bottom) of unstained whole cells showing the subcellular localization of the U deposits in the WT<sub>p<sup>+</sup></sub>, WT<sub>p<sup>-</sup></sub>, PilA<sup>-</sup>, and pRG5::pilA strains (left to right). Bar, 0.5  $\mu$ m.

The activity was biological in nature, as heat-killed WT<sub>p<sup>+</sup></sub> and WT<sub>p<sup>-</sup></sub> controls did not remove U(VI) significantly ( $0.02 \pm 0.04$  and  $0.05 \pm 0.02$  mM, respectively). X-ray Absorption Near Edge Structure (XANES) spectroscopy confirmed the reductive nature of the U removal activity and measured an average of 70-85% U(IV) in all samples (Fig. 2.1, top). Furthermore, the expression of the *pilA* gene relative to the internal control *recA* did not change during the assay (Fig. 2.2), thus ruling out any *de novo* pilin transcription.

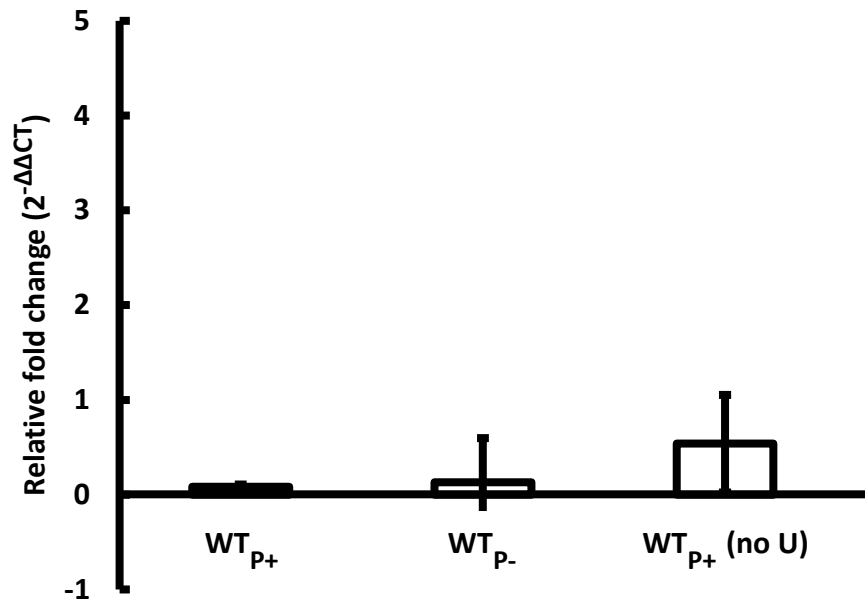


**FIGURE 2.2: Fold change expression of *pilA* relative to *recA* in resting cell suspensions of the  $WT_{p+}$  and  $WT_{p-}$  strains after 6 h of incubation with 1 mM U(VI) acetate. A  $WT_{p+}$  control incubated in reaction buffer without U(VI) acetate also is shown ( $WT_{p+}$  (no U)).**

The extent of U(VI) removal also corresponded well with the levels of piliation, which were measured as the protein content of purified PilA-containing pili samples (Fig. 2.3).

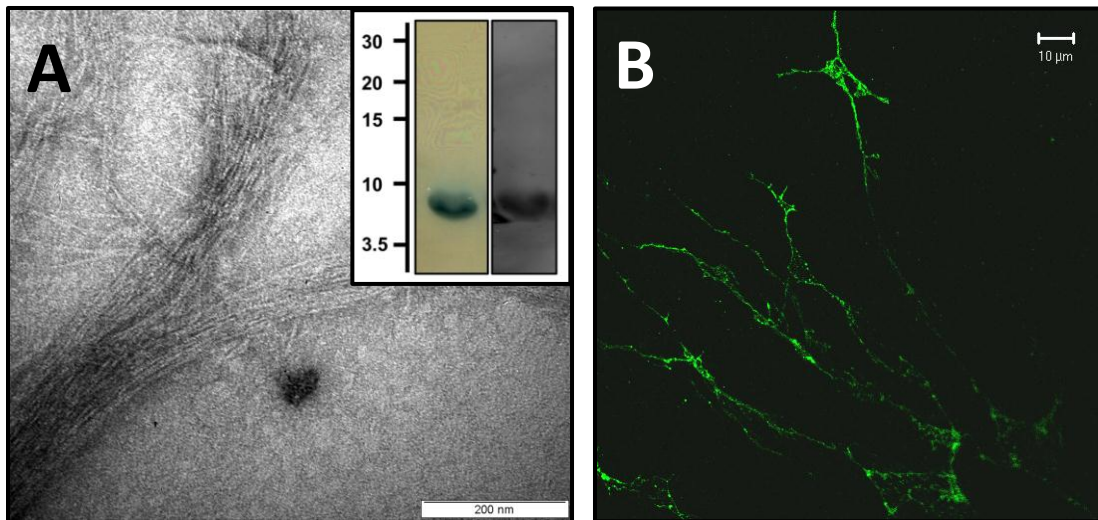


**FIGURE 2.3: Micrographs of purified pilus fibers.** TEM (A) and CLSM (B) micrographs of, respectively, negatively-stained and anti-PilA immunodetected pilus fibers (displayed as green) isolated as detergent-insoluble fractions in the WT<sub>P+</sub>. Inset in (A): SDS-PAGE Tricine gel (left) and Western blot using anti-PilA polyclonal antibodies (right) showing the depolymerization of the purified pili into the PilA peptide subunits. Numbers at left are molecular mass standards in kDa and were used to estimate the apparent mass of the PilA band (6.6 kDa, as predicted for the mature PilA based on amino acid sequence). For interpretation of the references to color in this and all other figures, the reader is referred to the electronic version of this dissertation.

The level of pRG5::*pilA* piliation ( $3.6 \pm 1.7 \mu\text{g pili}/\text{OD}_{600}$ ) was 2.5-fold higher than WT<sub>P+</sub> ( $1.5 \pm 0.1 \mu\text{g}/\text{OD}_{600}$ ), which matched well with its superior capacity to remove U(VI) from solution ( $1.8 \pm 1.0$ -fold higher than WT<sub>P+</sub>). By contrast, WT<sub>P-</sub> and PilA<sup>-</sup> samples had no detectable pili protein and reduced less U(VI).

The location of the U reductase system was studied by examining the cellular localization of the U deposits in unstained whole cells by TEM (Fig. 2.1, bottom). The pilated strains, WT<sub>P+</sub> and pRG5::*pilA*, preferentially deposited the U extracellularly and in a monolateral fashion, consistent with the localization of *Geobacter*'s conductive pili to one side

of the cell (55). The pili filaments were interspersed with the dense deposits (Fig. 2.4, inset).

Elemental composition analyses of the pili-associated deposits by TEM-EDS in the WT<sub>P+</sub>

confirmed the presence of U (Fig. 2.4).

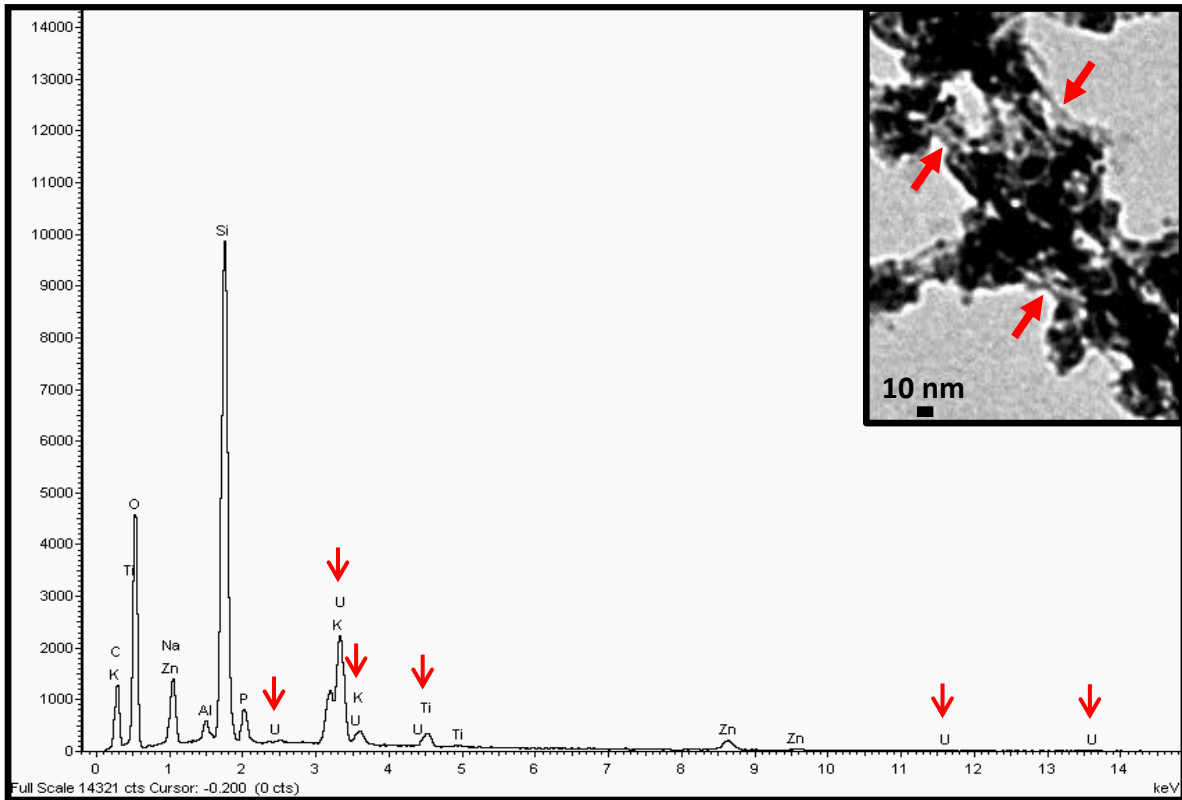


**FIGURE 2.4: Energy dispersive X-ray spectrum of the pili-associated electron-dense deposits imaged by TEM.** Uranium peaks are highlighted with red arrows. Inset shows pili filaments (red arrows) interspersed with the electron-dense uranium deposits. The text in this figure is not meant to be readable, but is for visual reference only.

In contrast, extracellular U mineralization in the non-piliated strains, WT<sub>P-</sub> and PilA<sup>-</sup> was limited to the cell's outer membrane and to membrane vesicles. TEM thin sections of the unstained cells confirmed the presence of extracellular, needle-like U deposits in the pilated strains as well as discrete regions of U deposition on the outer membrane (Fig. 2.5).

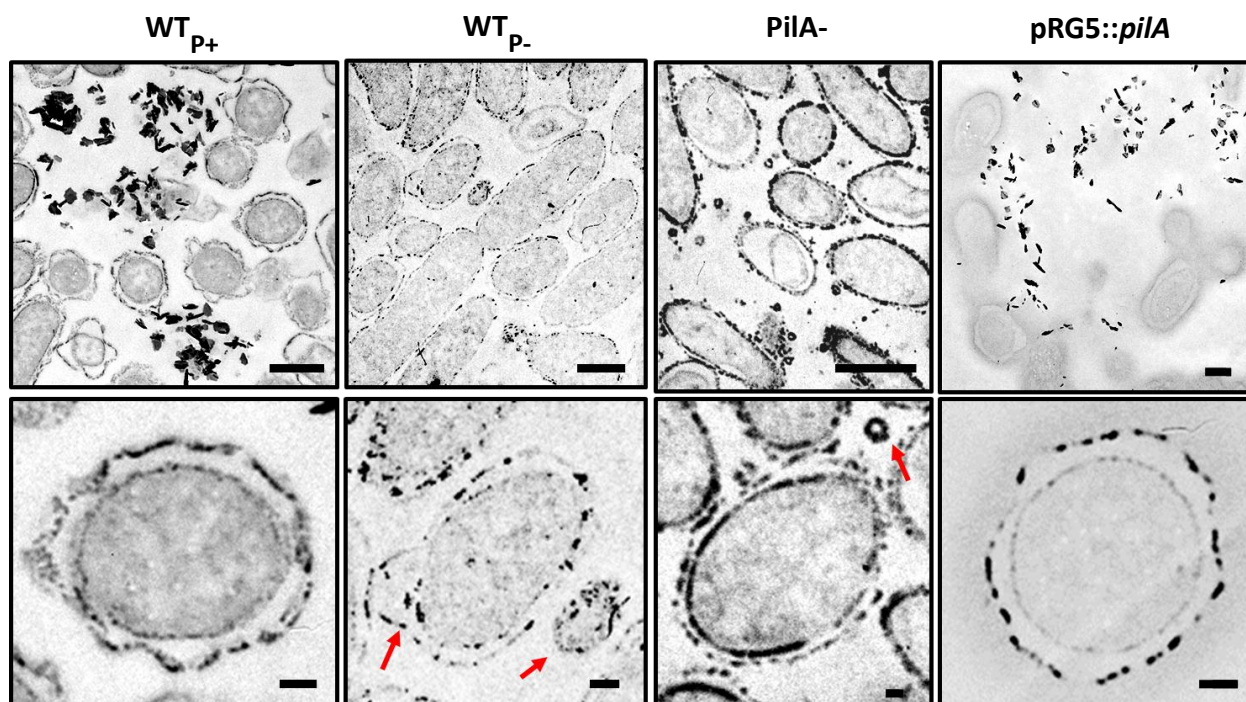


**FIGURE 2.5:** Subcellular localization of uranium deposits by TEM analyses of thin sections of pili-expressing ( $WT_{p+}$  and  $pRG5::pilA$ ) and non-expressing ( $WT_{p-}$  and  $PilA^-$ ) cells. Top panels show large fields (bar, 500 nm) and bottom panels show close-ups of a representative cell (bar, 100 nm). Needle-like extracellular precipitates are noticeable in the top micrographs of the piliated strains, which is consistent with pili-associated uranium deposits. Discrete uranium deposits on the outer membrane are also noticeable in most cells of the  $WT_{p+}$  and  $WT_{p-}$  and in a few cells of the  $pRG5::pilA$  strain, while fully mineralized outer membranes and periplasmic deposition is the observed in most  $PilA^-$  cells (top and bottom panels). Mineralized membrane vesicles budding from the cell ( $WT_{p-}$ ) or detached ( $PilA^-$ ) are indicated with red arrows.

Only a few cells ( $8 \pm 3\%$  of the  $WT_{p+}$  and  $<1\%$  of the  $pRG5::pilA$ ) had periplasmic mineralization.

Outer membrane foci of U deposition were also noticeable in the  $WT_{p-}$  cells, but more cells ( $37 \pm 13\%$  of the cells) had periplasmic deposition. The increased periplasmic mineralization in the  $WT_{p-}$  cannot be attributed to a differential expression of outer membrane *c*-cytochromes, as

outer membrane protein fractions had the same heme profile and content as the WT<sub>P+</sub> (Fig. 2.6).

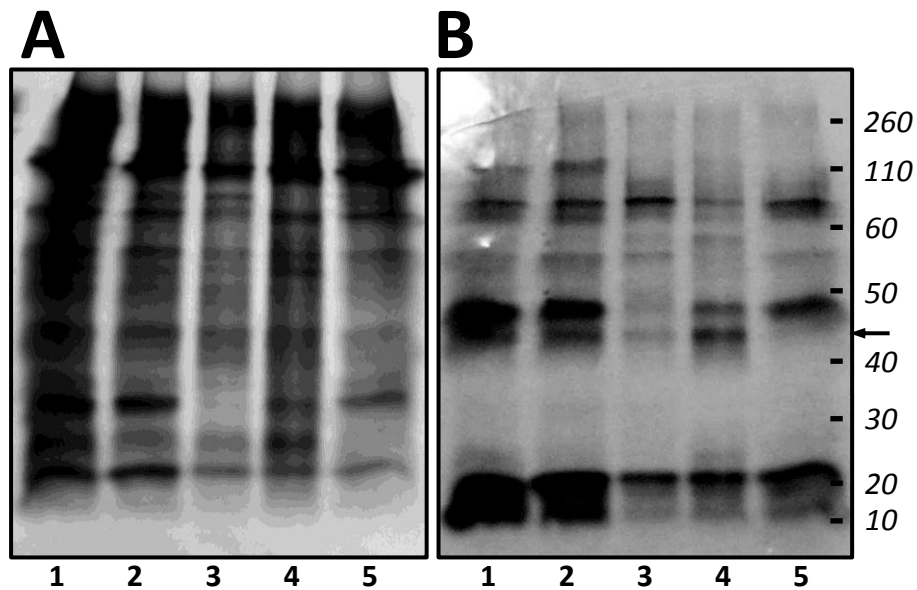


**FIGURE 2.6: SDS-PAGE profiling of mechanically detached outer membrane proteins.** Samples were resolved in 12% (wt/vol) SDS-PAGE gels and silver-stained for total protein (A) and for heme content (B). Approximately 2.5  $\mu\text{g}$  of protein were loaded per lane. Lanes: 1, WT<sub>P+</sub>; 2, WT<sub>P-</sub>; 3, PilA<sup>-</sup> mutant; 4, pRG5::*pilA*; and 5, OmcS<sup>-</sup> mutant. Numbers at right are molecular weight standards in kilodaltons. The migration of the OmcS c-cytochrome is marked with an arrow.

Periplasmic mineralization was more pronounced ( $85 \pm 12\%$  of the cells) in the PilA<sup>-</sup> mutant (Fig. 2.5), which was also partially defective in outer membrane c-cytochrome production (Fig. 2.6). This suggests that outer membrane c-cytochromes also contribute to the extracellular reduction of U(VI). It is unlikely that the outer membrane c-cytochrome OmcS, which has been hypothesized to mediate electron transfer between the conductive pili and metals (35), contributed to the pili-mediated reduction of U, because the pRG5::*pilA* strain expressed OmcS

at wild-type levels (Fig. 2.6) yet reduced more U than the WT<sub>p+</sub> (Fig. 2.1A) and proportionally to the levels of conductive pili assembled. Furthermore, the pRG5::*pilA* strain also had a defect in outer membrane, heme-containing proteins (Fig. 2.6), yet cells had very little U deposition in their cell envelope (Fig. 2.5). This is consistent with the pili functioning as the primary site for U reduction.

**X-ray absorption fine structure (EXAFS) analyses demonstrate the reduction of U(VI) to mononuclear U(IV).** U L<sub>III</sub>-edge EXAFS spectra were modeled to determine the atomic coordination about U and characterize the U(IV) product in all the strains (28). Models for the EXAFS spectra included signals from neighboring P, U, and Fe atoms, but only C neighbors were found to accurately reproduce the measured spectra. The spectra were best described by a mixture of U(IV) and U(VI) coordinated by C-containing ligands. Only the *PilA*<sup>-</sup> mutant required an additional P ligand. A U signal corresponding to the U-U distance in uraninite at 3.87 Å was tested but was inconsistent with the measured spectra. Fig. 2.7 shows the magnitude of the Fourier transformed spectra and models for each spectrum.

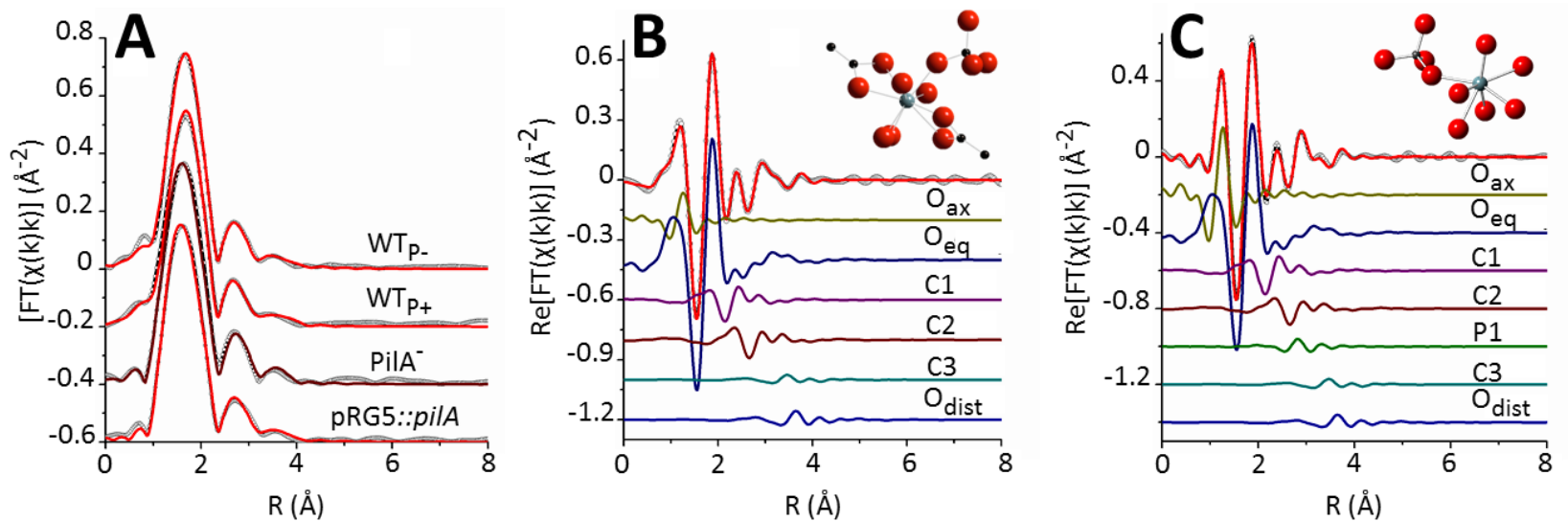


**FIGURE 2.7: U  $L_{III}$ -edge EXAFS spectra and models.** (A) Magnitude of Fourier transform spectra are offset for clarity. Real part of Fourier transform of  $WT_{p+}$  (B) and  $PilA^-$  (C). The components of the model are shown offset beneath the total model. Insets in B and C show the U(IV) moiety that is consistent with the measured EXAFS spectra (U(IV), light grey; O, red; C, black; P, dark grey)

Fig. 2.7B and 2.7C show, as examples, the contribution of each path in the model in the real part of the Fourier transform for the  $WT_{P+}$  and  $PiA^-$  cells and insets show a molecular moiety of the U(IV) atomic environment that is consistent with the measured EXAFS. The  $WT_{P+}$  model includes one C ligand bound to two O atoms of U in a bidentate fashion and followed by a distant C atom (C3) and another C ligand bonded to one O atom of U(IV) in a monodentate fashion and attached to a distant O atom (Odist). This model was simultaneously refined to all spectra and was insufficient to reproduce the  $PiA^-$  spectrum, which required an additional monodentate P ligand (Fig. 2.7C). The distances and  $\sigma^2$  values used to model the spectra are listed in Table 2.1. The coordination numbers (Table 2.2) are consistent with 1 to 2 bidentate C ligands and 2 monodentate C ligands per U atom.

**TABLE 2.1: EXAFS modeling results for  $R$  and  $\sigma^2$ \***

Path	CN	$R$ (Å)	$\sigma^2$ ( $\cdot 10^{-3}$ Å <sup>2</sup> )
Oax	Noax	$1.79 \pm 0.01$	2 <sup>†</sup>
Oeq	Noeq	$2.37 \pm 0.01$	$15 \pm 1$
C1	Nc1	$2.94 \pm 0.01$	$5 \pm 2$
C2	Nc2	$3.43 \pm 0.01$	$5 \pm 2$
Oax1-Oax2	Noax	$3.58 \pm 0.01$	4 <sup>†</sup>
Oax1-U-Oax2	Noax	$3.58 \pm 0.01$	4 <sup>†</sup>
Oax1-U-Oax1	2Noax	$3.58 \pm 0.01$	8 <sup>†</sup>
P1*	Np1	$3.57 \pm 0.05$	$5 \pm 2$
C3	Nc1	$4.41 \pm 0.02$	$5 \pm 2$
C1-C3	2Nc1	$4.41 \pm 0.02$	$5 \pm 2$
C1-C3-C1	Nc1	$4.41 \pm 0.02$	$5 \pm 2$
Odist	Nc2	$4.55 \pm 0.02$	$5 \pm 2$
C2-Odist	2Nc2	$4.58 \pm 0.02$	$5 \pm 2$
C2-Odist-C2	Nc2	$4.60 \pm 0.02$	$5 \pm 2$

CN, coordination number.

<sup>†</sup> Value held.

\*P1A<sup>-</sup> mutant data set only.

**TABLE 2.2: EXAFS modeling results for coordination numbers**

Data set	Noax	Noeq	C1	P1	C2
WT <sub>P+</sub>	$0.3 \pm 0.1$	$7.6 \pm 0.4$	$1.8 \pm 0.3$	-	$2.5 \pm 0.4$
WT <sub>P-</sub>	$0.4 \pm 0.1$	$7.5 \pm 0.3$	$1.7 \pm 0.3$	-	$2.5 \pm 0.4$
P1A <sup>-</sup>	$0.9 \pm 0.1$	$7.1 \pm 0.4$	$2.0 \pm 0.4$	$0.5 \pm 0.3$	$2.3 \pm 0.5$
pRG5:: <i>pilA</i>	$0.8 \pm 0.1$	$7.1 \pm 0.4$	$1.6 \pm 0.3$		$2.3 \pm 0.5$

The number of Oax atoms (Noax) was also used to estimate the amount of U(IV) in these samples, as there are two Oax atoms for each U(VI) atom and none for U(IV) (28). An average of 3-4 replicates for each strain gives the values of  $72 \pm 16\%$  (WT<sub>P+</sub>),  $81 \pm 6\%$  (pRG5::*pilA*),  $85 \pm 5\%$  (WT<sub>P-</sub>), and  $76 \pm 10\%$  (P1A<sup>-</sup>). This provides additional evidence that, while the extent of U(VI)

removal depended on the expression of the pili, the ability of the cells to reduce the immobilized U(VI) to U(IV) did not.

**U reduction via pili as a cellular protective mechanism.** The reverse correlation between piliation and periplasmic mineralization suggested that the pili-mediated reduction prevented U from permeating and being reduced in the periplasm, thus preserving vital functions of the cell envelope. To test this, we used the fluorogenic RedoxSensor<sup>TM</sup> Green dye to measure the vitality (or levels of vital reactions of the cell, in this case the cell's reductase activity) of the strains after U exposure in reference to unexposed controls. The vitality remaining after U exposure was higher in the pilated strains and proportional to the levels of piliation (pRG5::*pilA*>WT<sub>p+</sub>) (Fig. 2.8A).

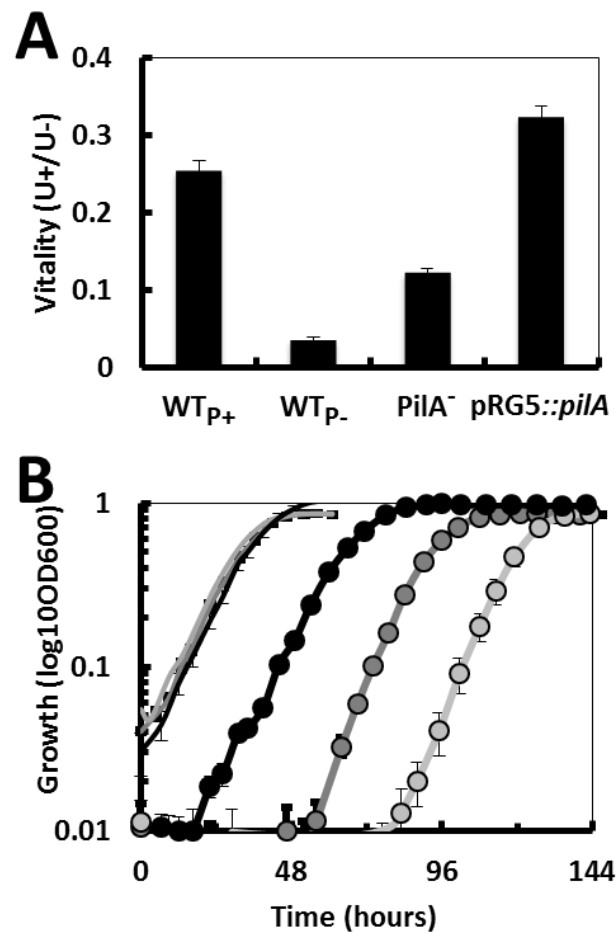


**FIGURE 2.8: Effect of U(VI) exposure on cell vitality and viability.** (A) Vitality was measured as bacterial reductase (respiratory) activity with the RedoxSensor dye in resting cells of the pili-expressing (WT<sub>p+</sub> and *pRG5::pilA*) and non-expressing (WT<sub>p-</sub> and PilA<sup>-</sup>) strains and expressed as the ratio of relative fluorescence units emitted by from cells incubated with (U<sup>+</sup>) or without (U<sup>-</sup>) U. (B) Growth recovery of resting cells of the *pRG5::pilA* (black), WT<sub>p+</sub> (dark gray), and WT<sub>p-</sub> (light gray) after 6 h of U exposure (circles) in comparison to controls without U (lines).

Inasmuch as the RedoxSensor dye can also serve as a proxy for the integrity of the cell envelope and the cell's viability (19), these results suggested that the cell viability was also higher in the piliated strains. To test this, we recovered the resting cells in growth medium and studied the cell's survival (defined as the cell's ability to maintain its integrity and undertake division (4))

after exposure to U as a function of the length of the *lag* phase (Fig. 2.8B). While cells that had not been exposed to U recovered rapidly and simultaneously, the strains exposed to U recovered in a step-wise fashion. The *lag* phase was shortest (~ 18 h) in the hyperpiliated pRG5::*pilA* cells, followed by the WT<sub>P+</sub> (~56 h) and the WT<sub>P-</sub> (~81 h), and correlated well with the levels of periplasmic mineralization of the strains ( $R^2 = 0.947$ ). The PilA<sup>-</sup> mutant recovery was similar to the other non-piliated strain, WT<sub>P-</sub>, yet more variable (*lag* phases ranging from 72 to 82 h). It also grew faster (~9 h doubling time compared to ~11 h for the WT and pRG5::*pilA* strains) than the other strains, which is expected to accelerate recovery. Despite these differences, the survival rates (calculated as the reverse of the length of the *lag* phase) of all the strains followed a linear regression ( $R^2 = 0.908$ ) with the levels of pili protein.

## DISCUSSION

**Physiological relevance of the extracellular reduction of U by *Geobacter's* pili.** Our results show that cells that assembled pili immobilized a greater amount of U and also prevented it from permeating inside the periplasm, where it would have otherwise been reduced nonspecifically by *c*-cytochromes and other low potential electron donors (71). As a result, the extracellular reduction of U via pili also preserved the vital functions of the cell envelope and the cell's viability. This mechanism is consistent with field studies showing that the indigenous *Geobacter* community that is stimulated during *in situ* bioremediation is metabolically active (23, 72) and gains energy for growth from the reduction of Fe(III) oxides (9,

14), a process that requires the expression of the conductive pili (55). We used a temperature-dependent regulatory switch (see *Materials and Methods*) to produce WT controls (WT<sub>p-</sub>) that did not assemble pili, yet had WT levels and profiles of outer membrane cytochromes. The lack of pili in the WT<sub>p-</sub> strain significantly diminished the cell's ability to reduce U(VI), increased the degree of periplasmic mineralization, and reduced the respiratory activity of the cell envelope and the cell's viability. WT<sub>p-</sub> cells also had extensive outer membrane vesiculation, a process linked to the selective detoxification of unwanted periplasmic materials by cells undergoing cell envelope stress (45). Similarly, the inability of a PiliA<sup>-</sup> mutant to produce pili impaired the yields of U reduction. This mutant strain also had reduced outer membrane cytochrome content and, as a result, more U traversed the outer membrane and precipitated in the periplasm. The fact that the pili of *G. sulfurreducens* catalyze the extracellular reductive precipitation of U under physiological conditions conducive to growth, is also in agreement with early studies with *G. metallireducens* suggesting that the reduction of U is extracellular (17) and coupled to cell growth (42). In these studies (17, 42), cells were grown with Fe(III) citrate as an electron acceptor, which are culture conditions that promote pili expression in *G. metallireducens* (10) but not in *G. sulfurreducens* (55). Thus, the extracellular precipitation and sustained removal of U reported for *G. metallireducens* is consistent with pili catalyzing the reaction as well.

**Reduction of U to mononuclear U(IV) phases.** Despite differences in the mechanism and yields of U reduction, the strains with the lowest levels of periplasmic mineralization (WT<sub>p+</sub>, pRG5::*pilA* and WT<sub>p-</sub>) produced similar U L<sub>III</sub>-edge EXAFS spectra that were modeled as

mostly U(IV) coordinated by C-containing ligands in bidentate and monodentate fashion and that lacked any Fe- or P-containing ligands. The bidentate C1-C3 ligand is likely biological in nature as reported for the carboxyl coordinations involving amino acids and lipopolysaccharide sugars (5, 6, 37). In contrast, the  $\text{PilA}^-$  mutant, which had the highest degree of periplasmic mineralization, required an additional monodentate P ligand. This signal was small with a coordination number of  $0.5 \pm 0.3$ , indicating that, on average, 50% of the U atoms contained a P ligand while the other 50% shared the atomic coordination of the other strains. Alternative interpretations such as 25% or 12.5% of U atoms with 2 or 4 P ligands, respectively, are unlikely because the CN values for the C1 and C2 signals did not decrease proportionally (50% and 75%, respectively). It is also unlikely that the low levels of U(VI) reduced by the  $\text{PilA}^-$  strain contributed to the distinct spectra, because  $\text{WT}_{p-}$  cells reduced less U(VI) and did not require a P ligand for U coordination. The P coordination and the generalized periplasmic mineralization observed in the  $\text{PilA}^-$  mutant cells suggest that U(VI) permeated deep and fast into the cell envelope, where it formed carboxyl and phosphoryl coordinated complexes with periplasmic proteins and the peptidoglycan layer (5, 6) and membrane phospholipids (34), respectively.

The formation of a mononuclear U(IV) phase has also been reported for other bacteria of relevance to U bioremediation (7, 15), yet contrasts with earlier reports of uraninite formation by *Geobacter* spp. (17, 62). The chemical composition of the medium can influence the nature of the reduced U mineral (15). We used a bicarbonate buffer and conditions used in previous studies with *G. sulfurreducens* (63), whereas studies reporting uraninite formation used PIPES-buffered solutions (62) or bicarbonate-buffered uncontaminated groundwater (17).

Evidence for the microbial reduction of U(VI) to non-uraninite U(IV) products is also emerging from field-scale studies (7, 29), whereas uraninite formation has been linked to conditions of reduced bioreducing activities (27, 30). This suggests that abiotic factors may contribute to the formation of uraninite.

**Model for the reduction of U(VI) by *Geobacter* bacteria.** The direct correspondence observed between piliation, extent of U(VI) reduction, cell envelope respiratory activities and cell viability support a model in which the conductive pili function as the primary mechanism for U reduction and cellular protection (Fig. 2.9).

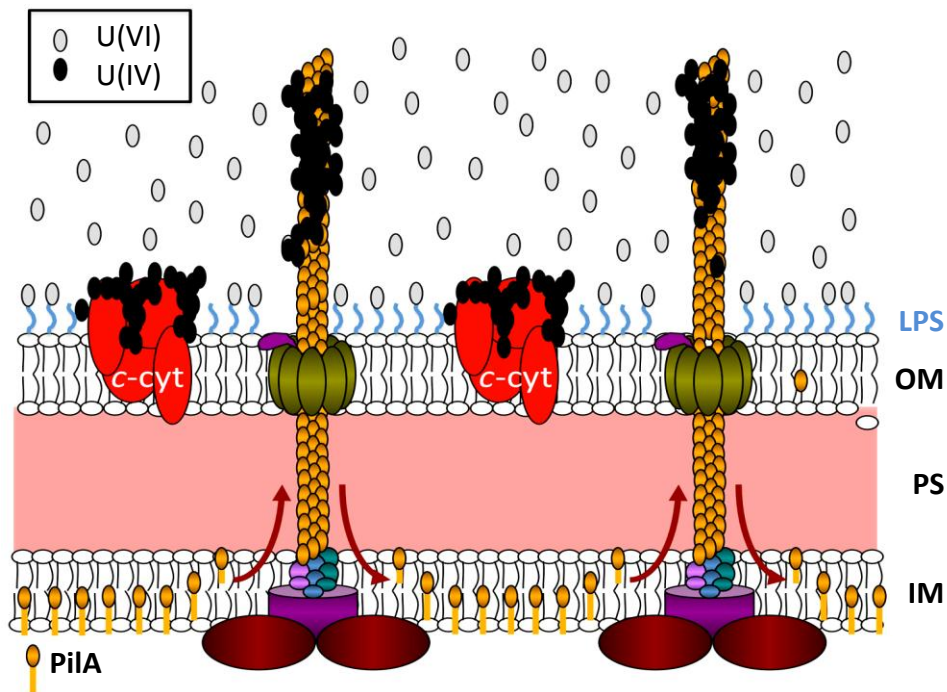


**FIGURE 2.9: Model for the extracellular reduction of U(VI) to U(IV).** Conductive pili function as primary uranium reductases, with c-cytochrome foci (c-cyt) as secondary reduction sites. IM, inner membrane; PS, periplasmic space; OM, outer membrane; LPS, lipopolysaccharide; PiIA, pilin subunit.

Pili can reach several  $\mu\text{m}$  in length, thereby increasing the redox-active surface area available for binding and reducing U(VI) outside the cell. Although most of the U reduced by the pilated

cells was extracellular and associated with the pili, discrete regions of the outer membrane also participated in the reduction of U. In *G. sulfurreducens* most of the redox activity of the outer membrane is provided by abundant *c*-cytochromes that decorate the cell surface as defined foci (52). Thus, they could provide a mechanism for reducing U in localized regions of the membrane and preventing it from permeating into the periplasm. In support of this, the PilA<sup>-</sup> mutant cells, which had reduced outer membrane cytochrome content, preferentially reduced U in the periplasm. Some of the most abundant metalloproteins on the outer membrane of *G. sulfurreducens* also are loosely bound to and easily detach from the membrane (46, 47, 52), providing a natural mechanism for releasing the U deposits. Some of these cytochromes also may be anchored to a recently identified exopolysaccharide matrix (56), which may promote the extracellular reduction of U. Furthermore, although some areas of the outer membrane were devoid of U reductase activity, U(VI) was effectively prevented from permeating into the periplasm. The outer leaflet of the outer membrane of Gram-negative bacteria is mostly composed of lipopolysaccharide (LPS), which acts as an efficient permeability barrier against soluble toxic compounds (53). *G. sulfurreducens* produces a rough LPS, i.e., it is composed of lipid A and a core oligosaccharide but lacks the *O*-antigen (69). The core oligosaccharide is the most highly charged region of the LPS and is stabilized by metallic cations (60). Models suggest that rough LPS preferentially chelates and immobilizes uranyl ions over other ions (37) and produces carboxyl and hydroxyl coordinations (37), which is consistent with the C and O ligands modeled from the EXAFS spectra. This suggests that the rough LPS of *G. sulfurreducens* also functions as a protective barrier to prevent U(VI) from penetrating in the cell envelope.

**Implications for the *in situ* bioremediation of U.** An insufficient knowledge of the biological mechanisms of contaminant transformation often limits the performance of *in situ* subsurface bioremediation and long-term stewardship strategies. The identification of *Geobacter's* pili as their primary U reductase provides a much-needed, fundamental mechanistic understanding of U reduction by *Geobacter* spp. required to design effective *in situ* bioremediation strategies. Analyses of transcript abundance for key *Geobacteraceae* genes are useful tools to predict the metabolic and physiological state of *Geobacter* bacteria during *in situ* bioremediation (21-24), yet provide no information about the mechanism of U bioreduction. However, similar tools could be applied to monitor the activity of conserved components of *Geobacter's* pilus apparatus to assess the effectiveness of *in situ* bioremediation schemes. The possibility that conductive appendages such as the pili of *Geobacter* are a widespread mechanism for U reduction also warrants special attention. The production of conductive appendages has been demonstrated in another U-reducing bacterium, *Shewanella oneidensis* (18). Furthermore, nanowire-mediated electrical currents have been proposed to couple spatially separated geochemical processes in sediments (50). The extracellular needle-like U deposits observed in TEM thin sections of the piliated strains of *G. sulfurreducens* (Fig. 2.5) also resembled the uraninite structures of *Desulfovibrio desulfuricans* biofilms (44), which some authors have suggested represent mineralized nanowire-like appendages (71). Thus, the contribution of microbial nanowires to U reduction may be significant and, therefore, relevant for the optimization of *in situ* bioremediation strategies.

## REFERENCES

## REFERENCES

1. **Anderson, R. T., H. A. Vrionis, I. Ortiz-Bernad, C. T. Resch, P. E. Long, R. Dayvault, K. Karp, S. Marutzky, D. R. Metzler, A. Peacock, D. C. White, M. Lowe, and D. R. Lovley.** 2003. Stimulating the in situ activity of *Geobacter* species to remove uranium from the groundwater of a uranium-contaminated aquifer. *Appl. Environ. Microbiol.* **69**:5884-5891.
2. **Ausubel, F. M., R. Brent, R. E. Kingston, D. D. Moore, J. G. Seidman, J. A. Smith, and K. Struhl (ed.).** 1995. *Current protocols in Molecular Biology*, vol. 2. John Wiley & Sons, Inc.
3. **Balch, W. E., G. E. Fox, L. J. Magrum, C. R. Woese, and R. S. Wolfe.** 1979. Methanogens: reevaluation of a unique biological group. *Microbiol. Rev.* **43**:260-296.
4. **Barer, M. R., and C. R. Harwood.** 1999. Bacterial viability and culturability. *Adv. Microb. Physiol.* **41**:93-137.
5. **Barkleit, A., H. Moll, and G. Bernhard.** 2009. Complexation of uranium(VI) with peptidoglycan. *Dalton Trans.*:5379-5385.
6. **Benavides-Garcia, M. G., and K. Balasubramanian.** 2009. Structural insights into the binding of uranyl with human serum protein apotransferrin. Structure and spectra of protein-uranyl interactions. *Chem. Res. Toxicol.* **22**:1613-1621.
7. **Bernier-Latmani, R., H. Veeramani, E. D. Vecchia, P. Junier, J. S. Lezama-Pacheco, E. I. Suvorova, J. O. Sharp, N. S. Wigginton, and J. R. Bargar.** 2010. Non-uraninite products of microbial U(VI) reduction. *Environ. Sci. Technol.* **44**:9456-9462.
8. **Butler, J. E., N. D. Young, and D. R. Lovley.** 2010. Evolution of electron transfer out of the cell: comparative genomics of six *Geobacter* genomes. *BMC genomics* **11**:40.
9. **Chang, Y. J., P. E. Long, R. Geyer, A. D. Peacock, C. T. Resch, K. Sublette, S. Pfiffner, A. Smithgall, R. T. Anderson, H. A. Vrionis, J. R. Stephen, R. Dayvault, I. Ortiz-Bernad, D. R. Lovley, and D. C. White.** 2005. Microbial incorporation of <sup>13</sup>C-labeled acetate at the field scale: detection of microbes responsible for reduction of U(VI). *Environ. Sci. Technol.* **39**:9039-9048.
10. **Childers, S. E., S. Ciuffo, and D. R. Lovley.** 2002. *Geobacter metallireducens* accesses insoluble Fe(III) oxide by chemotaxis. *Nature* **416**:767-769.
11. **Collinson, S. K., L. Emody, K. H. Muller, T. J. Trust, and W. W. Kay.** 1991. Purification and characterization of thin, aggregative fimbriae from *Salmonella enteritidis*. *J. Bacteriol.* **173**:4773-4781.

12. **Coppi, M. V., C. Leang, S. J. Sandler, and D. R. Lovley.** 2001. Development of a genetic system for *Geobacter sulfurreducens*. *Appl. Environ. Microbiol.* **67**:3180-3187.
13. **Davey, M. E., and M. J. Duncan.** 2006. Enhanced biofilm formation and loss of capsule synthesis: deletion of a putative glycosyltransferase in *Porphyromonas gingivalis*. *J Bacteriol* **188**:5510-5523.
14. **Finneran, K. T., R. T. Anderson, K. P. Nevin, and D. R. Lovley.** 2002. Potential for Bioremediation of uranium-contaminated aquifers with microbial U(VI) reduction. *Soil & Sediment Contamination* **11**:339-357.
15. **Fletcher, K. E., M. I. Boyanov, S. H. Thomas, Q. Wu, K. M. Kemner, and F. E. Loffler.** 2010. U(VI) reduction to mononuclear U(IV) by *Desulfitobacterium* species. *Environ. Sci. Technol.* **44**:4705-4709.
16. **Goransson, M., K. Forsman, and B. E. Uhlin.** 1989. Regulatory genes in the thermoregulation of *Escherichia coli* pili gene transcription. *Genes Dev.* **3**:123-130.
17. **Gorby, Y. A., and D. R. Lovley.** 1992. Enzymatic uranium precipitation. *Environ. Sci. Technol.* **26**:205-207.
18. **Gorby, Y. A., S. Yanina, J. S. McLean, K. M. Rosso, D. Moyles, A. Dohnalkova, T. J. Beveridge, I. S. Chang, B. H. Kim, K. S. Kim, D. E. Culley, S. B. Reed, M. F. Romine, D. A. Saffarini, E. A. Hill, L. Shi, D. A. Elias, D. W. Kennedy, G. Pinchuk, K. Watanabe, S. Ishii, B. Logan, K. H. Nealson, and J. K. Fredrickson.** 2006. Electrically conductive bacterial nanowires produced by *Shewanella oneidensis* strain MR-1 and other microorganisms. *Proc. Natl. Acad. Sci. USA* **103**:11358-11363.
19. **Gray, D., R. S. Yue, C. Y. Chueng, and W. Godfrey.** 2005. Bacterial vitality detected by a novel fluorogenic redox dye using flow cytometry.
20. **Holmes, D. E., S. K. Chaudhuri, K. P. Nevin, T. Mehta, B. A. Methe, A. Liu, J. E. Ward, T. L. Woodard, J. Webster, and D. R. Lovley.** 2006. Microarray and genetic analysis of electron transfer to electrodes in *Geobacter sulfurreducens*. *Environ. Microbiol.* **8**:1805-1815.
21. **Holmes, D. E., T. Mester, R. A. O'Neil, L. A. Perpetua, M. J. Larrahondo, R. Glaven, M. L. Sharma, J. E. Ward, K. P. Nevin, and D. R. Lovley.** 2008. Genes for two multicopper proteins required for Fe(III) oxide reduction in *Geobacter sulfurreducens* have different expression patterns both in the subsurface and on energy-harvesting electrodes. *Microbiology* **154**:1422-1435.
22. **Holmes, D. E., K. P. Nevin, and D. R. Lovley.** 2004. In situ expression of *nifD* in *Geobacteraceae* in subsurface sediments. *Appl. Environ. Microbiol.* **70**:7251-7259.

23. **Holmes, D. E., K. P. Nevin, R. A. O'Neil, J. E. Ward, L. A. Adams, T. L. Woodard, H. A. Vrionis, and D. R. Lovley.** 2005. Potential for quantifying expression of the *Geobacteraceae* citrate synthase gene to assess the activity of *Geobacteraceae* in the subsurface and on current-harvesting electrodes. *Appl. Environ. Microbiol.* **71**:6870-6877.
24. **Holmes, D. E., R. A. O'Neil, M. A. Chavan, L. A. N'Guessan, H. A. Vrionis, L. A. Perpetua, M. J. Larrahondo, R. DiDonato, A. Liu, and D. R. Lovley.** 2009. Transcriptome of *Geobacter uraniireducens* growing in uranium-contaminated subsurface sediments. *ISME J.* **3**:216-230.
25. **Istok, J. D., J. M. Senko, L. R. Krumholz, D. Watson, M. A. Bogle, A. Peacock, Y. J. Chang, and D. C. White.** 2004. *In situ* bioreduction of technetium and uranium in a nitrate-contaminated aquifer. *Environ. Sci. Technol.* **38**:468-475.
26. **Kalyuzhnaya, M. G., M. E. Lidstrom, and L. Chistoserdova.** 2008. Real-time detection of actively metabolizing microbes by redox sensing as applied to methylotroph populations in Lake Washington. *ISME J.* **2**:696-706.
27. **Kelly, S. D., D. Hesterberg, and B. Ravel.** 2008. Analysis of soils and minerals using X-ray absorption spectroscopy., p. 367-463. *In* A. L. Ulery and L. R. Drees (ed.), *Methods of soil analysis; Part 5: Mineralogical methods*. Soil Science Society of America, Madison, WI.
28. **Kelly, S. D., K. M. Kemner, M. I. Boyanov, E. J. O'Loughlin, B. H. Jeon, M. O. Barnett, W. D. Burgos, B. A. Dempsey, and E. E. Roden.** 2005. Comparison of U Valence State Ratio Determined from U L3-Edge XANES to EXAFS Measurements. *Advanced Photon Source Activity Report 2003*.
29. **Kelly, S. D., K. M. Kemner, J. Carley, C. Criddle, P. M. Jardine, T. L. Marsh, D. Phillips, D. Watson, and W. M. Wu.** 2008. Speciation of uranium in sediments before and after *in situ* biostimulation. *Environ. Sci. Technol.* **42**:1558-1564.
30. **Kelly, S. D., W. M. Wu, F. Yang, C. S. Criddle, T. L. Marsh, E. J. O'Loughlin, B. Ravel, D. Watson, P. M. Jardine, and K. M. Kemner.** 2010. Uranium transformations in static microcosms. *Environ. Sci. Technol.* **44**:236-242.
31. **Kim, B. C., C. Leang, Y. H. Ding, R. H. Glaven, M. V. Coppi, and D. R. Lovley.** 2005. OmcF, a putative c-Type monoheme outer membrane cytochrome required for the expression of other outer membrane cytochromes in *Geobacter sulfurreducens*. *J. Bacteriol.* **187**:4505-4513.
32. **Kim, B. C., and D. R. Lovley.** 2008. Investigation of direct vs. indirect involvement of the c-type cytochrome MacA in Fe(III) reduction by *Geobacter sulfurreducens*. *FEMS Microbiol. Lett.* **286**:39-44.

33. **Kim, B. C., X. Qian, C. Leang, M. V. Coppi, and D. R. Lovley.** 2006. Two putative *c*-type multiheme cytochromes required for the expression of OmcB, an outer membrane protein essential for optimal Fe(III) reduction in *Geobacter sulfurreducens*. *J. Bacteriol.* **188**:3138-3142.
34. **Koban, A., and G. Bernhard.** 2007. Uranium(VI) complexes with phospholipid model compounds--a laser spectroscopic study. *J. Inorg. Biochem.* **101**:750-757.
35. **Leang, C., X. Qian, T. Mester, and D. R. Lovley.** 2010. Alignment of the *c*-type cytochrome OmcS along pili of *Geobacter sulfurreducens*. *Appl. Environ. Microbiol.* **76**:4080-4084.
36. **Lin, W. C., M. V. Coppi, and D. R. Lovley.** 2004. *Geobacter sulfurreducens* can grow with oxygen as a terminal electron acceptor. *Appl. Environ. Microbiol.* **70**:2525-2528.
37. **Lins, R. D., E. R. Vorpapel, M. Guglielmi, and T. P. Straatsma.** 2008. Computer simulation of uranyl uptake by the rough lipopolysaccharide membrane of *Pseudomonas aeruginosa*. *Biomacromolecules* **9**:29-35.
38. **Lloyd, J. R., J. Chesnes, S. Glasauer, D. J. Bunker, F. R. Livens, and D. R. Lovley.** 2002. Reduction of actinides and fission products by Fe(III)-reducing bacteria. *Geomicrobiol. J.* **19**:103-120.
39. **Lovley, D. R.** 2001. Bioremediation. Anaerobes to the rescue. *Science* **293**:1444-1446.
40. **Lovley, D. R., R. C. Greening, and J. G. Ferry.** 1984. Rapidly growing rumen methanogenic organism that synthesizes coenzyme M and has a high affinity for formate. *Appl. Environ. Microbiol.* **48**:81-87.
41. **Lovley, D. R., and E. J. P. Phillips.** 1988. Novel mode of microbial energy metabolism: organic carbon oxidation coupled to dissimilatory reduction of iron or manganese. *Appl. Environ. Microbiol.* **54**:1472-1480.
42. **Lovley, D. R., E. J. P. Phillips, Y. A. Gorby, and E. R. Landa.** 1991. Microbial reduction of uranium. *Nature* **350**:413-416.
43. **Marshall, M. J., A. S. Beliaev, A. C. Dohnalkova, D. W. Kennedy, L. Shi, Z. Wang, M. I. Boyanov, B. Lai, K. M. Kemner, J. S. McLean, S. B. Reed, D. E. Culley, V. L. Bailey, C. J. Simonson, D. A. Saffarini, M. F. Romine, J. M. Zachara, and J. K. Fredrickson.** 2006. *c*-Type cytochrome-dependent formation of U(IV) nanoparticles by *Shewanella oneidensis*. *PLoS Biol.* **4**:e268.
44. **Marsili, E., H. Beyenal, L. Di Palma, C. Merli, A. Dohnalkova, J. E. Amonette, and Z. Lewandowski.** 2005. Uranium removal by sulfate reducing biofilms in the presence of carbonates. *Wat. Sci. Technol.* **52**:49-55.

45. **McBroom, A. J., and M. J. Kuehn.** 2007. Release of outer membrane vesicles by Gram-negative bacteria is a novel envelope stress response. *Mol. Microbiol.* **63**:545-558.
46. **Mehta, T., S. E. Childers, R. Glaven, D. R. Lovley, and T. Mester.** 2006. A putative multicopper protein secreted by an atypical type II secretion system involved in the reduction of insoluble electron acceptors in *Geobacter sulfurreducens*. *Microbiology* **152**:2257-2264.
47. **Mehta, T., M. V. Coppi, S. E. Childers, and D. R. Lovley.** 2005. Outer membrane *c*-type cytochromes required for Fe(III) and Mn(IV) oxide reduction in *Geobacter sulfurreducens*. *Appl. Environ. Microbiol.* **71**:8634-8641.
48. **Newville, M.** 2001. IFEFFIT: Interactive EXAFS analysis and FEFF fitting. *J. Synch. Rad.* **8**:322-324.
49. **Ng, S. Y., B. Chaban, and K. F. Jarrell.** 2006. Archaeal flagella, bacterial flagella and type IV pili: a comparison of genes and posttranslational modifications. *J. Mol. Microbiol. Biotechnol.* **11**:167-191.
50. **Nielsen, L. P., N. Risgaard-Petersen, H. Fossing, P. B. Christensen, and M. Sayama.** 2010. Electric currents couple spatially separated biogeochemical processes in marine sediment. *Nature* **463**:1071-1074.
51. **North, N. N., S. L. Dollhopf, L. Petrie, J. D. Istok, D. L. Balkwill, and J. E. Kostka.** 2004. Change in bacterial community structure during in situ biostimulation of subsurface sediment cocontaminated with uranium and nitrate. *Appl. Environ. Microbiol.* **70**:4911-4920.
52. **Qian, X., G. Reguera, T. Mester, and D. R. Lovley.** 2007. Evidence that OmcB and OmpB of *Geobacter sulfurreducens* are outer membrane surface proteins. *FEMS Microbiol. Lett.* **277**:21-27.
53. **Raetz, C. R., and C. Whitfield.** 2002. Lipopolysaccharide endotoxins. *Annu. Rev. Biochem.* **71**:635-700.
54. **Ravel, B., and M. Newville.** 2005. ATHENA, ARTEMIS, HEPHAESTUS: Data analysis for X-ray absorption. *J. Synch. Rad.* **12**:537-541.
55. **Reguera, G., K. D. McCarthy, T. Mehta, J. S. Nicoll, M. T. Tuominen, and D. R. Lovley.** 2005. Extracellular electron transfer via microbial nanowires. *Nature* **435**:1098-1101.
56. **Rollefson, J. B., C. S. Stephen, M. Tien, and D. R. Bond.** 2011. Identification of an extracellular polysaccharide network essential for cytochrome anchoring and biofilm formation in *Geobacter sulfurreducens*. *J. Bacteriol.* **193**:1023-1033.

57. **Sahu, S. N., S. Acharya, H. Tuminaro, I. Patel, K. Dudley, J. E. LeClerc, T. A. Cebula, and S. Mukhopadhyay.** 2003. The bacterial adaptive response gene, *barA*, encodes a novel conserved histidine kinase regulatory switch for adaptation and modulation of metabolism in *Escherichia coli*. *Mol. Cell Biochem.* **253**:167-177.
58. **Sanford, R. A., Q. Wu, Y. Sung, S. H. Thomas, B. K. Amos, E. K. Prince, and F. E. Loffler.** 2007. Hexavalent uranium supports growth of *Anaeromyxobacter dehalogenans* and *Geobacter* spp. with lower than predicted biomass yields. *Environ. Microbiol.* **9**:2885-2893.
59. **Schagger, H., and G. von Jagow.** 1987. Tricine-sodium dodecyl sulfate-polyacrylamide gel electrophoresis for the separation of proteins in the range from 1 to 100 kDa. *Anal. Biochem.* **166**:368-379.
60. **Schindler, M., and M. J. Osborn.** 1979. Interaction of divalent cations and polymyxin B with lipopolysaccharide. *Biochemistry* **18**:4425-4430.
61. **Schmittgen, T. D., and K. J. Livak.** 2008. Analyzing real-time PCR data by the comparative C<sub>T</sub> method. *Nat. Protoc.* **3**:1101-1108.
62. **Sharp, J. O., E. J. Schofield, H. Veeramani, E. I. Suvorova, D. W. Kennedy, M. J. Marshall, A. Mehta, J. R. Bargar, and R. Bernier-Latmani.** 2009. Structural similarities between biogenic uraninites produced by phylogenetically and metabolically diverse bacteria. *Environ. Sci. Technol.* **43**:8295-8301.
63. **Shelobolina, E. S., M. V. Coppi, A. A. Korenevsky, L. N. DiDonato, S. A. Sullivan, H. Konishi, H. Xu, C. Leang, J. E. Butler, B. C. Kim, and D. R. Lovley.** 2007. Importance of *c*-Type cytochromes for U(VI) reduction by *Geobacter sulfurreducens*. *BMC Microbiol.* **7**:16.
64. **Silhavy, T. J., D. Kahne, and S. Walker.** 2010. The bacterial cell envelope. *Cold Spring Harb. Perspect. Biol.* **2**:a000414.
65. **Silverman, M., R. Belas, and M. Simon.** 1984. Genetic control of bacterial adhesion, p. 95-107. *In* K. C. Marshall (ed.), *Microbial adhesion and aggregation*. Springer-Verlag, Berlin.
66. **Stern, E. A., and S. M. Heald.** 1983. Basic principles and applications of EXAFS, p. 995-1014. *In* E. E. Koch (ed.), *Handbook of Synchrotron Radiation*, vol. 10. North-Holland, New York.
67. **Strom, M. S., and S. Lory.** 1993. Structure-function and biogenesis of the type IV pili. *Annu. Rev. Microbiol.* **47**:565-596.

68. **Thomas, P. E., D. Ryan, and W. Levin.** 1976. An improved staining procedure for the detection of the peroxidase activity of cytochrome P-450 on sodium dodecyl sulfate polyacrylamide gels. *Anal. Biochem.* **75**:168-176.
69. **Vinogradov, E., A. Korenevsky, D. R. Lovley, and T. J. Beveridge.** 2004. The structure of the core region of the lipopolysaccharide from *Geobacter sulfurreducens*. *Carbohydr. Res.* **339**:2901-2904.
70. **Wall, D., and D. Kaiser.** 1999. Type IV pili and cell motility. *Mol. Microbiol.* **32**:1-10.
71. **Wall, J. D., and L. R. Krumholz.** 2006. Uranium reduction. *Annu. Rev. Microbiol.* **60**:149-166.
72. **Wilkins, M. J., N. C. Verberkmoes, K. H. Williams, S. J. Callister, P. J. Mouser, H. Elifantz, L. N'Guessan A, B. C. Thomas, C. D. Nicora, M. B. Shah, P. Abraham, M. S. Lipton, D. R. Lovley, R. L. Hettich, P. E. Long, and J. F. Banfield.** 2009. Proteogenomic monitoring of *Geobacter* physiology during stimulated uranium bioremediation. *Appl. Environ. Microbiol.* **75**:6591-6599.
73. **Wu, W. M., J. Carley, T. Gentry, M. A. Ginder-Vogel, M. Fienen, T. Mehlhorn, H. Yan, S. Carroll, M. N. Pace, J. Nyman, J. Luo, M. E. Gentile, M. W. Fields, R. F. Hickey, B. Gu, D. Watson, O. A. Cirpka, J. Zhou, S. Fendorf, P. K. Kitanidis, P. M. Jardine, and C. S. Criddle.** 2006. Pilot-scale in situ bioremediation of uranium in a highly contaminated aquifer. 2. Reduction of U(VI) and geochemical control of U(VI) bioavailability. *Environ. Sci. Technol.* **40**:3986-3995.
74. **Zabinsky, S. I., J. J. Rehr, A. Ankudinov, R. C. Albers, and M. J. Eller.** 1995. Multiple-scattering calculations of X-ray-absorption spectra. *Phys. Rev. B* **52**:2995-3009.

## CHAPTER 3

### THE ROLE OF *GEOBACTER SULFURREDUCTENS* BIOFILMS IN THE IMMOBILIZATION AND REDUCTION OF URANIUM

The following individuals contributed to the work presented in this chapter:

**Allison Speers:** Analysis of COMSTAT data, collaborated on U experiments

**Blair Bullard:** Assisted with the development of biofilm and U assays

**Shelly Kelly (EXAFS Analysis):** EXAFS experiments and data analysis

## ABSTRACT

Biofilms formed by dissimilatory metal reducers are of interest to develop permeable biobarriers for the immobilization and reductive precipitation of soluble contaminants such as uranium. Thus, we studied the kinetics of U(VI) removal and reduction by biofilms formed by the metal-reducing bacterium *Geobacter sulfurreducens*. The biofilms removed twofold more U(VI) from solution than planktonic cells, and linearly for up to 24 h. Despite the prolonged exposure to uranium, the biofilm cells were viable and active, as indicated by their respiratory activity, which was higher than in control biofilms not exposed to uranium. Furthermore, we measured similar respiratory activities in cells from biofilms exposed to concentrations of uranium as high as 2.5 mM, and approximately 70% of this activity was still detected in biofilm cells exposed to 5mM concentrations for 24 h. Thus, the biofilms were able to maintain their redox activities despite the high concentrations of uranium and prolonged exposure. The ability to remove U(VI) from solution was similar in monolayered and multilayered biofilms and was not proportional to increases in biofilm biomass and thickness. Hence, the ability to remove uranium depended on the area of the biofilm that was exposed to the soluble contaminant. By contrast, the reduction of uranium increased as the biofilms grew in biomass and height and was dependent on the expression of *Geobacter* conductive pili. As with pili-expressing planktonic cells, the reduced uranium mineral associated with the biofilms was a mononuclear U(IV) phase involving carbon ligands. Taken together these results demonstrate that the stage of biofilm development, as well as the specific components expressed at that stage determines its contribution to U transformations.

## INTRODUCTION

Since World War II uranium (U) has been mined extensively for its use in nuclear weapons, and as a power source, resulting in the production of significant amounts of contaminated groundwater and sediment worldwide (1, 18). One remediation strategy that has shown promise is the stimulation of the native microbial community *in situ*. With the addition of an electron donor, the native microbes are able to reduce soluble U(VI) to sparingly soluble U(IV), thus preventing migration of the contaminant in groundwater (2, 9, 20, 31, 43). Concurrent with the reduction of U(VI) is the enrichment the *Geobacteraceae* family of dissimilatory metal-reducing organisms (2, 9, 31, 42).

The energy for growth of the *Geobacteraceae* during *in situ* bioremediation comes from the reduction of Fe(III) oxides, an electron acceptor more prevalent than U in the subsurface (13). The reduction of Fe(III) oxides requires the expression of *Geobacter's* conductive pilus nanowires (34), which recent studies from our group have also implicated as their primary U reductase (10).

The expression of conductive pili by *Geobacter* also leads to cell aggregation and the formation of biofilms (35, 36). Biofilm development is often assumed in the subsurface, particularly at the matrix-well screen interface and rock fractures, but evidence of biofilms in the bulk aquifer matrix is scarce (6). Recent studies (23) at the Rifle IFRC site demonstrated that field-scale addition of acetate to groundwater also stimulated the growth of *Geobacter* spp. in the sediment particles. Furthermore, their growth shifted from the groundwater to the solid phases during the field-scale acetate addition, where they out-competed other organisms. This suggested that *Geobacter* cells transitioned from planktonic to biofilm physiologies during the

active phase of U reduction following the addition of the electron donor. However, the contribution of *Geobacter* biofilms to uranium removal and reduction has never been investigated. This contrasts with the availability of studies about U transformations mediated by *Geobacter* planktonic cells (10, 14, 25, 27, 40) or by biofilms formed by other metal-reducing bacteria such as *Desulfovibrio* (5, 29) and *Shewanella* (7, 39).

Hence, we investigated the role of *Geobacter* biofilms in the immobilization and reduction of uranium using the model representative *Geobacter sulfurreducens*, for which a genetic system (11), sequenced genome (30), and developed biofilm protocols have been described previously (35, 36). Here we show that *G. sulfurreducens* biofilms immobilize and reduce more uranium than planktonic cells and are also able to tolerate exposure to higher concentrations of the contaminant for prolonged periods of time. As with planktonic cells, the biofilms reduced the soluble U(VI) to a mononuclear U(IV) mineral phase that included carbon ligands. The ability to immobilize uranium was independent of the biofilm biomass and height. However, U reduction correlated well with increases in biofilm biomass and height and was dependent on the expression of the cell's conductive pili. These findings support the notion that *Geobacter* biofilms contribute to the immobilization and reduction of U in the subsurface, and highlight their potential as permeable biobarriers for the bioremediation of uranium contaminants.

## **MATERIALS AND METHODS**

**Strains and culture conditions.** Wild-type (WT) *G. sulfurreducens* PCA (ATCC 51573), a pilin-deficient mutant ( $PilA^-$ ) (34), and its genetically complemented strain (pRG5::*pilA*) (34) were routinely cultured in fresh water (FW) medium (26) with the modifications described

previously (10), and supplemented with 15mM acetate and 40mM fumarate (FWAF). The medium was dispensed into serum bottles, sparged with N<sub>2</sub>:CO<sub>2</sub> (80:20), sealed with butyl rubber stoppers (Bellco) and aluminum tear-off seals (Wheaton), and autoclaved 30 minutes. Biofilms were grown on 6-well cell-culture-treated plates (Corning), or glass coverslips (Corning) (36). Prior to inoculation the glass coverslips were acid-washed overnight with a 50/50 (vol/vol) HCl/NO<sub>3</sub><sup>-</sup> mixture or a 15% (vol/vol) HCl/H<sub>2</sub>O mixture, rinsed thoroughly with ddH<sub>2</sub>O, and inserted into sliced rubber stoppers (4 coverslips/stopper), as previously described (36). Immediately prior to inoculation, the stopper-coverslip assembly was autoclaved in FW medium lacking vitamins, minerals, acetate, and fumarate. Each stopper-coverslip assembly was placed in a sterile 50 ml conical tube (Corning). Biofilm assays were inoculated with an early stationary-phase FWAF culture to a final OD<sub>600</sub> of 0.04, grown anaerobically inside a vinyl glove bag (Coy Labs) with a H<sub>2</sub>:CO<sub>2</sub>:N<sub>2</sub> (7:10:83) atmosphere, and incubated at 30°C for 24, 48, or 72 h, as specified.

For determination of the total protein content of the biofilms, biofilms were grown for 24, 48 or 72 h in 6-well plates, scraped off, and harvested by centrifugation (5 min, 12,000 x *g*). The resulting cell pellet was boiled for 1 h in 2M NaOH, allowed to cool, and then neutralized with an equal volume of 2M HCl. The sample was centrifuged to remove cellular debris, and the resulting supernatant analyzed for total protein content. Protein was quantified using a Pierce Microplate BCA Protein Assay Kit (reducing reagent compatible, Thermo Scientific) with BSA

standards, according to the manufacturer's specifications. Protein was measured as an OD<sub>562</sub> on a Tecan Sunrise Plate Reader (Tecan, Inc.).

**U(VI) resting cell suspension and biofilm assays.** The ability of cells to remove U(VI), provided as uranyl acetate, from solution was assayed in resting planktonic and biofilm cell suspensions using protocols adapted from those described previously (40). Heat-killed and uninoculated controls were also included to rule out any abiotic removal activity or absorption. Resting biofilm suspensions were prepared from biofilms grown on stopper-coverslip assemblies for 24, 48, or 72 h, as described above. The culture broth was decanted, the assembly rinsed gently with sterile, anaerobically-prepared wash buffer (40), and 20 ml of reaction buffer (40) supplemented with 20 mM sodium acetate and 1 mM uranyl acetate (Electron Microscopy Sciences) prepared in 30mM bicarbonate buffer was added. Resting planktonic and biofilm cell suspensions were incubated for 24 h at 30°C. Following incubation, 500 µl samples of the supernatant were removed, filtered (0.22 µm Millex-GS filter, Millipore), acidified in 2% nitric acid (500 µL), and stored at -20°C. For kinetic studies of U(VI) removal, samples were taken every 6 h. All procedures were performed inside an anaerobic glove bag, as described above. The concentration of U(VI) in the acidified samples was measured using a Platform Inductively Coupled Plasma Mass Spectrometer (ICP-MS) (Micromass, Thermo Scientific) or a Kinetic Phosphorescence Analyzer (KPA) (Chemchek).

**Vitality fluorescent assays.** The respiratory activity of biofilm cells after exposure to uranium was assayed using the fluorescent RedoxSensor vitality kit (Invitrogen), as previously described. WT biofilms were grown on coverslips for 48 h and incubated in reaction buffer with

1 mM, 2.5 mM and 5 mM concentrations of uranyl acetate. Control biofilms incubated in reaction buffer without uranyl acetate were also included. After 24 h of incubation, the reaction buffer was decanted from the tubes and the stopper-coverslip assemblies were washed with wash buffer. The biofilms were then scraped from the assembly and resuspended in 1 ml reaction buffer. Samples were vortexed briefly, mixed 1:1 with Redox dye solution, and incubated 10 min before measuring fluorescence (490nm excitation, 520nm emission) on a SpectraMax M5 plate reader (Molecular Devices). The respiratory activity of the biofilms was calculated as the fluorescence emission of the Redox Sensor dye relative to the metabolic activity of controls without uranium. Separate aliquots of the samples were stained with SYTO 9 (Invitrogen) to confirm that the samples had the same amount of cells.

**Microscopy.** Biofilm growth on 6-well plates was examined by Confocal Laser Scanning Microscopy (CLSM). Following the specified incubation period, planktonic growth was carefully removed and the remaining biofilm was stained with LIVE/DEAD BacLight Bacterial Viability Kit (Invitrogen) dye solution, following the manufacturer's recommendations. The biofilms were stained for approximately 15 min, washed once in PBS, and imaged on a Zeiss Pascal LSM microscope (Carl Zeiss Microscopy, LLC) equipped with an Achroplan 40x/0,80W dipping objective. COMSTAT analyses were carried out using images from three biological replicates, with 6-10 distinct fields-of-view (1,024 x 1,024 pixels, 0.22  $\mu\text{m}/\text{pixel}$ ) for each. Images were collected every 1.14  $\mu\text{m}$ , and projections were created using Zeiss LSM Image Browser software (Carl Zeiss Microscopy, LLC). The structure of the biofilms was characterized using COMSTAT image analysis software using connected volume filtration to remove noise in the data, as described previously (17).

When indicated, the biofilms were also examined with a Scanning Electron Microscope (SEM). Biofilms were grown for 48 h on round glass coverslips (12-mm diameter), and exposed to 1mM uranyl acetate for 24 h. The biofilms were then fixed at 4°C for 1-2 h in 4% glutaraldehyde, rinsed briefly in 0.1M sodium phosphate buffer, and dehydrated in a series of ethanol washes (25%, 50%, 75%, 95%, 10 minutes each), followed by three 10 min washes in 100% ethanol. The samples were critical-point dried using a Blazers 010 critical point dryer (Blazers Union Ltd.) with liquid CO<sub>2</sub> as the transitional fluid. Once dry, the coverslips containing the biofilm samples were mounted on aluminum stubs using epoxy glue and coated with ~10 nm of osmium using a NEOC-AT osmium coater (Meiwafosis Co., Ltd.). Samples were examined with a JEOL JSM-7500F SEM equipped with an Energy Dispersive Spectroscopy (EDS) 30mm<sup>2</sup> detector crystal for elemental analyses.

**X-ray Absorption Spectroscopy (XAS) analyses.** The valence and speciation of U in the biofilms was estimated by XANES (X-ray Absorption Near Edge Spectroscopy) and EXAFS (Extended X-ray Absorption Fine Structure Analysis), respectively. For these analyses, biofilms were grown on stopper-coverslip assemblies, and exposed to U for 24 h, as described above. After rinsing the assemblies gently with wash buffer, the biofilm biomass was scraped off the assemblies using and resuspended in 2 ml of reaction buffer. The cells were then harvested by centrifugation (12,000xg, 10 min), loaded into custom-made plastic holders, and stored at -80°C (10). All procedures were carried out in an anaerobic chamber, and samples were kept frozen during XAS measurements. XANES and EXAFS measurements were performed using standard beamline parameters (22) and a multielement Ge detector in fluorescence mode using

the PNC-CAT beamline 20-BM at the Advanced Photon Source (Argonne National Laboratory). Data obtained from XANES and EXAFS analysis was processed according to the combination of protocols described previously (10).

**SDS-PAGE and heme-stain of proteins of the biofilm EPS matrix.** The exopolysaccharide matrix (EPS) was extracted from biofilms grown 48 h on 6-well plates using a modification of a protocol described previously (8, 38). Briefly, biofilms were scraped and collected in reaction buffer. The solution was centrifuged for 10 minutes at 13,000 $\times$ g and the resulting pellet was resuspended in 1/5 volume of TNE and vortexed for 1 min. SDS was added to a final concentration of 0.1%, and the solution was mixed at room temperature for 5 min. The samples were then passed 10 times through an 18G needle, and centrifuged at 15,500 $\times$ g to collect the sheared materials as an insoluble fraction. The resulting pellet was washed 5 times before resuspending it in 10mM Tris-HCl, pH 7.5.

To identify heme-containing proteins in the EPS matrix, 20  $\mu$ g of protein from each EPS isolation was boiled for 10 min and separated on a 12% Mini-Protean TGX gel (BioRad) at 250V for 30 min. The Novex Sharp markers (Invitrogen) were used as a molecular weight standard. Heme-containing proteins were visualized on the gel with N,N,N',N'-tetramethylbenzidine staining, as described previously (10, 41). A duplicate gel was run in parallel and stained for total protein using Coomassie Brilliant Blue G-250 (BioRad) according to the manufacturer's recommendations.

## RESULTS AND DISCUSSION

**Enhanced U(VI) immobilization and tolerance by biofilms.** The kinetics of U(VI) immobilization were investigated in resting 48 h biofilms in reference to planktonic cells (Fig. 3.1A).

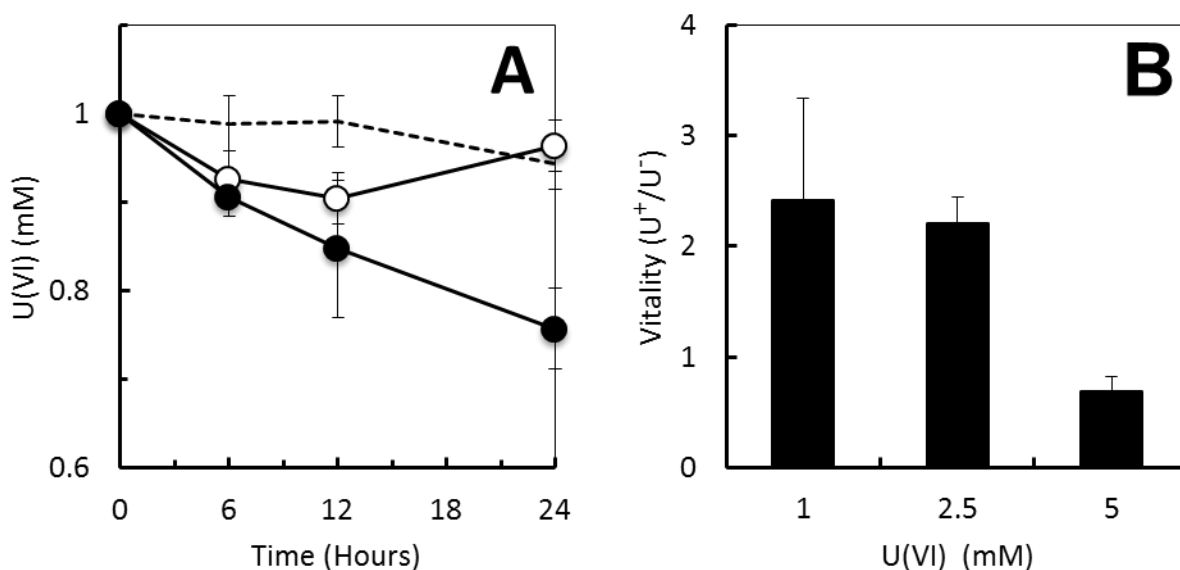


**FIGURE 3.1: Biofilms maintain vital activities through 24 h of U exposure.** (A) Removal of U(VI) from solution by 48 h biofilms of *G. sulfurreducens* (solid symbols) showing the linearity of the reaction for 24 hours. Controls with planktonic cells (open symbols) and uninoculated biofilm assemblies (dashed line) are also shown. (B) Effect of 24 h exposure to increasing concentrations of U(VI) (1, 2.5, and 5 mM) on the respiratory activity of 48-h biofilms (vitality measured with the RedoxSensor dye and expressed as the ratio of relative fluorescence units emitted by cells incubated with ( $U^+$ ) and without ( $U^-$ ) U).

The rates of U removal during the first 6-12 h were similar in planktonic cells and biofilms. However, while the biofilms immobilized U linearly for up to 24 h, the removal activities of the planktonic cells stopped after 12 h and the cell-associated U was solubilized again. As a result, the biofilms immobilized twice as much U as the planktonic cells. Cell viability, which is crucial for assessing the capacity for U(VI) reduction, can only be preserved in

planktonic cells for the first 7 h under the conditions used in this assay (40). After this time, osmotic pressure causes the cells to lyse and the viability of the resting cells declines rapidly. The sustained removal of U by the biofilms suggests that the biofilms remain viable and metabolically active even after prolonged exposure to the contaminant. To investigate this, we used the fluorogenic RedoxSensor Green dye to measure the respiratory activities of biofilm cells exposed to U for 24 h ( $U^+$ ) in reference to unexposed biofilm controls ( $U^-$ ) (Fig 3.1B). The dye yields green fluorescence when modified by the bacterial reductases, which are mostly located in the electron transport system of the cell envelope (15, 21). As respiration is a vital activity of the cell, the dye also measures the cell's vitality and serves as a proxy for the cell's viability (10). As shown in Fig. 3.1B, the respiratory activities of biofilm cells exposed to 1mM U for 24 h were 2.4-fold higher than control biofilms incubated under identical conditions but without U. This is likely because they are able to use the U as an electron acceptor, while the unchallenged controls are not supplemented with an electron acceptor and therefore are not actively metabolizing. This high rate of vitality contrasts with the more than 70% decrease in respiratory activities reported for planktonic cells incubated with U for 6 h in reference to unexposed controls (10). Furthermore, similar increases in respiratory activities were measured in biofilms exposed to 2.5 mM concentrations of U for 24 h and decreases in respiratory activity (ca. 70%) were only measured after exposing the biofilms to 5 mM concentrations of U for the same period of time. Thus, the results are consistent with increased respiratory activities and cell viability in cells within biofilms.

**Extracellular reduction of U by biofilms.** Approximately 67% ( $\pm 4\%$ ) of the U(VI) immobilized by 48 h biofilms after 24 h was reduced to U(IV). Thus, the immobilization of U(VI)

by the biofilms was coupled to its reduction of U(IV). Examination of the biofilms after exposure to 1 mM U for 24 h by SEM showed needle-like, extracellular precipitates that coated the biofilm microcolonies (Fig. 3.2A), which elemental analyses with an EDS detector confirmed to be composed of U (Fig. 3.A.1).

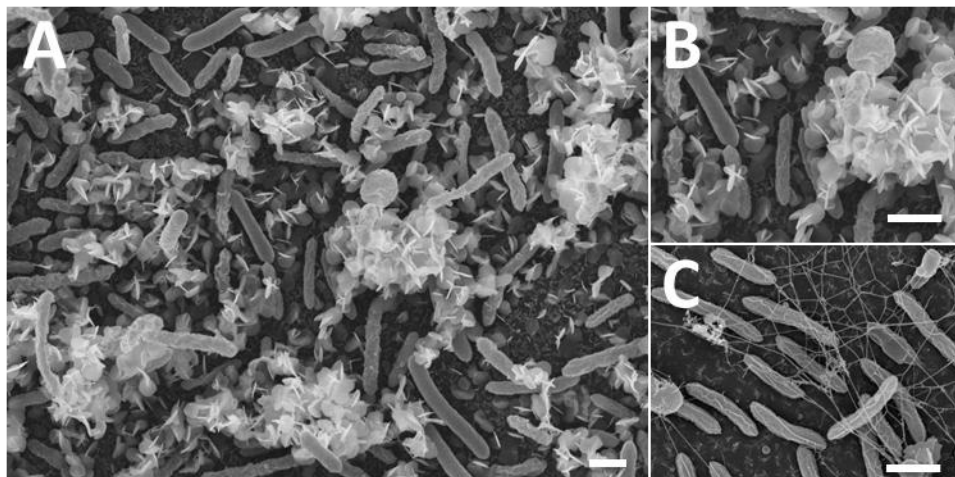


**FIGURE 3.2: SEM micrographs of 48 h biofilms** exposed to U for 24 h (A and B) showing the extracellular needle-like, white precipitates of uranium associated with the biofilm microcolonies. Control biofilms not exposed to U are also shown (C). Scale bar, 1  $\mu\text{m}$ .

At higher magnification (Fig. 3.2B and C) the U precipitates were observed as interspersed with extracellular filaments, some with diameters (ca. 4 nm) matching well the diameters reported for the conductive pili of *G. sulfurreducens* (34) and some with larger diameters (ca. 15-20 nm) consistent with dehydrated EPS fibers (38). The conductive pili of *G. sulfurreducens* are required for microcolony formation during biofilm formation by *G. sulfurreducens* (36) and are also the primary U reductase of planktonic cells (10). Thus, they could also play a similar role in U reduction by the biofilms. On the other hand, the EPS matrix of *G. sulfurreducens* anchors several *c*-cytochromes involved in metal reduction in *G.*

*sulfurreducens* (38) and could, therefore, contribute to the U reductase activities of the biofilms.

As the biofilms grow and mature, more conductive pili and more EPS matrix with c-cytochromes are available to participate in the redox reactions of the biofilms. Hence, we studied the ability of biofilms grown for 24, 48 and 72 h to immobilize and reduce U(VI) after 24 h of exposure to the contaminant (Fig. 3.3A).

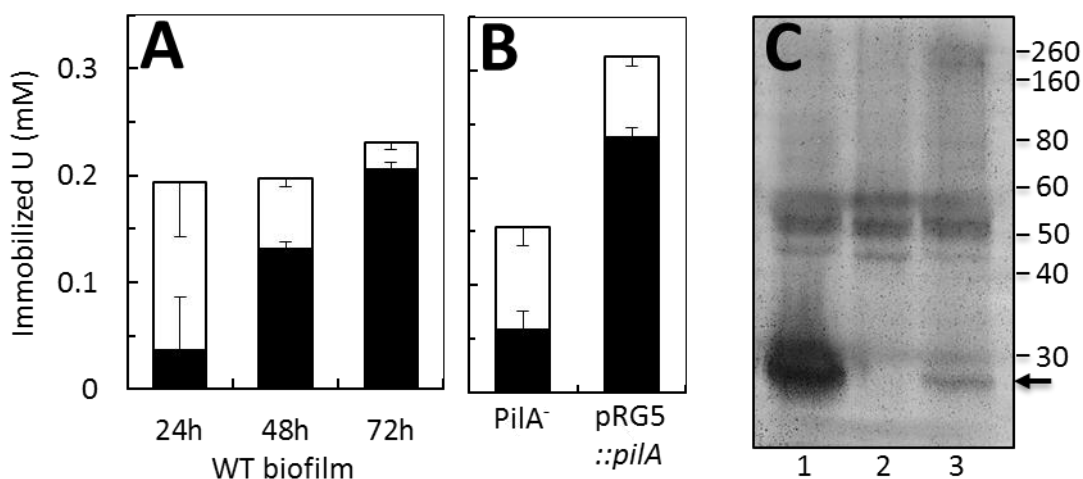


**FIGURE 3.3: U(VI) immobilization/reduction, and cytochrome profile of the WT, Pila<sup>-</sup>, and pRG5::pila strains.** (A-B) Reduction of U(VI) (open blocks) to U(IV) (solid blocks) by WT biofilms grown for 24, 48 and 72 h (A) and by 48 h biofilms of the pilin-deficient Pila<sup>-</sup> mutant and the hyperpilated pRG5::pila strain (B). (C) Heme-stained SDS-PAGE of protein extracted from the EPS matrix of 48 h biofilms of the WT (lane 1), Pila<sup>-</sup> (lane 2), and pRG5::pila (lane 3) strains. Numbers at the right are relative molecular weights of protein markers in kDa. The arrow points at the migration of the small, processed form of the OmcZ c-cytochrome (OmcZ<sub>S</sub>).

While the removal activities of the biofilms were similar, U reduction increased proportionally to the biofilm age and was highest in the 72 h biofilms (Fig. 3.3A). CLSM micrographs of the biofilms revealed visual differences in biofilm thickness and structure in 24, 48, and 72 h biofilms (Fig. 3.4A and 3.A.2).

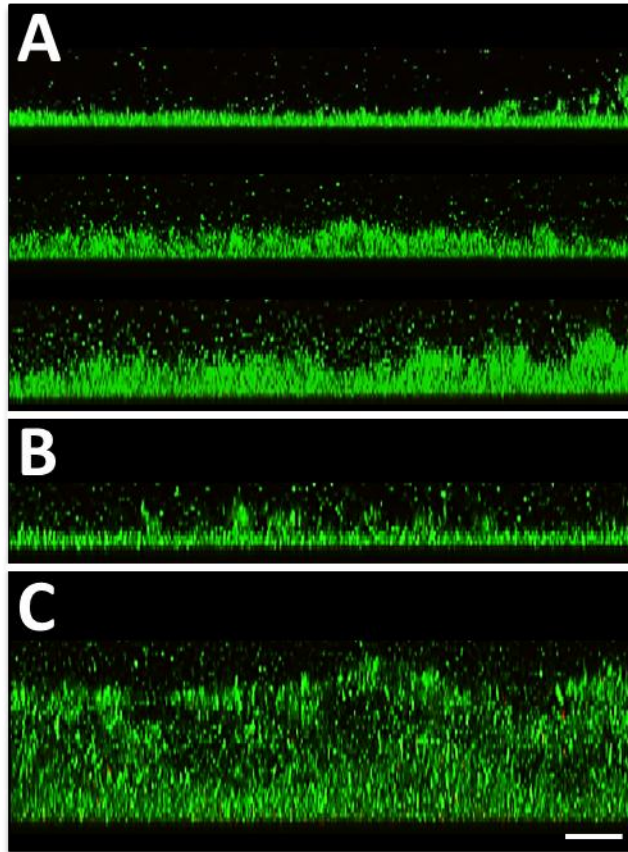


**FIGURE 3.4: CLSM micrographs showing side view projections of (A) WT (24, 48 and 72 h), (B)  $PilA^-$  (48 h), and (C)  $pRG5::pilA$  (48 h) biofilms stained with the BacLight viability kit (green, live cells; red, dead cells). Scale bar, 20  $\mu\text{m}$ . The top view projections corresponding to these images are shown in Fig. 3.A.2.**

Biofilm parameters calculated using the COMSTAT analysis software such as biomass, thickness and surface area, increased linearly during the first 48 h of biofilm growth and remained unchanged in 72 h biofilms (Fig. 3.A.3, Table 3.1). Interestingly, the surface coverage and surface to volume ratio values did not change substantially as the biofilms aged (Fig. 3.A.3, Table 3.1).

**TABLE 3.1: COMSTAT analysis**

Biofilm	Total biomass ( $\mu\text{m}^3/\mu\text{m}^2$ )	Average Thickness ( $\mu\text{m}$ )	Surface Area ( $\text{mm}^2$ )	Surface Coverage (%)	Surface to volume ratio ( $\mu\text{m}^2/\mu\text{m}^3$ )
WT 24h	6.4 ± 1.0	7.8 ± 1.1	0.6 ± 0.1	80.7 ± 5.2	2.9 ± 0.3
WT 48h	10.6 ± 1.3	13.3 ± 1.8	1.2 ± 0.1	91.8 ± 1.7	3.6 ± 0.4
WT 72h	10.6 ± 3.3	13.9 ± 3.9	1.0 ± 0.2	92.2 ± 6.6	3.1 ± 0.4
<i>PilA</i> <sup>-</sup> 48h	5.2 ± 0.7	6.8 ± 1.0	0.6 ± 0.1	77.8 ± 3.6	3.4 ± 0.3
pRG5:: <i>pilA</i> 48h	43.4 ± 14.8	60.1 ± 18.9	6.1 ± 2.5	99.5 ± 0.5	4.4 ± 1.3

This is similar to our earlier observation that the U removal activities of the biofilms do not change substantially as the biofilms age (Fig. 3.3A). This and the extracellular location of the U precipitates (Fig. 3.2) suggest that U is preferentially immobilized at the biofilm surface exposed to liquid milieu.

None of the biofilm parameters calculated (Fig. 3.A.3) matched the linear increases in U reductive activities observed as the biofilms aged between 48 and 72 h (Fig. 3.3A). Biofilm formation is a developmental process, consisting of specific stages such as attachment, microcolony formation and biofilm maturation (32). The transition from one stage of biofilm development to the next involves extensive gene reprogramming so that specific biofilm components and activities are expressed (16, 28). Consistent with this, we measured linear increases in the total protein content of the biofilms, which includes the protein from the cells

and from the biofilm matrix (Fig. 3.A.4), that cannot be accounted for by increases in cell numbers calculated as biomass in the COMSTAT analyses (Fig. 3.A.3). This supports the notion that there are specific redox-active components expressed during biofilm formation that catalyze the reduction of U.

**Role of conductive pili and c-cytochromes of the biofilm matrix in U reduction.** We further investigated the role of the biofilm pili in U reduction by studying the ability of 48 h biofilms of a pilin-deficient ( $PilA^-$ ) mutant to immobilize and reduce U compared to its genetically complemented strain pRG5::*pilA* (Fig. 3.3B). The mutant carries a deletion in the gene encoding the pilin subunit (34), which reduces the ability of planktonic cells to reduce U extracellularly (10). The mutant biofilms attached and grew on the surface but had fewer microcolonies (Fig. 3.4B and Fig. 3.A.2). By contrast, its genetically complemented strain, pRG5::*pilA*, which is hyperpilated (10), formed very thick biofilms after only 48 h of incubation (Fig. 3.4C and Fig. 3.A.2). In general, all the biofilm parameters measured in the mutant biofilms (such as biomass, thickness, surface coverage, etc.) were similar to those measured in 24 h biofilms of the WT strain (Fig. 3.A.3), consistent with the previously reported role of *Geobacter* pili in microcolony formation (36). Not surprisingly, the mutant biofilms also removed and reduced less U than 48 h WT biofilms (Fig. 3.3B). By contrast, the hyperpilation of the strain pRG5::*pilA* promoted biofilm formation (Fig. 3.4C and 3.A.2) and resulted in substantial increases in biofilm biomass, thickness and surface area but similar values for surface coverage and surface:volume ratio (Fig. 3.A.3). The hyperpilated biofilms also removed 1.6 times more U than the WT biofilms and reduced 76% ( $\pm 3\%$ ) of U(VI) to U(IV) (Fig. 3.3B).

When compared to 48 h WT biofilms, the U removal and reduction activities of the  $PilA^-$

and pRG5::*pilA* biofilms correlated strongly with the biofilm biomass and average thickness ( $R^2 = 0.99$ ), but required a logarithmic fit. This indicates that a biofilm's ability to adsorb or reduce U based solely on its biomass characteristics is finite. Hence, increases in biofilm biomass cannot solely account for the differences in U removal and reduction observed in the biofilms formed by strains with different levels of piliation. Interestingly, we observed a positive linear correlation between surface coverage and U removal ( $R^2 = 0.82$ ). Surface coverage represents the amount of cells attached to the substratum, or biofilm confluence (17). The roughness coefficient is a measurement of the variations in biofilm thickness (17). Thus, a lower roughness coefficient indicates a more uniform biofilm and a higher coefficient a more variable one. Taken together these results demonstrate that the thickness/biomass of a biofilm can be used as an initial prediction of the amount of U that can be immobilized and reduced, but the ultimate determination of the U transformation phenotype is made by structural characteristics determined by specific biofilm components, such as the pilus nanowires.

As the  $\text{PilA}^-$  mutant also has defects in outer membrane *c*-cytochromes required for metal reduction such as OmcS (10) and these cytochromes are anchored in the biofilm EPS matrix (37), we examined the heme-containing proteins associated with the biofilm matrix of the WT,  $\text{PilA}^-$  and pRG5::*pilA* biofilms (Fig. 3.3C). Interestingly, a band with a relative molecular weight similar to that of OmcS (~47KDa) (33) was present in both the WT and the  $\text{PilA}^-$  mutant matrices. The only heme-containing band present in the WT matrix and absent in the  $\text{PilA}^-$  matrix was one with a relative molecular weight of 30 KDa. This size matches that of OmcZ<sub>S</sub>, a

processed isoform of the OmcZ cytochrome of *G. sulfurreducens* that is required for optimal current production by anode biofilms in microbial fuel cells (19). In vitro studies show that the purified OmcZ<sub>S</sub> protein can reduce U (19). Thus, OmcZ<sub>S</sub> could contribute to the reduction of U in the biofilms as well. Interestingly, the pRG5::*pilA* heme-stain profile also shows defects in OmcZ<sub>S</sub> levels (Fig. 3.3C), yet produces more conductive pili and reduces more U than the WT biofilms (Fig. 3.3B). Furthermore, we observed a strong linear correlation ( $R^2 = 0.999$ ) between the levels of piliation of the three strains grown under pili-inducing conditions (25°C) and the extent of U reduction by the biofilms (Fig. 3.A.4B). Hence, the results support the notion that the conductive pili are the primary U reductase of the biofilms.

**XAS analyses.** U L3-edge EXAFS spectra from WT and *PilA*<sup>-</sup> biofilms were modeled to determine the atomic coordination about U. The spectra were best described by a mixture of U(IV) and U(VI) coordinated by carbon atoms. The magnitude of the Fourier transformed spectra and models are shown in Fig 3.5A, with the spectra offset for clarity.

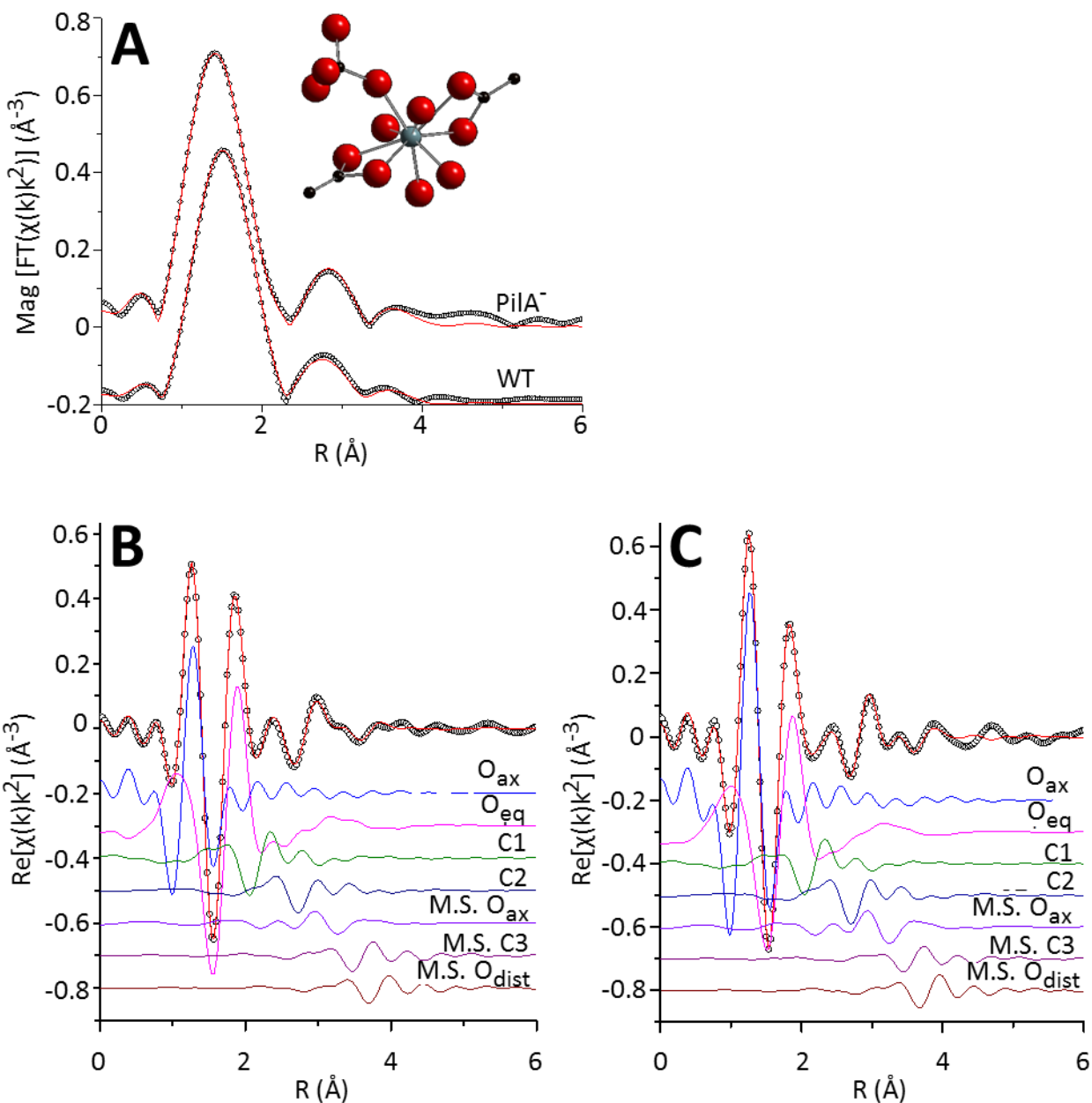


**FIGURE 3.5: U  $L_{III}$ -edge XAFS spectra. EXAFS spectra and model.** (A) Magnitude of Fourier transform spectra are offset for clarity in descending order  $\text{PiIA}^-$ , and WT. The real part of Fourier transform of WT (B) and  $\text{PiIA}^-$  (C) is also shown. The components of the model are shown offset beneath the total model and measured spectrum. Also shown is the U(IV) moiety that is consistent with the measured EXAFS spectra for both WT and  $\text{PiIA}^-$  (inset). U(IV) (grey) is coordinated by oxygen (red) atoms and two bidentate carbon (black) ligands and one monodentate carbon ligand.

A molecular moiety that is consistent with both the WT and  $\text{PilA}^-$  model is shown in the inset. Fig 3.5B and 3.5C show the contribution of each path in the model in the real part of the Fourier transform for the WT and  $\text{PilA}^-$  samples, respectively. The model includes two types of carbon ligands. One of the C-ligands is bound to two oxygen atoms of U in a bidentate fashion and is followed by a distant carbon (C3) atom. The other C-ligand is bound to one oxygen atom of U in a monodentate fashion and is attached to 3 distant oxygen (Odist) atoms. Multiple scattering paths from distant C3 and Odist atoms were included in the model. This model was simultaneously refined to both spectra. The distances and  $\sigma^2$  values used to model the spectra are listed in Table 3.A.1. Table 3.A.2 lists the coordination numbers. The coordination numbers are consistent with 1 to 2 bidentate C-ligands and 1 to 2 monodentate C-ligands per U atom. The number of Oax atoms can be used to estimate the amount of U(IV) in these samples, since there are two Oax atoms for each U(VI) atom and no Oax atoms for U(IV). The Noax values indicate that  $\text{PilA}^-$  and WT contain approximately 25%, and 48% U(IV) with an estimated uncertainty of 10%. These values are consistent with U XANES measurements indicating more U(IV) in the WT sample as compared to the  $\text{PilA}^-$  sample.

Our previous studies with planktonic cultures required the addition of a phosphorus ligand to model U reduction in the  $\text{PilA}^-$  strain (10), which we hypothesized was the result of U permeating deep into the cell envelope and complexing with phosphorous-containing substrates such as peptidoglycan (3), periplasmic proteins (4), and membrane phospholipids (24). Interestingly, although the  $\text{PilA}^-$  biofilms showed a distinct U removal and reduction

defect, the model that fit the EXAFS spectra did not require a phosphorous ligand, suggesting that U may not have permeated in the cells but, rather, was immobilized and reduced by other extracellular components of the biofilm matrix. Biofilm physiology is substantially different from that of planktonic cultures (12). Thus, other yet to be identified biofilm components are likely to contribute to the redox activities of the biofilms.

**Implications for bioremediation.** The results of this study demonstrate the relevance of biofilms to U transformations in the subsurface, and highlight the distinct contributions of each stage of development, as well as the necessity to better understand the physiology of bacteria in the subsurface. Further studies into the U reduction activity and development of *Geobacter* biofilms could contribute to the implementation of novel bioremediation strategies, potentially including the use of biofilms as bioreactive barriers.

## APPENDIX

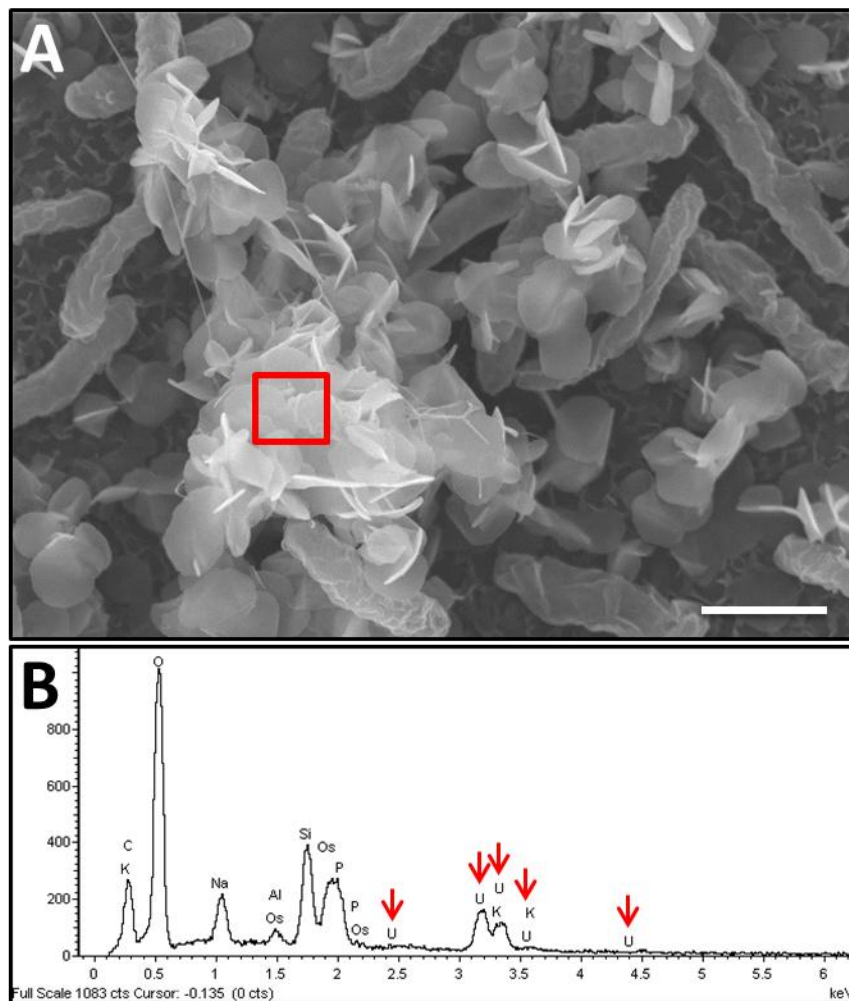


**FIGURE 3.A.1: SEM micrograph and EDS analysis of U precipitates.** (A) SEM micrograph of 48 h biofilms exposed to U for 24 h, with the area of EDS analysis indicated by the red box. (B) EDS spectrum of the white precipitates within the boxed region, with U peaks indicated by red arrows. Scale bar, 1  $\mu\text{m}$ . The text in this figure is not meant to be readable, but is for visual reference only.

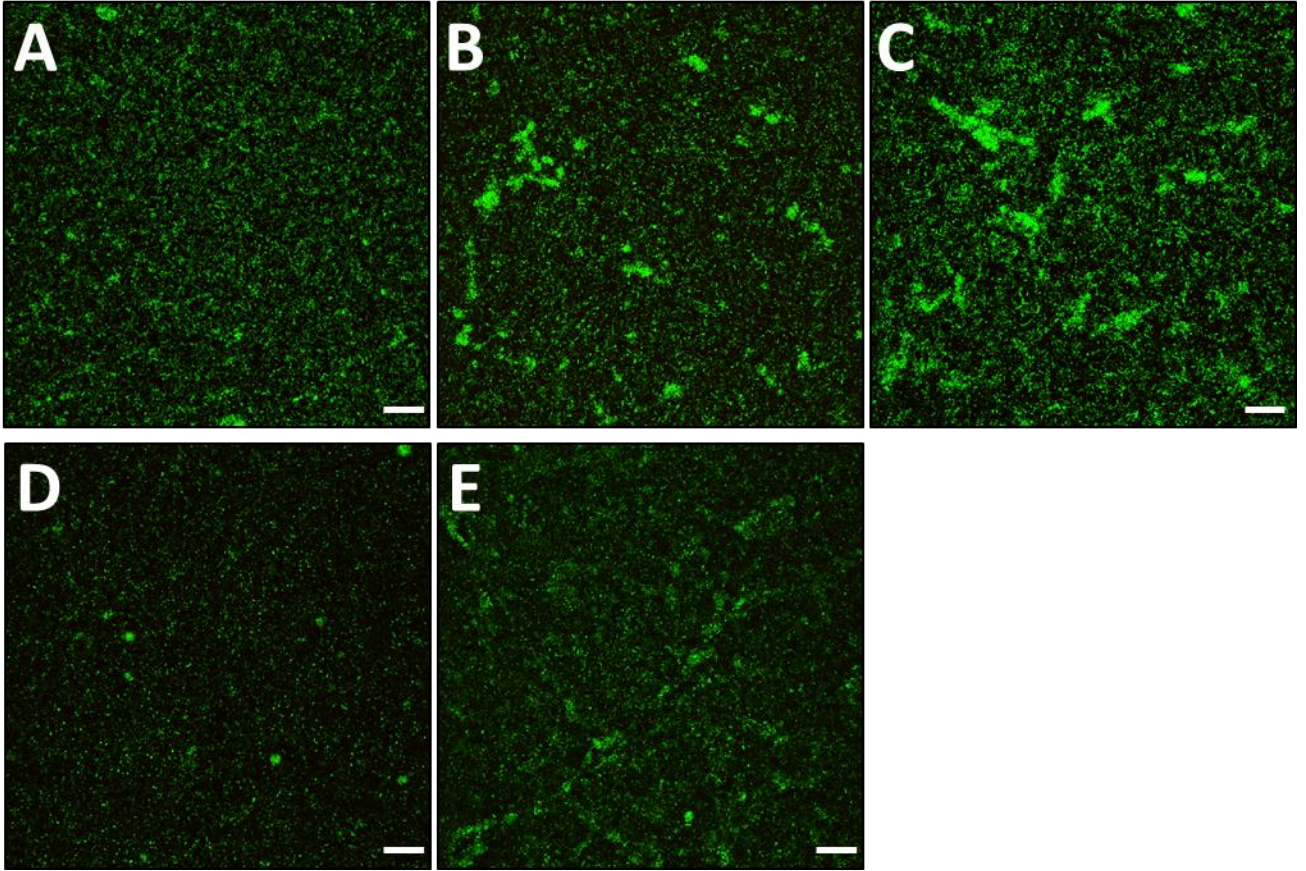


**FIGURE 3.A.2: CLSM micrographs showing top view projections of 24, 48, and 72 h WT (A), 48 h  $PilA^-$  (B), and 48h pRG5::*pilA* (C) biofilms stained with BacLight viability kit (green, live cells; red, dead cells). Scale bar, 20  $\mu\text{m}$ .**

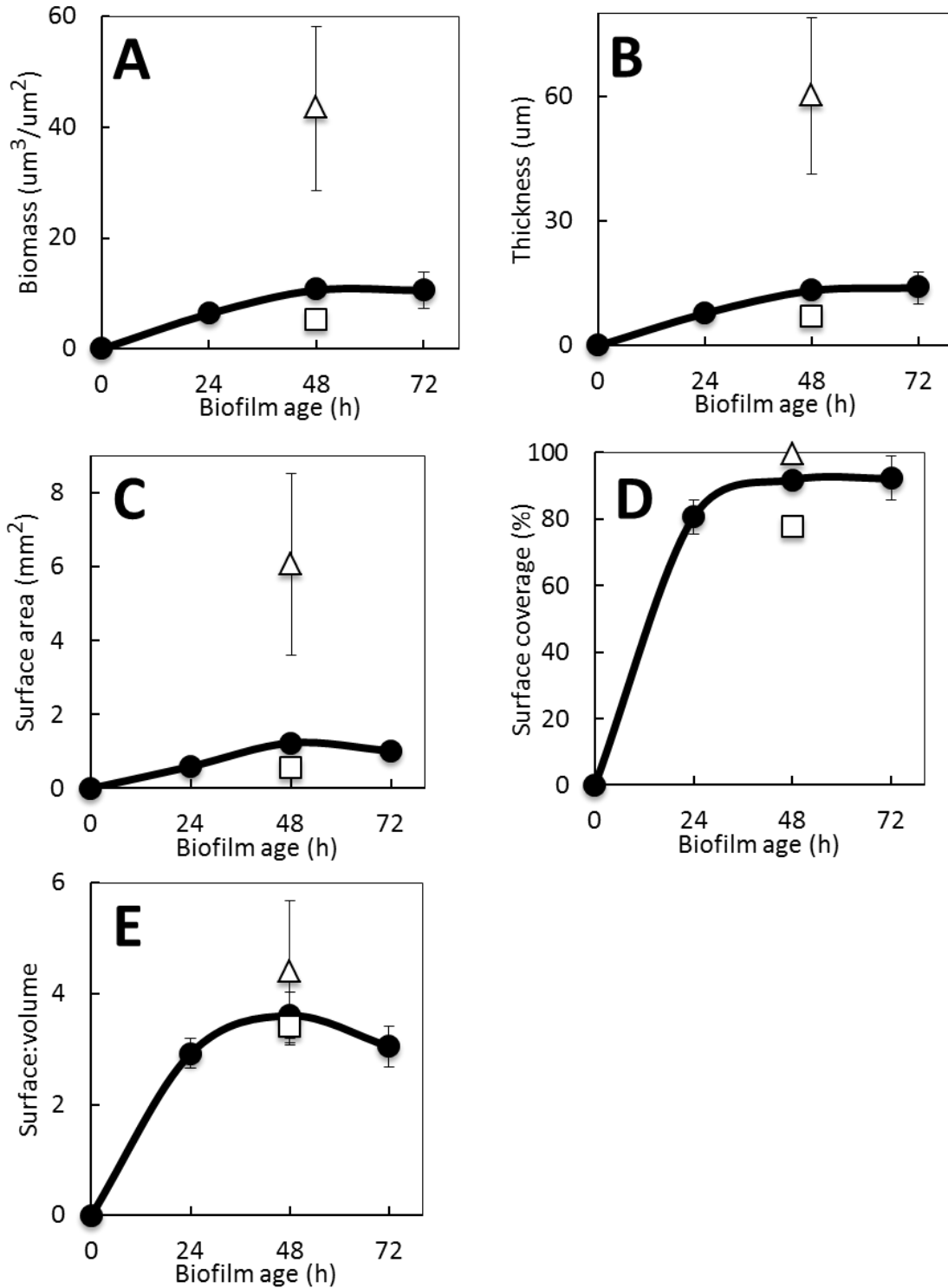


**FIGURE 3.A.3: Correlation of biofilm age and biofilm biomass (A), thickness (B), surface area (C), surface coverage (D), and surface:volume ratio (E).** Values were determined using COMSTAT analysis software (17). WT (black circles),  $\text{PiA}^-$  (squares), and  $\text{pRG5}::\text{pila}$  (triangles) strains are shown.

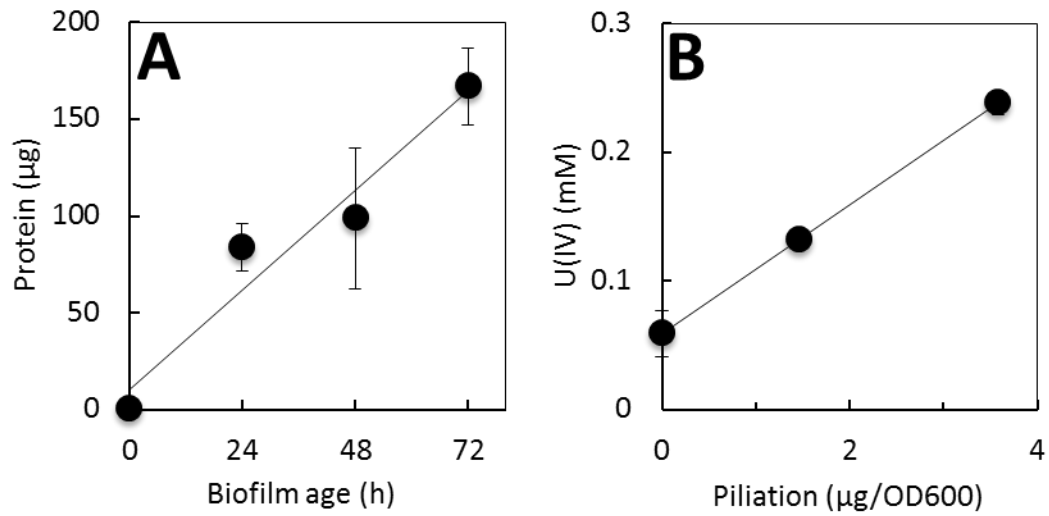


**FIGURE 3.A.4: Linear correlation between the total protein content of biofilms and biofilm age ( $R^2=0.94$ ) (A) and between piliation (planktonic cells grown under pili-inducing conditions at 25°C) and U reduction by 48 h biofilms of the WT,  $PilA^-$  and pRG5::*pilA* strains ( $R^2 = 0.999$ ) (B).**

**Table 3.A.1: EXAFS modeling results for R and  $\sigma^{2**}$** 

Path	CN	R (Å)	$\sigma^2$ ( $\cdot 10^{-3} \text{ \AA}^2$ )
Oax	Noax	$1.80 \pm 0.01$	1*
Oeq	Noeq	$2.38 \pm 0.02$	**
C1	Nc1	$2.86 \pm 0.01$	$2 \pm 7$
C2	Nc2	$3.49 \pm 0.03$	$2 \pm 7$
Oax1-Oax2	Noax	$3.61 \pm 0.02$	2*
Oax1-U-Oax2	Noax	$3.61 \pm 0.02$	2*
Oax1-U-Oax1	2Noax	$3.61 \pm 0.02$	4*
C3	Nc1	$4.54 \pm 0.07$	$2 \pm 7$
C1-C3	2Nc1	$4.54 \pm 0.07$	$2 \pm 7$
C1-C3-C1	Nc1	$4.54 \pm 0.07$	$2 \pm 7$
Odist	Nc2	$4.69 \pm 0.08$	$2 \pm 7$
C2-Odist	2Nc2	$4.72 \pm 0.08$	$2 \pm 7$
C2-Odist-C2	Nc2	$4.74 \pm 0.08$	$2 \pm 7$

\*value held, \*\*PilA:  $25 \pm 6$ , WT:  $18 \pm 4$

**Table 3.A.2: EXAFS modeling results for coordination numbers**

Data Set	Noax	Noeq	C1	C2
PilA-	$1.5 \pm 0.1$	$6.9 \pm 2.2$	$1.2 \pm 0.7$	$1.2 \pm 0.7$
WT	$1.0 \pm 0.1$	$6.3 \pm 1.4$	$1.4 \pm 0.7$	$1.4 \pm 0.8$

## REFERENCES

## REFERENCES

1. **Agency for Toxic Substances and Disease Registry, A. S. T. D. R.** 2011. Toxicological profile for uranium. *In* P. H. S. Department of Health and Human Services (ed.), Atlanta, GA.
2. **Anderson, R. T., H. A. Vrionis, I. Ortiz-Bernad, C. T. Resch, P. E. Long, R. Dayvault, K. Karp, S. Marutzky, D. R. Metzler, A. Peacock, D. C. White, M. Lowe, and D. R. Lovley.** 2003. Stimulating the in situ activity of *Geobacter* species to remove uranium from the groundwater of a uranium-contaminated aquifer. *Appl. Environ. Microbiol.* **69**:5884-5891.
3. **Barkleit, A., H. Moll, and G. Bernhard.** 2009. Complexation of uranium(VI) with peptidoglycan. *Dalton Trans* **27**:5379-5385.
4. **Benavides-Garcia, M. G., and K. Balasubramanian.** 2009. Structural insights into the binding of uranyl with human serum protein apotransferrin structure and spectra of protein-uranyl interactions. *Chemical research in toxicology* **22**:1613-1621.
5. **Beyenal, H., R. K. Sani, B. M. Peyton, A. C. Dohnalkova, J. E. Amonette, and Z. Lewandowski.** 2004. Uranium immobilization by sulfate-reducing biofilms. *Environ. Sci. Technol.* **38**:2067-2074.
6. **Cao, B., B. Ahmed, and H. Beyenal.** 2010. Immobilization of Uranium in Groundwater Using Biofilms, p. 1-37. *In* V. Shah (ed.), *Emerging Environmental Technologies*, vol. Volume II. Springer Netherlands.
7. **Cao, B., B. Ahmed, D. W. Kennedy, Z. Wang, L. Shi, M. J. Marshall, J. K. Fredrickson, N. G. Isern, P. D. Majors, and H. Beyenal.** 2011. Contribution of extracellular polymeric substances from *Shewanella* sp. HRCR-1 biofilms to U(VI) immobilization. *Environ. Sci. Technol.* **45**:5483-5490.
8. **Chang, B. Y., and M. Dworkin.** 1994. Isolated fibrils rescue cohesion and development in the Dsp mutant of *Myxococcus xanthus*. *J Bacteriol* **176**:7190-7196.
9. **Chang, Y. J., P. E. Long, R. Geyer, A. D. Peacock, C. T. Resch, K. Sublette, S. Pfiffner, A. Smithgall, R. T. Anderson, H. A. Vrionis, J. R. Stephen, R. Dayvault, I. Ortiz-Bernad, D. R. Lovley, and D. C. White.** 2005. Microbial incorporation of <sup>13</sup>C-labeled acetate at the field scale: detection of microbes responsible for reduction of U(VI). *Environ. Sci. Technol.* **39**:9039-9048.
10. **Cologgi, D. L., S. Lampa-Pastirk, A. M. Speers, S. D. Kelly, and G. Reguera.** 2011. Extracellular reduction of uranium via *Geobacter* conductive pili as a protective cellular mechanism. *Proc Natl Acad Sci U S A* **108**:15248-15252.

11. **Coppi, M. V., C. Leang, S. J. Sandler, and D. R. Lovley.** 2001. Development of a genetic system for *Geobacter sulfurreducens*. *Appl. Environ. Microbiol.* **67**:3180-3187.
12. **Costerton, J. W., Z. Lewandowski, D. E. Caldwell, D. R. Korber, and H. M. Lappin-Scott.** 1995. Microbial biofilms. *Annu Rev Microbiol* **49**:711-745.
13. **Finneran, K. T., R. T. Anderson, K. P. Nevin, and D. R. Lovley.** 2002. Potential for Bioremediation of uranium-contaminated aquifers with microbial U(VI) reduction. *Soil & Sediment Contamination* **11**:339-357.
14. **Gorby, Y. A., and D. R. Lovley.** 1992. Enzymatic uranium precipitation. *Environ. Sci. Technol.* **26**:205-207.
15. **Gray, D., R. S. Yue, C. Y. Chueng, and W. Godfrey.** 2005. Bacterial vitality detected by a novel fluorogenic redox dye using flow cytometry, American Society for Microbiology Meeting. American Society for Microbiology.
16. **Harrison, J. J., H. Ceri, and R. J. Turner.** 2007. Multimetal resistance and tolerance in microbial biofilms. *Nat. Rev. Microbiol.* **5**:928-938.
17. **Heydorn, A., A. T. Nielsen, M. Hentzer, C. Sternberg, M. Givskov, B. K. Ersboll, and S. Molin.** 2000. Quantification of biofilm structures by the novel computer program COMSTAT. *Microbiology* **146 ( Pt 10)**:2395-2407.
18. **Hu, Q. H., J. Q. Weng, and J. S. Wang.** 2010. Sources of anthropogenic radionuclides in the environment: a review. *Journal of environmental radioactivity* **101**:426-437.
19. **Inoue, K., X. Qian, L. Morgado, B. C. Kim, T. Mester, M. Izallalen, C. A. Salgueiro, and D. R. Lovley.** 2010. Purification and characterization of OmcZ, an outer-surface, octaheme c-type cytochrome essential for optimal current production by *Geobacter sulfurreducens*. *Appl Environ Microbiol* **76**:3999-4007.
20. **Istok, J. D., J. M. Senko, L. R. Krumholz, D. Watson, M. A. Bogle, A. Peacock, Y. J. Chang, and D. C. White.** 2004. *In situ* bioreduction of technetium and uranium in a nitrate-contaminated aquifer. *Environ. Sci. Technol.* **38**:468-475.
21. **Kalyuzhnaya, M. G., M. E. Lidstrom, and L. Chistoserdova.** 2008. Real-time detection of actively metabolizing microbes by redox sensing as applied to methylotroph populations in Lake Washington. *ISME J.* **2**:696-706.
22. **Kelly, S. D., K. M. Kemner, J. Carley, C. Criddle, P. M. Jardine, T. L. Marsh, D. Phillips, D. Watson, and W. M. Wu.** 2008. Speciation of uranium in sediments before and after *in situ* biostimulation. *Environ. Sci. Technol.* **42**:1558-1564.

23. **Kerkhof, L. J., K. H. Williams, P. E. Long, and L. R. McGuinness.** 2011. Phase Preference by Active, Acetate-Utilizing Bacteria at the Rifle, CO Integrated Field Research Challenge Site. *Environmental science & technology* **45**:1250-1256.
24. **Koban, A., and G. Bernhard.** 2007. Uranium(VI) complexes with phospholipid model compounds--a laser spectroscopic study. *Journal of inorganic biochemistry* **101**:750-757.
25. **Lloyd, J. R., J. Chesnes, S. Glasauer, D. J. Bunker, F. R. Livens, and D. R. Lovley.** 2002. Reduction of actinides and fission products by Fe(III)-reducing bacteria. *Geomicrobiol. J.* **19**:103-120.
26. **Lovley, D. R., and E. J. P. Phillips.** 1988. Novel mode of microbial energy metabolism: organic carbon oxidation coupled to dissimilatory reduction of iron or manganese. *Appl. Environ. Microbiol.* **54**:1472-1480.
27. **Lovley, D. R., E. J. P. Phillips, Y. A. Gorby, and E. R. Landa.** 1991. Microbial reduction of uranium. *Nature* **350**:413-416.
28. **Mah, T. F., B. Pitts, B. Pellock, G. C. Walker, P. S. Stewart, and G. A. O'Toole.** 2003. A genetic basis for *Pseudomonas aeruginosa* biofilm antibiotic resistance. *Nature* **426**:306-310.
29. **Marsili, E., H. Beyenal, L. Di Palma, C. Merli, A. Dohnalkova, J. E. Amonette, and Z. Lewandowski.** 2007. Uranium immobilization by sulfate-reducing biofilms grown on hematite, dolomite, and calcite. *Environ. Sci. Technol.* **41**:8349-8354.
30. **Méthé, B. A., K. E. Nelson, J. A. Eisen, I. T. Paulsen, W. Nelson, J. F. Heidelberg, D. Wu, M. Wu, N. Ward, M. J. Beanan, R. J. Dodson, R. Madupu, L. M. Brinkac, S. C. Daugherty, R. T. DeBoy, A. S. Durkin, M. Gwinn, J. F. Kolonay, S. A. Sullivan, D. H. Haft, J. Selengut, T. M. Davidsen, N. Zafar, O. White, B. Tran, C. Romero, H. A. Forberger, J. Weidman, H. Khouri, T. V. Feldblyum, T. R. Utterback, S. E. Van Aken, D. R. Lovley, and C. M. Fraser.** 2003. Genome of *Geobacter sulfurreducens*: metal reduction in subsurface environments. *Science* **302**:1967-1969.
31. **North, N. N., S. L. Dollhopf, L. Petrie, J. D. Istok, D. L. Balkwill, and J. E. Kostka.** 2004. Change in bacterial community structure during in situ biostimulation of subsurface sediment cocontaminated with uranium and nitrate. *Appl. Environ. Microbiol.* **70**:4911-4920.
32. **O'Toole, G., H. B. Kaplan, and R. Kolter.** 2000. Biofilm formation as microbial development. *Annu. Rev. Microbiol.* **54**:49-79.
33. **Qian, X., T. Mester, L. Morgado, T. Arakawa, M. L. Sharma, K. Inoue, C. Joseph, C. A. Salgueiro, M. J. Maroney, and D. R. Lovley.** 2011. Biochemical characterization of purified OmcS, a c-type cytochrome required for insoluble Fe(III) reduction in *Geobacter sulfurreducens*. *Biochimica et biophysica acta* **1807**:404-412.

34. **Reguera, G., K. D. McCarthy, T. Mehta, J. S. Nicoll, M. T. Tuominen, and D. R. Lovley.** 2005. Extracellular electron transfer via microbial nanowires. *Nature* **435**:1098-1101.
35. **Reguera, G., K. P. Nevin, J. S. Nicoll, S. F. Covalla, T. L. Woodard, and D. R. Lovley.** 2006. Biofilm and nanowire production lead to increased current in microbial fuel cells. *Appl. Environ. Microbiol.* **72**:7345-7348.
36. **Reguera, G., R. B. Pollina, J. S. Nicoll, and D. R. Lovley.** 2007. Possible Nonconductive Role of *Geobacter sulfurreducens* Pilus Nanowires in Biofilm Formation. *J. Bacteriol.* **189**:2125-2127.
37. **Rollefson, J. B., C. E. Levar, and D. R. Bond.** 2009. Identification of genes involved in biofilm formation and respiration via mini-Himar transposon mutagenesis of *Geobacter sulfurreducens*. *J Bacteriol* **191**:4207-4217.
38. **Rollefson, J. B., C. S. Stephen, M. Tien, and D. R. Bond.** 2011. Identification of an extracellular polysaccharide network essential for cytochrome anchoring and biofilm formation in *Geobacter sulfurreducens*. *J Bacteriol* **193**:1023-1033.
39. **Sani, R. K., B. M. Peyton, and A. Dohnalkova.** 2008. Comparison of uranium(VI) removal by *Shewanella oneidensis* MR-1 in flow and batch reactors. *Water Res.* **42**:2993-3002.
40. **Shelobolina, E. S., M. V. Coppi, A. A. Korenevsky, L. N. DiDonato, S. A. Sullivan, H. Konishi, H. Xu, C. Leang, J. E. Butler, B. C. Kim, and D. R. Lovley.** 2007. Importance of c-Type cytochromes for U(VI) reduction by *Geobacter sulfurreducens*. *BMC Microbiol.* **7**:16.
41. **Thomas, P. E., D. Ryan, and W. Levin.** 1976. An improved staining procedure for the detection of the peroxidase activity of cytochrome P-450 on sodium dodecyl sulfate polyacrylamide gels. *Analytical biochemistry* **75**:168-176.
42. **Wilkins, M. J., N. C. Verberkmoes, K. H. Williams, S. J. Callister, P. J. Mouser, H. Elifantz, L. N'Guessan A, B. C. Thomas, C. D. Nicora, M. B. Shah, P. Abraham, M. S. Lipton, D. R. Lovley, R. L. Hettich, P. E. Long, and J. F. Banfield.** 2009. Proteogenomic monitoring of *Geobacter* physiology during stimulated uranium bioremediation. *Appl. Environ. Microbiol.* **75**:6591-6599.
43. **Wu, W. M., J. Carley, T. Gentry, M. A. Ginder-Vogel, M. Fienen, T. Mehlhorn, H. Yan, S. Carroll, M. N. Pace, J. Nyman, J. Luo, M. E. Gentile, M. W. Fields, R. F. Hickey, B. Gu, D. Watson, O. A. Cirpka, J. Zhou, S. Fendorf, P. K. Kitanidis, P. M. Jardine, and C. S. Criddle.** 2006. Pilot-scale in situ bioremediation of uranium in a highly contaminated aquifer. 2. Reduction of U(VI) and geochemical control of U(VI) bioavailability. *Environ. Sci. Technol.* **40**:3986-3995.

## CHAPTER 4

### GENETIC ANALYSIS OF BIOFILM DEVELOPMENT IN *GEOBACTER* *SULFURREDUCTENS*

The following individuals contributed to the work presented in this chapter:

**Allison Speers:**

Collaborated on the development of a mutagenesis system, and the optimization of the biofilm assay used for the mutant screening.

**Anne Otwell and John Rotondo:**

Undergraduate researchers who assisted with the construction of the mutant library, biofilm screening assays, and sequencing associated with this project.

## ABSTRACT

As discussed in Chapter 3, *Geobacter sulfurreducens* biofilms are able to reduce uranium for prolonged periods of time without compromising the cell's viability. Our studies also demonstrated that each biofilm developmental stage contributes differently to U transformations, with reductase activity becoming more prominent in the later stages, and independent of the quantity of biomass. This led us to investigate the components expressed at each stage of growth in order to develop molecular markers that could allow us to assess the developmental stage of *Geobacter* bacteria in the subsurface, and to better predict their U reductase activity.

To identify genes involved in biofilm development, we developed a transposon mutagenesis system coupled with a high-throughput biofilm screening assay. Our partial screening of a transposon-insertion library allowed the identification of genes required for attachment, microcolony formation, and biofilm maturation in *G. sulfurreducens*. Our results confirmed the essential role of the pilus nanowires in biofilm development, and identified additional genes with cell envelope biogenesis and electron transfer functions that have not previously been implicated in biofilm formation by *G. sulfurreducens*.

## INTRODUCTION

It is now widely accepted that, in their natural environment, bacteria live predominately as part of surface-attached communities termed biofilms (14, 15, 17). For this reason, biofilm development has often been assumed in the subsurface, particularly at the matrix-well screen interface and rock fractures, but evidence of biofilms in the bulk aquifer matrix is scarce (7). Dissimilatory iron reducers in the genus *Geobacter* are natural inhabitants of subsurface aquifers and sediments (10). These bacteria gain energy for growth by coupling the oxidation of electron donors such as acetate to soluble and insoluble electron acceptors (30). The natural electron acceptor of *Geobacter* bacteria is insoluble Fe(III) oxides, which are abundant in subsurface groundwater and sediments (19). *In vitro* studies with the model representative *Geobacter sulfurreducens* have shown that the bacterial cells attach and grow as biofilms on Fe(III) coatings, a process that requires the expression of *G. sulfurreducens* conductive pili to provide structural support for the biofilms and mediate long-range electron transfer across the multilayered community (47). *G. sulfurreducens* also forms electroactive biofilms on the anode electrode of a microbial fuel cell (46). Furthermore, the growth of the electroactive biofilm requires the expression of the conductive pili and is proportional to current production (46). Evidence is also emerging from environmental studies that *Geobacter* bacteria form biofilms in the subsurface and that these biofilms mediate redox reactions such as the reductive precipitation of soluble uranium contaminants. The field-scale addition of acetate to groundwater stimulates planktonic growth and uranium reduction by *Geobacter* spp. (3). However, the growth of the planktonic population shifted from the groundwater to the solid phases during the field-scale acetate addition, and, once in the sediment, the *Geobacter* spp.

out-competed other organisms (25) . This suggested that *Geobacter* cells transitioned from planktonic to biofilm physiologies during the active phase of U reduction following the addition of the electron donor.

As shown in Chapter 3, we have demonstrated that the biofilms formed by *G. sulfurreducens* can reductively precipitate uranium. The biofilms immobilized more uranium than planktonic cells for prolonged periods of time without compromising the cells viability even when exposed at high (up to 2.5 mM) concentrations of uranium, thus showing great potential for the development of permeable biobarriers that immobilize uranium and limit its mobility in the aqueous phases. The reduced uranium was a mononuclear phase and was predominantly extracellular and associated with the biofilm pili and exopolysaccharide (EPS) matrix. We observed a linear correlation between piliation and the uranium reductase activities of the biofilms, suggesting that the conductive pili, as in planktonic cells (11), are the primary site for uranium reduction in the biofilms. We also identified the extracellular *c*-cytochrome OmcZ<sub>S</sub> (22) in the EPS matrix and evidence suggested that it could contribute to uranium reduction in the biofilms. However, the uranium reductase abilities of biofilms of a mutant deficient in pili production and OmcZ<sub>S</sub> expression were not completely abolished. Thus, other biofilms components may contribute to the reduction of uranium by the biofilms.

Also in Chapter 3, we showed that the uranium reductase activities of *G. sulfurreducens* biofilms increase as the biofilms mature, although the biofilm biomass did not change substantially. Bacterial biofilm formation is a developmental process that goes through defined stages as cells transition from planktonic growth to a sessile community. These stages consist of

attachment to the surface, the formation of microcolonies, biofilm maturation, and dispersal (39). Each developmental stage involves the expression of a unique set of genes, which confers on the biofilm a distinct physiology. As biofilms grow and mature, for example, they display increased resistance to antimicrobial agents and heavy metals (21, 32). Thus, it is important to develop molecular markers that can allow us to assess the developmental stage of *Geobacter* bacteria in the subsurface and predict the redox reactions that they can catalyze.

Transposon mutagenesis has been successfully used to identify genes involved in biofilm development in a variety of organisms (31, 40, 41, 44, 48, 60). Transposon-insertion mutants in genes required to transition from one developmental stage to the next are interrupted at that specific stage and can be identified in high-throughput screenings that quantify the biofilm biomass. Crystal violet, for example, is most often used to stain the biofilm biomass and the biofilm-associated dye can then be solubilized with acids or organic solutions and quantified spectrophotometrically (42). Transposon mutagenesis has also recently been used to identify genes required for attachment and electron transfer to electrodes and Fe(III) oxides by *G. sulfurreducens* (48, 49). This, and the availability of assays to investigate biofilm formation in this organism (47, 49), prompted us to develop a transposon mutagenesis method and a high-throughput biofilm screening assay to investigate the molecular basis of biofilm development in *G. sulfurreducens*. Here we show results from a partial screening of a transposon-mutant library of *G. sulfurreducens* and the identification of genes required for attachment, microcolony formation and biofilm maturation in this organism. The genetic screening confirmed the essential role of the pilus nanowires in biofilm development in this organism, and also identified

a number of genes involved in cell envelope biogenesis and electron transfer that have not been previously implicated in biofilm formation.

## **MATERIALS AND METHODS**

**Strains and culture conditions.** Wild-type (WT) *Geobacter sulfurreducens* PCA (ATCC 51573) was routinely cultured at 30°C in NB medium supplemented with 15mM acetate and 40mM fumarate (NBAF) (12). When indicated, fresh water medium (11, 30) supplemented with 15mM acetate and 40mM fumarate (FW 15A/40F), fresh water medium supplemented with 30mM acetate and 40mM fumarate (FW 30A/40F), or minimal medium (DB) supplemented with 30mM acetate and 40mM fumarate (DB 30A/40F) (34, 48, 53) were used. All media were sparged with N<sub>2</sub>:CO<sub>2</sub> (80:20), sealed with butyl rubber stoppers, and autoclaved prior to use. All procedures were performed anaerobically inside a vinyl glove bag (Coy Labs, Grass Lake, MI) containing a H<sub>2</sub>:CO<sub>2</sub>:N<sub>2</sub> (7:10:83) atmosphere.

**Biofilm assays.** To determine the conditions most conducive to biofilm growth and high-throughput screening, a variety of growth media, commercially-available 96-well plates, and chemical coatings with different surface characteristics (Table 4.A.1) were compared. Biofilms were incubated at 30°C for 24, 48, or 72 hours, as indicated. After the specified incubation period, planktonic growth was discarded and the biofilms were stained with 0.1% (w/v) crystal violet for 20 min, as described previously (31, 42).

Four solvents were tested to solubilize the biofilm-associated dye (Table 4.A.1), and their optimal absorption wavelength was also investigated. Each plate was de-stained for 20

minutes with the appropriate solvent, and the optical density (OD) was measured at three wavelengths contained by its maximum absorption peak (580 nm, 590 nm, and 600 nm). Unless otherwise indicated, plates were de-stained with the best solvent (33% acetic acid) and the OD of the crystal violet-acetic acid solution was measured at 580 nm using a SpectraMax M5 Plate Reader (Molecular Devices).

**Confocal Laser Scanning Microscopy (CLSM).** Biofilms were cultured and imaged in flat-bottomed Costar cell culture cluster 6-well plates (Corning), which have the same binding properties as the Corning 96-well plates selected for the biofilm screening (Corning microwell selection guide, 2011). Cells were grown as specified in FW 30A/40F, FW 15A/40F, or DB 30A/40F for 24, 48, for 72 h before discarding the liquid culture containing the planktonic cells. The biofilm was stained approximately 15 min with the BacLight LIVE/DEAD fluorescent stain (Invitrogen) according to the manufacturer's recommendations, and the dye solution was replaced with PBS for imaging. Biofilms were imaged using the 488 nm and 543 nm lasers on a Zeiss LSM Pascal microscope (Carl Zeiss Microscopy) equipped with an Achromplan 40x/0,80W dipping objective.

**Transposon mutagenesis.** Mid-log phase WT cultures were serially transferred at least three times in NBAF medium and the cells were then harvested and treated to make electrocompetent cells as described previously (12). The commercially available linear EZ-Tn5 Transposome complex (Epicentre Biotechnologies) (20) was electroporated into wild-type *G. sulfurreducens* electrocompetent cells using an Eppendorf 2510 Electroporator operated at 1470 volts. Cells were recovered for ~18 h in NBAF medium and plated on NBAF plating media supplemented with 50 µg/ml kanamycin ( $KM^{50}$ ) to select for insertion mutants. A library of ca.

4,000 Tn5-insertion mutants was constructed using colonies isolated from seven independent rounds of electroporation. Ten colonies were randomly picked and the location of the transposon insertion was investigated by Southern blot to rule out the presence of hot spots of insertion in the genome and rates of single Tn5 insertions. To ensure the Tn5 insertion was stably maintained in the absence of kanamycin, a randomly-selected mutant was transferred for 16 and 58 days in kanamycin-free NBAF, then dilution plated on solidified NBAF medium with and without  $KM^{50}$ , and the number of resulting colonies was compared.

**High-throughput biofilm screening.** Kanamycin-resistant colonies were transferred to flat-bottom 96-well Costar cell culture cluster microtiter plates (Corning) containing 200  $\mu$ l FW 30A/40F per well. The microtiter plates were incubated until visible turbidity was apparent (~3-5 days), and then transferred at least 3 times prior to inoculation of a biofilm assay. 10% (v/v) of the culture in each well was then transferred to the well of a microtiter plated containing fresh medium, and the plates were incubated at 30°C for 72 h. All steps were carried out in an anaerobic glove bag (Coy), as described above. The plates were then removed from the glove bag, the liquid culture with the planktonic cells discarded, and the biofilms were stained with crystal violet, as described above. The plates were then allowed to dry in a fume hood overnight and visually inspected to identify wells with less or more crystal violet staining than a WT control well. The mutants having a distinct crystal violet staining were selected for a quantitative secondary screening. Each mutant of interest was re-assayed in six replicates in reference to the wild type. The crystal violet associated with the biofilm was dissolved in 33% acetic acid for 20 min and the absorbance of the crystal violet solution was measured at 580 nm

on a SpectraMax M5 (Molecular Devices) or a Tecan Sunrise Plate Reader (Tecan, Inc.). Those mutants with a reproducible biofilm phenotype (biofilm defective or enhanced) were inoculated to a final OD<sub>600</sub> of 0.04 in FW 30/40 medium in a 96-well plate and their growth at 30°C was monitored spectrophotometrically (OD<sub>600</sub>) every hour in a Tecan Sunrise plate reader.

**Identification of transposon-insertion sites.** The transposon insertion site of mutants of interest was investigated first via rescue cloning (26), and if unsuccessful, via direct genomic sequencing (Britton Lab, personal communication), and/or arbitrary/touchdown PCR techniques (6, 27, 40, 41, 44, 60). Genomic DNA (gDNA) was purified using the MasterPure DNA Purification Kit (Epicentre Biotechnologies) according to the manufacturer's specifications. All sequencing reactions were performed at the Genomics Core of the Research Technology Support Facility (Michigan State University).

**Rescue cloning.** 1 µg genomic gDNA was digested overnight with HindIII (New England Biolabs) and self-ligated using T4 Ligase (Invitrogen) according to the manufacturer's specifications. The resulting plasmids were transformed into chemically-competent *pir*<sup>+</sup> *Escherichia coli* and plated on LB agar supplemented with KM<sup>50</sup>. Colonies were picked and grown in liquid LB with KM<sup>50</sup> before isolating the plasmid DNA using the ZR Plasmid Miniprep-Classic Kit (Zymo Research). Sequencing of the Tn5 flanking regions was carried out using the provided Tn5 reverse sequencing primer (KAN-2-RP-1). Sequences of primers used in this work are listed in Table 4.1.

**TABLE 4.1: Primers**

Primer Name	Sequence	Reference
KAN-2-FP-1	5'-ACCTACAACAAAGCTCTCATCAACC-3'	(26, 27)
KAN-2-RP-1	5'-GCAATGTAACATCAGAGATTTTGAG-3'	(26, 27)
ARB1	5'-GGCCACGCGTCGACTAGTACNNNNNNNNNNGATAT-3'	(40, 41, 60)
ARB2	5'-GGCCACGCGTCGACTAGTAC-3'	(40, 41, 60)
ARB6	5'-GGCCACGCGTCGACTAGTACNNNNNNNNNACGCC-3'	(40, 41, 60)
APYBAF1	5'-CGGAATCCGTGTTAAATATGGTATTGTGATNGAYKSNGGNTC-3'	(27)
HIB17	5'-CGGAATCCGGATNGAYKSNGGNTC-3'	(27)
Tn5-F	5'-GCATTACAGGGTGTCTCAA-3'	This work
Tn5-R	5'-ATTCCGACTGGTCCAACATC-3'	This work

**Arbitrary PCR.** An arbitrary PCR protocol was used, as described previously (41, 60). Briefly, the first round of PCR uses a primer unique to the transposon (KAN-2-RP-1) and arbitrary primers (ARB1 and ARB6) designed to hybridize randomly on the chromosome. The second round of PCR coupled the KAN-2-RP-1 primer with a primer specific for the 5' end of the arbitrary primers (ARB2). All PCR reactions were performed on a Mastercycler egradient S (Eppendorf) using Go-Taq Green Mastermix (Promega) according to the manufacturer's specifications. The first round of PCR was carried out using the following conditions: 95°C for 2 min, followed by 30 cycles of 94°C for 30 s, 50°C for 30 s, and 74°C for 1 min, followed by a final 5 min extension step at 74°C. The subsequent round of PCR amplification consisted of: 95°C for 2 min, followed by 5 cycles of 94°C for 30 s, 30°C for 30 s, and 74°C for 1 min, then 30 cycles of 94°C for 30 s, 30°C for 45 s, and 74°C for 1 min, and lastly followed by a final 5 min extension step at 74°C. PCR products were run on a 1.2% agarose gel, stained with ethidium

bromide, visualized on an Alphascreen 2200 (Cell Biosciences) and bands were extracted using the Zymoclean Gel DNA Recovery kit. Sequencing was carried out using the KAN-2-RP-1 primer.

For mutants that failed to produce a sequence using the above methods, alternative arbitrary PCR methods were used, as described previously (27). The “touchdown” method of arbitrary PCR involves an initial high annealing temperature (60°C), with a 0.5°C drop each subsequent cycle, ending at 45°C. The Tn5-specific primers (KAN-2-FP-1 and KAN-2-RP-1) were coupled with arbitrary primers APYBAF1 and HIB17. PCRs were performed and DNA bands obtained as described above, except the following conditions were used: Touchdown protocol 1: 94°C for 8 min, followed by 30 cycles of 94°C for 1 min, 60°C-45°C for 1 min (each temperature), and 72°C for 1 min. This was followed by 10 cycles of 94°C for 1 min, 45°C for 1 min, and 72°C for 1 min. Touchdown protocol 2 was carried out as follows: 95°C for 5 min, followed by 25 cycles of 95°C for 45 s, 60°C-45°C for 45 s (each temperature), and 72°C for 2 min. This was followed by 25 cycles of 95°C for 45 s, 50°C for 45 s, and 72°C for 2 min.

**Mutant confirmation.** Mutants of interest were colony purified, re-sequenced, and subjected to Southern blotting to confirm the presence of a single Tn5 insertion. Genomic DNA was extracted and digested with EcoRI Fast Digest Enzyme (Fermentas) according to the manufacturer’s specifications. The digested DNA was run on an agarose gel and photographed, before Southern blotting was performed as previously described (4). A probe of the Tn5 insert was prepared by PCR amplifying the gene using primers Tn5-F and Tn5-R as well as DIG DNA labeling mix (Roche) and Taq polymerase (Invitrogen) according to the manufacturer’s

recommendations with an annealing temperature of 55 °C. Detection was carried out using the anti-digoxigenin-AP fab fragments (Roche) antibody and NBT/BCIP tablets (Roche).

**SDS-PAGE and heme-stain of proteins in biofilm EPS matrix.** EPS was extracted from biofilms grown for 72 h on 6-well plates using the protocol described in previous published works (8, 49), as well as in chapter 3 of this dissertation. Total protein content was quantified using the Pierce Microplate BCA Protein Assay Kit (reducing reagent compatible, Thermo Scientific) with BSA standards, according to the manufacturer's specifications. Protein was measured as an OD<sub>562</sub> on a Tecan Sunrise Plate Reader.

For analyses of heme-containing proteins in the biofilm EPS matrix, 20 µg of protein from each sample was boiled for 10 min in Laemmli loading buffer (BioRad) and run at 250 V for 30 min on a 12% Mini-Protean TGX gel (BioRad). Heme-containing proteins were identified using N,N,N',N'-tetramethylbenzidine staining (11, 54). A duplicate gel was run in parallel and stained for total protein using Coomassie Brilliant Blue R-250 (BioRad) according to the manufacturer's recommendations. The relative molecular weight of the proteins was estimated using the Novex Sharp molecular weight markers (Invitrogen) as a standard.

**U(VI) resting cell suspension biofilm assays.** The ability of cells to remove U(VI) from solution was assayed in resting biofilm cell suspensions using protocols adapted from those described previously (11, 51), and described in Chapter 3 of this dissertation. Uninoculated controls were also included to rule out any abiotic U absorption. Resting biofilm cell suspensions were prepared from biofilms grown for 72 h in FW 30A/40F on sterilized 60 mm glass petri dishes (Corning). The culture broth was carefully removed and the biofilms were

rinsed once with sterile, anaerobically-prepared wash buffer (51). This solution was replaced with reaction buffer (51) supplemented with 20 mM sodium acetate and 1 mM uranyl acetate (Electron Microscopy Sciences) prepared in 30mM bicarbonate buffer. The cell suspensions were incubated for up to 24 h at 30°C under strictly anaerobic conditions. The U removal activity was monitored periodically in 500 µL samples. The samples were filtered (0.22 µm Millex-GS filter, Millipore), acidified in 2% nitric acid (500 µL), and stored at -20°C. The concentration of U(VI) remaining in solution in the acidified samples was measured using a Kinetic Phosphorescence Analyzer (KPA) (Chemchek).

## RESULTS AND DISCUSSION

**Development of an assay to characterize biofilm developmental stages.** We investigated biofilm formation in *G. sulfurreducens* using several commercially-available 96-well plates. From all the microtiter plates tested, the tissue-culture-treated plate (Costar Cell Culture Cluster) supported the formation of the most robust biofilms (Fig. 4.A.1). Other chemical coatings such as Sigmacote (Fisherbrand plates coated), 0.01% poly-D-lysine hydrobromide, or graphite were not as effective. Biofilm formation was, for example, prevented in the graphite-coated plates, whereas Sigmacote and poly-D-lysine-coated plates resulted in biofilms with biomass ~80% of that measured in the uncoated control plates (Fig. 4.A.1). These differences in binding could be attributed to the hydrophobic and ionic interactions between the bacteria and the surfaces tested. The uncoated polystyrene and PVC 96-well plates (Fisherbrand, BD Falcon, Nunc MicroWell) are hydrophobic and neutrally charged, and have been used in previous

biofilm assays (40, 41, 48). Graphite is also hydrophobic, whereas Sigmacote is a neutral and hydrophobic film coating prepared from chlorinated organopolysiloxane in heptane. Thus, hydrophobic surfaces are unlikely to favor the cell-surface interactions needed in the first stages of biofilm formation. Poly-D-Lysine, on the other hand, is hydrophilic and positively charged. It is commonly used to promote the attachment of cells or molecules with a predominantly negative surface charge (Corning microplate selection guide, 2011; Corning assay surfaces, 2007). However, biofilm formation was similar in tissue-culture treated plates (Nunc MicroWell MaxiSorp, Corning Costar), which provide a hydrophilic and negatively-charged surface to promote the attachment of positively charged biomolecules (Corning microplate selection guide, 2011; Corning assay surfaces, 2007). Thus, the charge of the surface does not appear to affect cell attachment. The best performing plate, the Costar Cell Culture Cluster, is a tissue-culture-treated plate that presumably provides a hydrophilic surface for cell attachment; however, information about the chemical nature of the coating is not available. It promoted biofilm formation in *G. sulfurreducens* and was selected for further studies.

Four solvents are commonly used to de-stain crystal violet biofilms (Table 4.A.1) (37), and each was investigated for their suitability for our biofilm system. The maximum absorbance reported for these solvents (590nm for DMSO, 580nm for all others) was used to quantify the amount of crystal violet that was solubilized from *G. sulfurreducens* biofilms. All of the solvents effectively solubilized most of the biofilm-associated dye, with ethanol and acetic acid producing the highest absorbance values (Fig. 4.A.2). As ethanol evaporates faster and this can concentrate the crystal violet solution, we chose acetic acid as a solvent to solubilize the crystal violet associated to *G. sulfurreducens* biofilms.

The first biofilm assays described for *G. sulfurreducens* used glass coverslips and FW 15A/40F medium (47), which we used above to screen for surfaces suitable for biofilm assays. More recently, minimal media (DB) with excess electron donor (DB 30A/40F) was reported to enhance biofilm attachment in 96-well plates (48). This is not surprising as previous studies have noted the response of biofilms to nutritional cues (13, 41, 42, 61). Under the conditions of our biofilm assay, FW 15A/40F promoted biofilm formation more rapidly than the DB 30A/40F but the total biofilm biomass was similar in both (Fig 4.1A). However, providing an excess electron donor to the FW medium (FW 30A/40F) promoted biofilm formation and resulted in maximum biofilm growth at 72 h (Fig. 4.1A).

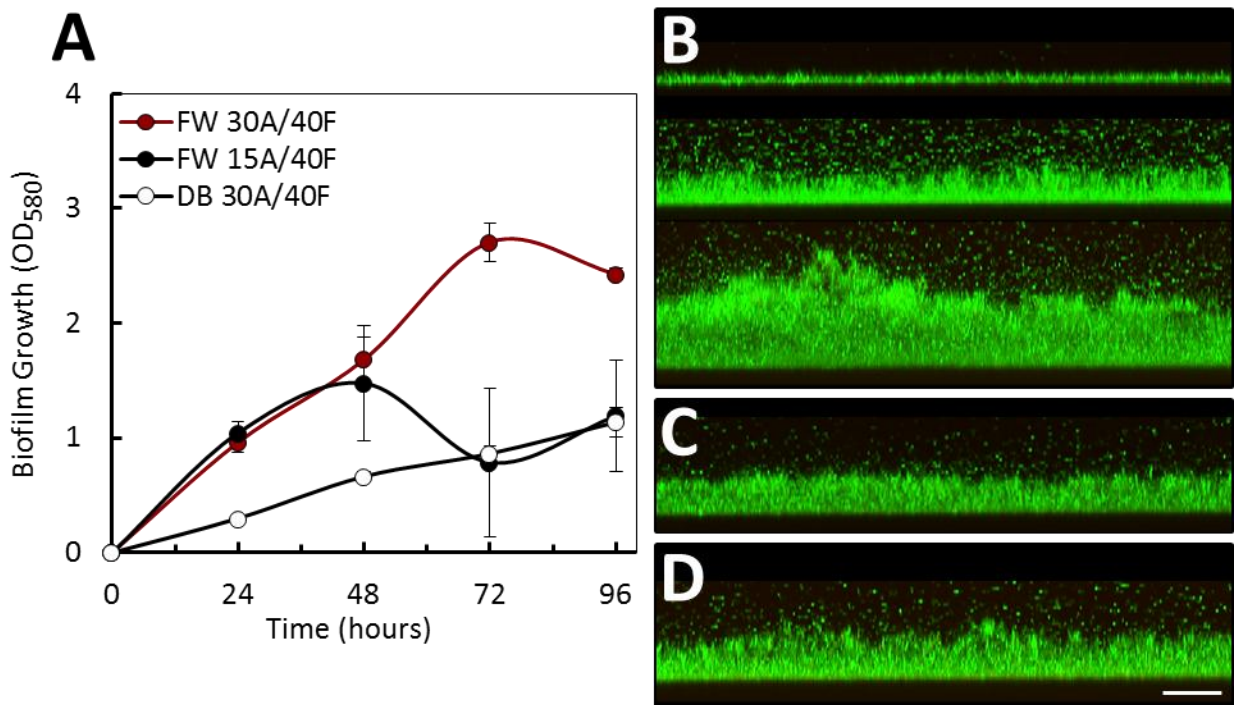


**FIGURE 4.1:** Comparison of the effect of growth medium type and electron donor (acetate) concentrations on biofilm formation (A). CLSM images of wild-type biofilms grown in FW 30A/40F (B) (24 (top), 48 (middle), and 72 (bottom) h growth), FW 15A/40F (72 h growth) (C), and DB 30A/40F (72 h growth) (D). Bar, 20  $\mu$ M.

CLSM micrographs of the FW 30A/40F biofilms revealed three distinct biofilm structures at 24 h (monolayer), 48 h (microcolonies) and 72 h (mature biofilms) (Fig. 4.1B), consistent with the developmental stages of initial attachment, microcolony formation, and maturation. The three stages were also easily distinguished based on the crystal violet values shown in Fig. 4.1A). For these reasons, we selected FW 30A/40F as the growth medium for the purposes of our screening.

**Identification of Tn5-insertion mutants with biofilm defects.** We used the Tn5 transposon to create a library of Tn5-insertion mutants. The transposon insertion was stable in the absence of antibiotic (kanamycin) pressure, as approximately 2 weeks of serial transfers yielded a 125% recovery on NBAF-KM<sup>50</sup> vs. NBAF-KM<sup>-</sup> ( $5 \times 10^4$  CFU/ml vs.  $4 \times 10^4$  CFU/ml), and approximately two months of serial transfers yielded a 76% recovery ( $1 \times 10^9$  CFU/ml vs.  $1.35 \times 10^9$  CFU/ml) on KM<sup>50</sup> media. Furthermore, Southern blot analyses of 10 mutant colonies picked at random revealed a single transposon insertion site and at random locations (data not shown), consistent with the random nature of the insertion and low likelihood of hot spots of insertion. We then screened a Tn5 transposon-insertion library of 3,840 mutants to identify mutants with both reduced and enhanced biofilm abilities. A primary visual screening identified 308 mutants. Of those, only 166 gave reproducible biofilm phenotypes in a quantitative secondary screen. Out of the 166 mutants, 13 had enhanced biofilms and were not investigated further. The remaining mutants have various degrees of biofilm defects and were grouped in categories based on their crystal violet values: “no attachment” (“-“, interrupted at the attachment stage of development, <5% of wild-type biofilms), “low” biofilm-formers (“+”,

corresponding to the microcolony stage, 5-40% of wild-type biofilms), and “medium” biofilm-formers (“++”, interrupted at the maturation stage, 40-80% of wild-type biofilms) (crystal violet de-staining values of representative mutants from each developmental stage are shown in Fig. 4.2).

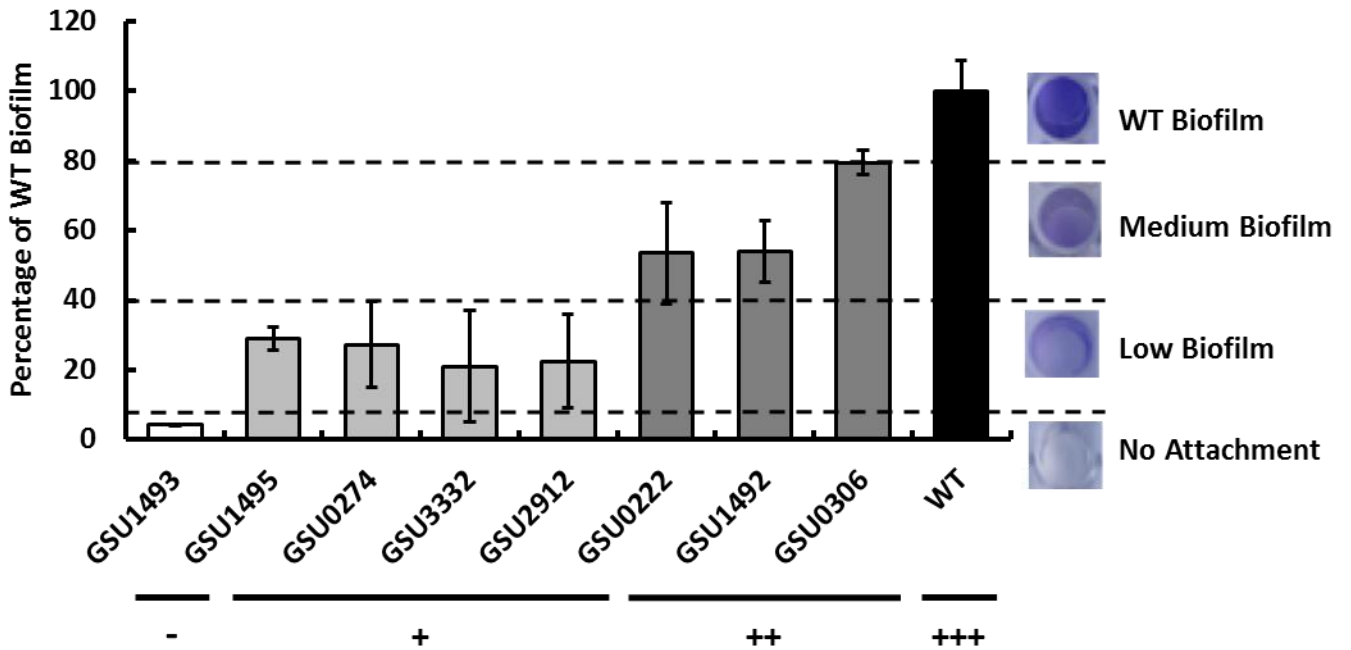


**FIGURE 4.2: Crystal violet staining of representative Tn5-insertion mutants.** Biofilm crystal violet staining values of in reference to the wild-type (left) and images (right) are shown. -, no attachment; +, low biofilm; ++, medium biofilm; +++, wild-type.

**Description of mutant groups.** Table 4.A.2 provides an exhaustive list of the biofilm-deficient mutants whose insertion site could be identified, the interrupted gene locus, the coordinates of the transposon insertion site, and growth phenotype. We identified genes from numerous functional categories including electron transfer, cell envelope biogenesis, signal transduction/regulation, metabolism, hypothetical/conserved hypothetical and unknown function.

**Cell envelope.** Cell envelope components identified in this screening that have previously been linked to biofilm formation in other bacteria include GSU3343 (SpoVR family protein, low biofilm), which has been hypothesized to be responsible for synthesis of cell wall peptidoglycan (5). Other examples include GSU1970 (polysaccharide biosynthesis protein, putative, low biofilm), which is homologous to *neuB* in *G. metallireducens* and other organisms, as well as GSU3460 (glycosyl transferase, group 2 family protein, medium biofilm). Both of these genes has been previously implicated in the synthesis of capsule polysaccharides (2, 16, 55, 58). In general, it appears that the expression of cell envelope biogenesis genes is required mainly for the early stages of biofilm formation, consistent with their role in promoting productive cell-surface interactions.

Interestingly, many of the genes identified in the regulation, metabolism, and unknown function categories were related to the biogenesis of the cell envelope, as well as electron transfer. Examples of this include no attachment mutant GSU3385 (phosphoenolpyruvate carboxykinase, *pckA*), which is involved in the conversion of oxaloacetate to phosphoenolpyruvate and CO<sub>2</sub> during the TCA cycle. Inactivation of this gene has been shown to prevent capsule biosynthesis in *Staphylococcus epidermidis* (50). Other metabolic genes include low biofilm-forming mutant GSU1942 (UDP-glucose/GDP-mannose dehydrogenase family protein), which has been implicated in EPS and capsule biosynthesis (38, 56), as well as medium biofilm-former GSU3321 (phosphoglucomutase/phosphomannomutase family protein) which is responsible for the formation of alginate and therefore the production of LPS in *Pseudomonas aeruginosa*. Expression of alginate has been correlated with the ability of cells to remain attached to the substratum during the biofilm developmental process (18). Similarly, *GntR*-like

regulators (GSU1626, low biofilm-former) have been identified in an EPS gene cluster in *Streptomyces* spp. (57). None of these mutants had defects in growth rates. Thus, they are likely involved in the synthesis of a cell surface capsule or EPS matrix that is necessary for cell attachment.

***Electron transfer.*** We identified genes predicted to regulate, directly or indirectly, the expression and functioning of electron transport components.

These genes included those involved in the biogenesis and regulation of the conductive pili, *c*-type cytochromes, and hydrogenases. Mutants carrying Tn5 insertions in *c*-type cytochromes were identified in the low and medium biofilm categories, suggesting that they are required for the development of multilayered biofilms and their maturation. Among the genes we identified several were unable to form microcolonies (GSU2912, GSU0274, and GSU3332, all cytochrome *c* family proteins), or mature biofilms (GSU0222, cytochrome *c* oxidase, subunit II). Information about these cytochromes is scarce. Mutants in GSU2912 are defective in the reduction of soluble Fe(III) citrate, but not the insoluble Fe(III) oxides (48). Mutants in GSU3332, a predicted outer membrane *c*-cytochrome, have defects in both uranium and Fe(III) oxide reduction (51), consistent with their role in extracellular electron transfer. No information is available for GSU0274 or for the cytochrome *c* oxidase of *G. sulfurreducens*. However, cytochrome *c* oxidase has previously been shown to be required for the later stages of biofilm formation in *Pseudomonas aeruginosa*, potentially because it is required for growth in anoxic environment, and oxygen gradients are common to the later stages of biofilm formation, such as the development of microcolonies (52).

Among the genes known to have an indirect effect, we identified one encoding a CRISPR-associated protein, *cas2* (GSU0058, low biofilm), which has been hypothesized to inhibit *c*-type cytochromes in *Pelobacter carbinolicus*, a close relative of *G. sulfurreducens* (1). Another gene of potential interest in electron transfer is the fibronectin type III domain protein (GSU1945, medium biofilm). Although annotated as a protein of “unknown function”, fibronectin domains are often linker domains that promote the binding and catalyses of substrates. Some cellulases, for example, have fibronectin domains to connect the catalytic and binding domains and promote the binding of the enzyme to cellulose fibers and its hydrolysis, presumably because it directs the cellulose into the active site and maintains the optimal interaction and orientation between it and the catalytic domain of the glycosyl hydrolase (24, 59). A similar function has been proposed for the fibronectin domain in the OmpB protein, a multicopper protein of *G. sulfurreducens* that promotes the association of the cell with insoluble Fe(III) oxides to facilitate electron transfer (36).

The mutants with the transposon inserted in pili biogenesis genes ranged from no attachment (GSU1493, *pilC*), low (GSU1492, *pilR*), and medium (GSU1495, *pilT-4*) biofilm-formers. This suggests that pili expression and function is required throughout the development of the biofilms, consistent with their role as structural components of the biofilm matrix and electronic conduits across the biofilms (46, 47). Similar genes homologues have been linked to the development of mature biofilms in other organisms (40, 41, 43-45, 47). In *G. sulfurreducens*, mutations in the *pilR* gene reduce the transcription of the *pilA* gene, which encodes the pilin subunit, as well as several *c*-cytochromes (23). As a result, a *pilR* mutant has defects in pili expression and cell-aggregation (23), which can lead to defects in biofilm

formation. Interestingly, although a *pilT-4* mutant was biofilm-deficient in our screening, it was previously reported to have enhanced biofilm capabilities (48). The biofilm screening used in this early report used DB 30A/40F medium, which we showed does not promote the growth of multilayered biofilms (Fig. 4.1A). Thus, the discrepancies in the reported phenotypes may have resulted from the different growth media used in both assays. The *pilT-4* gene is one of 4 *pilT* homologues identified in the genome of *G. sulfurreducens*. In other bacteria, PilT is an ATPase that powers pilus retraction and depolymerization (35, 62). As a result, mutations in *pilT* often lead to hyperpilated strains and enhanced biofilm abilities (35). The biofilms formed by hyperpilated strains often have tall mushroom-like pillars (9), which can easily break during the biofilm assay, thus leading to a biofilm-defective phenotype. Alternatively, *pilT-4* may not encode for a functional PilT ATPase in *G. sulfurreducens* or in the biofilms. We also identified a “no attachment” mutant with a transposon insertion in the *pilC* gene. PilC is an integral membrane protein associated with the pilus apparatus, and has been proposed to be involved in secretion, assembly, and/or stabilization of the pilus fiber (62). However, its role in pilus biogenesis has not been conclusively demonstrated. The finding that a *pilC* mutant cannot attach to the surface to initiate biofilm suggests that the pili of *G. sulfurreducens* could also be involved in the early stages of biofilm formation, when the cell attaches to the surface as a monolayer. However, the phenotype of the *pilC* mutant was variable, with some independent assays showing no attachment and others (Fig. 4.3A) showing medium biofilm formation. These differences could reflect differences in the growth rates or surface properties of the mutant cells in independent experiments, which are not uncommon in pili-deficient mutants in *G. sulfurreducens* (11). Thus, the results do not conclusive link pili expression to attachment.

**Role of pili in biofilm development and uranium immobilization.** We gained further insights into the role of pili in biofilm development by investigating the phenotypes of the three strains carrying mutations in pili genes: *pilC*::Tn5 (GSU1493, integral membrane protein, pili biogenesis), *pilR*::Tn5 (GSU1492,  $\sigma^{54}$ -dependent response regulator), and *pilT-4*::Tn5 (GSU1495, twitching motility protein PilT). The mutants were purified, their insertion site re-confirmed by sequencing, and a Southern blot was performed to demonstrate that the observed phenotype was the result of a single insertion event (Fig. 4.A.3). A new biofilm assay confirmed the biofilm defects in the *pilR* and *pilT-4* mutants; however, the *pilC*::Tn5 mutant attached to the surface but could not develop microcolonies (Fig. 4.3A). The uranium removal activities of the biofilms correlated well ( $R^2 = 0.90$ ) with the amount of biofilm biomass (Fig. 4.3B), suggesting that pili expression during biofilm maturation is necessary to maximize the removal potential of the biofilms.

As mutations leading to changes in pili expression can also result in defects in the expression of outer membrane *c*-cytochromes (11) and the cytochromes of the biofilm matrix (Chapter 3), we extracted the EPS matrix from the mutant biofilms and separated the proteins associated with the EPS matrix electrophoretically. The protein in the gel was then stained to identify the heme-containing proteins. The heme content and profile of the *pilC*::Tn5 mutant was similar to the WT (Fig. 4.3C). This is significant because all the mutations in pili biogenesis genes investigated thus far (11, 23) also lead to defects in *c*-cytochrome expression. Thus, defects in metal reduction in these mutants are difficult to interpret because of the pleiotropic nature of the mutations. Thus, this gene is a good molecular marker to link the activity of the

biofilms conductive pili to its reductive capabilities. By contrast, both *pilR*::Tn5 and *pilT-4*::Tn5 had defects in heme-containing proteins, including the OmcZ<sub>5</sub> c-cytochrome (~30 KDa) (Fig. 4.3C), which we previously correlated with the uranium reductive activities of *G. sulfurreducens* biofilms (chapter 3). The defects observed in the *pilR*::Tn5 are consistent with previous reports that demonstrated the differential regulation of a number of c-type cytochromes in a PilR<sup>-</sup> mutant (23). The *pilT-4*::Tn5 mutant biofilms also had a reduced heme content in the EPS matrix (Fig. 4.3C). As pili retraction leads to hyperpiliated strains (35), it is possible that overproducing pili affects c-cytochrome secretion, as we previously show for the hyperpiliated pRG5::*pilA* strain (11), which expresses the *pilA* gene from a medium-copy plasmid (45). It is interesting to note that planktonic cells of a PilT-4<sup>-</sup> mutant do not have any defect in the expression of outer membrane c-cytochromes (Bryan Schindler, unpublished data).

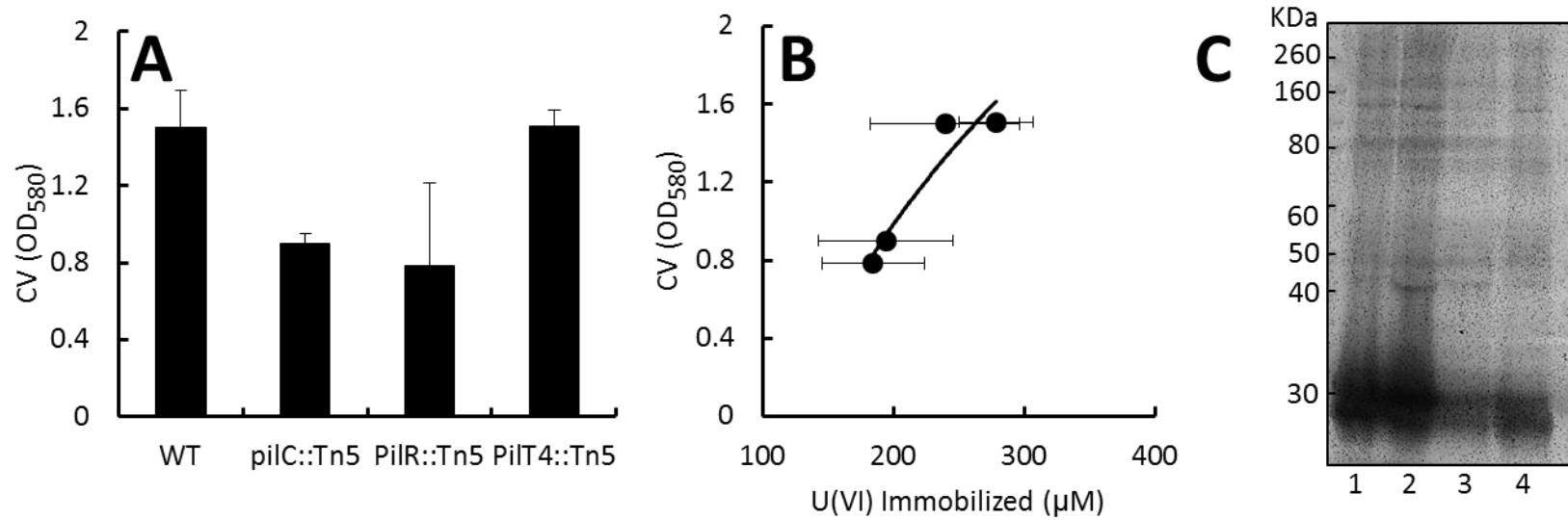


**FIGURE 4.3: Phenotypic characterization of selected mutants.** Biofilm assay (A), correlation between U removal and biomass (B), and heme content of EPS (C) are shown. Lane 1, WT; lane 2, *pilC::Tn5*; lane 3, *pilR::Tn5*; lane 4, *pilT4::Tn5*.

**Conclusions.** The results demonstrate that biofilm formation in *G. sulfurreducens* is a developmental process requiring the expression of specific genes at each stage. Genes encoding proteins for capsule and EPS synthesis were required in the early stages of attachment to form monolayered biofilms, consistent with the role of specific components of the cell's exterior at promoting cell-surface interactions. The conductive pili of *G. sulfurreducens* were required for the formation of microcolonies and for biofilm maturation, thus providing additional evidence for the requirement of pili expression as structural support and electronic connections in multilayered biofilms (46, 47). Interestingly, *c*-cytochromes were also required for the formation of microcolonies and biofilm maturation. As the biofilms increase in height, *c*-cytochromes in the biofilm EPS matrix promote long-range electron transfer across the biofilms, thereby supporting the growth of the biofilm cells (28). Taken together, the genetic analyses of biofilm development in *G. sulfurreducens* revealed conservation of components required for biofilm formation in other organisms but also unique components required for the electroactivity of the biofilms.

## **APPENDIX**

**TABLE 4.A.1: Plates, coatings, growth media, and solvents assessed for their use in the biofilm assay.**

<b>96-Well Plate</b>	<b>Manufacturer &amp; Catalog Number</b>
Nunc MicroWell Plate	Thermo Scientific Cat. No. 260836
Nunc MicroWell MaxiSorp Plate	Thermo Scientific Cat. No. 456537
Costar Cell Culture Cluster Plate	Corning Cat. No. 3595
Fisherbrand Clear Polystyrene Plate	Fisher Scientific Cat. No. 15-565-500
BD Falcon PVC Flexible U Bottom Plate	BD Biosciences Cat. No. 353911

<b>Coating</b>	<b>Manufacturer &amp; Catalog Number</b>
Sigmacote	Sigma-Aldrich Cat. No. SL2
0.01% Poly-D-Lysine Hydrobromide	Sigma-Aldrich Cat. No. P7886
Graphite (Ladd Carbon Evaporator)	Ladd Research

<b>Growth Medium</b>	<b>Reference</b>
FW 15A/40F	(29), with modifications described in (11)
FW 30A/40F	This work
DB 30A/40F	(33, 48, 53)

<b>Solvent</b>	<b>Absorption Wavelength</b>
100% DMSO	590nm
95% Ethanol	580nm
33% Acetic Acid	580nm
80% Ethanol: 20% Acetone	580nm

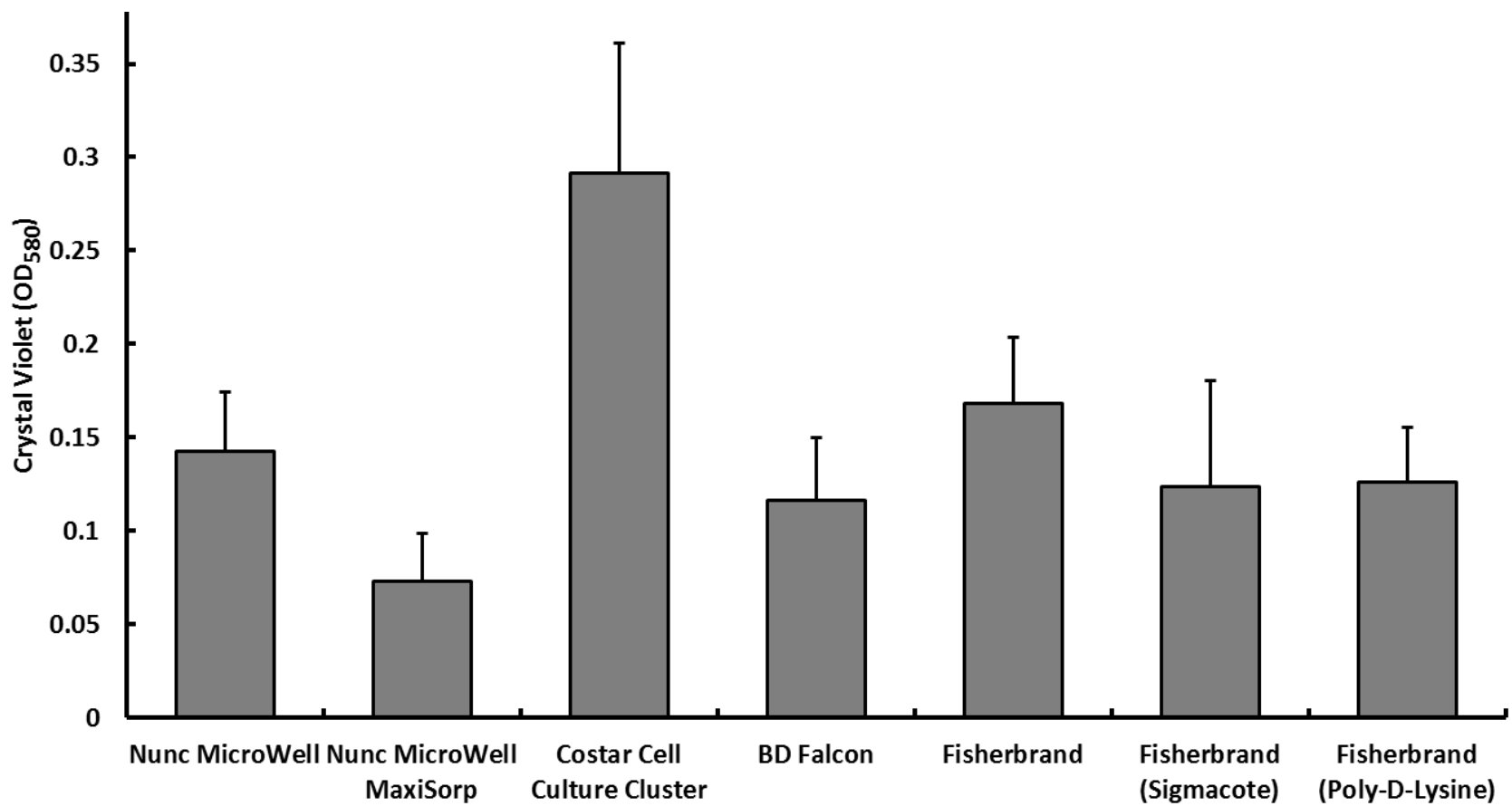
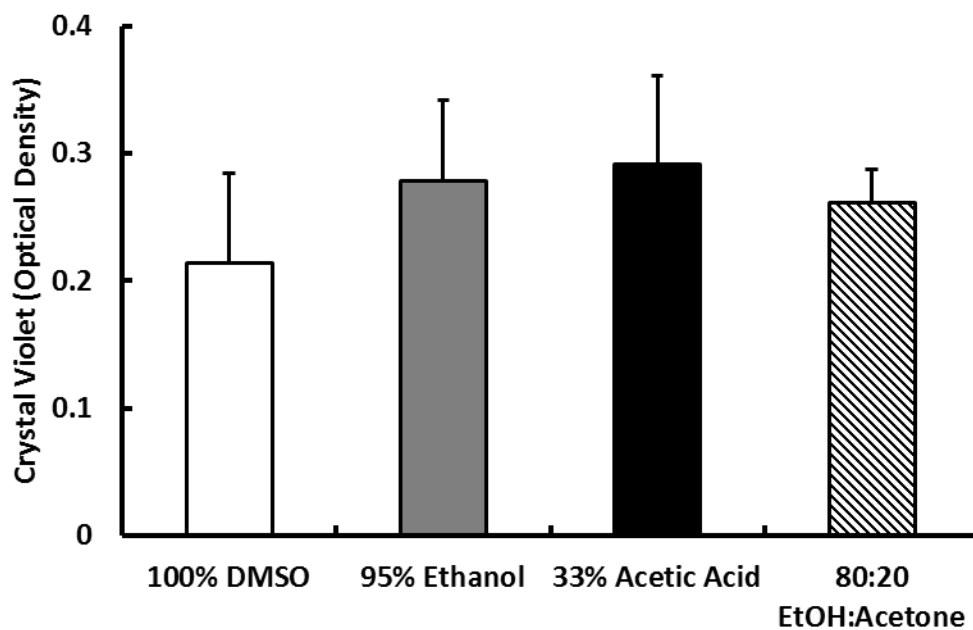


FIGURE 4.A.1: A selection of 96-well plates investigated for their ability to maximize *G. sulfurreducens* 72 h biofilm growth at 30°C.



**FIGURE 4.A.2: Selection of a solvent for de-staining of crystal violet biofilms.** A comparison of the ability of four solvents to dissolve crystal violet-stained biofilms. Shown here is the optical density read at the optimal absorbance for each solvent (DMSO, 590nm; all others, 580nm).

**TABLE 4.A.2: Transposon-insertion mutants displaying deficient or enhanced biofilm phenotypes**

Mutant	GSU locus <sup>a</sup>	Annotation <sup>b</sup>	Coordinate <sup>c</sup>	Growth Rate	Biofilm <sup>d</sup>
21 A2	2282	CBS Domain Protein	2498835-2498836	+	-
22 A10	1945	Fibronectin type III domain protein	2132741-2132742	+	-
29 B10	3385	Phosphoenolpyruvate Carboxykinase (pckA)	3723531-3723532	+	-
31 C5	1493	Type IV Pilus Biogenesis Protein PilC	1638348-1638349	-	-
24 D5	2912	Cytochrome C Family Protein	3209497-32099498	+	+
21 B1	0274	Cytochrome C Family Protein	283025-283026	+	+
7 G8	3332 <sup>e</sup>	Cytochrome C Family Protein	3661881-3661882	+	+
25 E1	3439	NADH Dehydrogenase I, G Subunit	3785649-3785650	+	+
21 A11	2762	Glycerol Kinase (glpK)	3043161-3043162	+	+
35 E2	1843	Metallo-beta-lactamase family protein (similar to RNA metabolizing)	2011467-2011468	+	+
19 C10	1227	ABC Transporter, ATP-Binding Protein	1330619-1330620	+	+
23 C2	1434	Peptide ABC transporter permease protein	1573183-1573184	+	+
17 C6	3363	Sigma-54-Dependent Transcriptional Regulator, Fis Family	3695163-3695164	+	+
19 H10	0253	Sensory Box Histidine Kinase	262719-262720	+	+
20 G1	3343	SpoVR-Like Family Protein	3671647-3671648	+	+
21 B2	1626	Transcriptional Regulator, GntR Family	1781558-1781559	+	+
21 D4	3118	DNA-Binding Response Regulator	3420238-3420239	+	+
23 D1	0281	Sensor histidine kinase, authentic frameshift (near cadherin gene)	310083-310084	+	+
27 E10	0474	Sensory Box/GGDEF	505038-505039	+	+
35 B2	1495	Sigma-54 dependent DNA-binding response regulator	1641425-1641426	+	+

**TABLE 4.A.2 (cont'd)**

25 B3	0058	CRISPR-associated protein, cas2 (298bp after –sRNA region)	74899-74900	+	+
22 H2	0002	RecF Protein	3030-3031	+	+
21 A4	2387	B12-Binding Domain	2616527-2616528	+	+
21 E9	3157	Hydrolase, alpha/beta fold family	3464948-3464949	+	+
23 H12	0978 <sup>e</sup>	Hypothetical Protein (in Phage Operon)	1055246-1055247	+	+
25 C2	0238	Radical SAM Domain Protein	246566-246567	+	+
19 H11	1261	ATP transporter, ATP binding protein	1373553-137354	+	+
21 A8	1700	NAD-dependent malic enzyme (maeB)	1862353-1862354	+	+
35 A3	0474	Sensory Box/GGDEF	505038-505039	+	+
35 B6	0474	Sensory Box/GGDEF	505038-505039	+	+
35 F6	1122	HD Domain Protein	1207423-1207424	+	+
35 G6	0992	Hypothetical protein	1073609-1073610	+	+
35 B7	3199	Chemotaxis protein CheA (CheA-3)	3507763-3507764	+	+
35 C7	0174	Acetyl-CoA Hydrolase/Transferase Family Protein	189971-189972	+	+
37 D2	1074	DNA-Binding Regulatory Protein, YebC/PmpR Family	1163749-1163750	+	+
37 D9	2403 <sup>e</sup>	Hypothetical Protein	2638633-2638633	+	+
37 F2	1949	Hypothetical Protein	2136757-2136758	+	+
39 F11	1942	UDP-Glucose/UDP-Mannose Dehydrogenase Family Protein	2127220-2127221	+	+
39 H1	1970	Polysaccharide Biosynthesis Protein, Putative	2161395-2161396	+	+
3 H11	3295	Conserved Hypothetical Protein	3614122-3614123	++	+
7 A11	0474	Sensory Box/GGDEF	505038-505039	+	+
7 C12	1485	Ribonuclease R, putative	1628979-1628980	+	+
1D9	1183	O-acetyl-L-homoserine sulfhydrylase	1290628-1290629	+	++
1 C8	2502	Spermine/Spermidine Synthase Family Protein	2756295-2756296	+	++
3 A1	3459/ 3460 <sup>e</sup>	Hypothetical Protein & Glycosyl transferase, group 2 family protein (between)	3804868-3804869	+	++

**TABLE 4.A.2 (cont'd)**

17 H7	1432	TRP Domain Protein	1569923-1569924	+	++
21 A5	0377	Glycine Cleavage System, P Protein, Subunit 1	411286-411287	+	++
26 H8	3457	Glycine Cleavage System Transcriptional Repressor, Putative	3804144-3804144	+	++
21 A9	0775	Sensor Histidine Kinase	832499-832500	+	++
21 B12	1337	Lipoprotein, Putative	1464937-1464938	+	++
21 C5	3321	Phosphoglucomutase/Phosphomannomutase Family Protein	3647205-3647206	+	++
21 F11	3399	Efflux Transporter, RND family, MFP Subunit	3739015-3739016	+	++
21 F12	0222	Cytochrome c oxidase, subunit II	230554-230555	+	++
22 H6	2319/2 320 <sup>e</sup>	Conserved Hypothetical (Upstream of CFA Operon) (245bp upstream), Hypothetical (9bp upstream)	2540037-2540038	+	++
23 E1	1672	Glycerate dehydrogenase (hprA)	1833040-1833041	+	++
23 E2	0180	Conserved Hypothetical Protein (near metabolic genes)	194573-194574	+	++
23 F1	0968	Hypothetical protein	1042230-1042231	+	++
24 A3	3318	Conserved Hypothetical Protein	3644746-3644747	+	++
24 A7	1185	Conserved Hypothetical Protein	1293096-1293097	+	++
24 B4	3418	Sigma 54-Dependent DNA-Binding Response Regulator	3761837-3761838	+	++
24 E2	3326	Conserved Hypothetical (Downstream of Exinuclease ABC (uvrA))	3655240-3655241	+	++
24 F8	2697	Multidrug Resistance Protein	2978002-2978003	+	++
24 G2	1945	Fibronectin type III domain protein	2132741-2132742	+	++
25 A8	0098 <sup>e</sup>	MglB Protein (29bp upstream)	113579-113580	+	++
25 D11	0238	Radical SAM Domain Protein	246566-246567	+	++
25 F6	2671	Hypothetical Protein	2946824-2946824	+	++
25 H10	1492	Twitching Motility Protein PilT (PilT-4)	1637002-1637003	+	++
26 B12	0306	Hydrogenase Maturation Protein (HypF)	339834-339833	+	++

**TABLE 4.A.2 (cont'd)**

26 H1	0302	Hypothetical Protein	331689-331690	+	++
28 G12	3158	Cysteine Synthase B (cysM)	3465380-3465381	+	++
35 C3	3459/3 460 <sup>e</sup>	Hypothetical Protein & Glycosyl transferase, group 2 family protein (between)	3804868-3804869	+	++
35 E8	1733	Branched-chain amino acid ABC transporter permease protein (livH)	1898384-1898385	+	++
35 F8	0728	Polyphosphate:AMP Phosphotransferase (pap)	775630-775631	+	++
35 H10	1358	Conserved Hypothetical Protein	1484097-1484098	+	++
35 G11	1009	GTP-Binding Protein	1090260-1090261	+	++
38 A8	0323 <sup>e</sup>	General Secretion Pathway Protein J, Putative (47bp upstream)	354290-354291	+	++
38 C5	1527	Conserved Hypothetical Protein	1674377-1674378	+	++
28 B8	2330/2 332	Conserved Hypothetical and Hypothetical (CFA Operon)	2550521-2550522	+	++++
28 B11	3386	Lipoprotein, putative	3723753-3723754	+	++++
28 H10	1007	GAF Domain/HD Domain Protein	1087571-1087572	+	++++
29 H10	0244	Radical SAM Domain Protein	251774-251775	+	++++
31 B9	0924	ABC Transporter, Permease Protein, Putative	993660-993661	+	++++
32 D9	3459/3 460	Hypothetical Protein & Glycosyl transferase, group 2 family protein (between)	3804868-3804869	+	++++
32 F12	2330/2 332	Conserved Hypothetical and Hypothetical (CFA Operon)	2550521-2550522	+	++++
1D1	0058	CRISPR-associated protein, cas2 (298bp after -sRNA region)	74899-74900	+	++++

<sup>a</sup> GSU locus containing the transposon insertion, <sup>b</sup> Annotation assigned by JCVI, <sup>c</sup> Genomic coordinate for the transposon insertion  
<sup>d</sup> Biofilm phenotype: no attachment (-), low (+), and medium (++) in reference to WT (+++), <sup>e</sup> Insertion just upstream of designated open reading frame

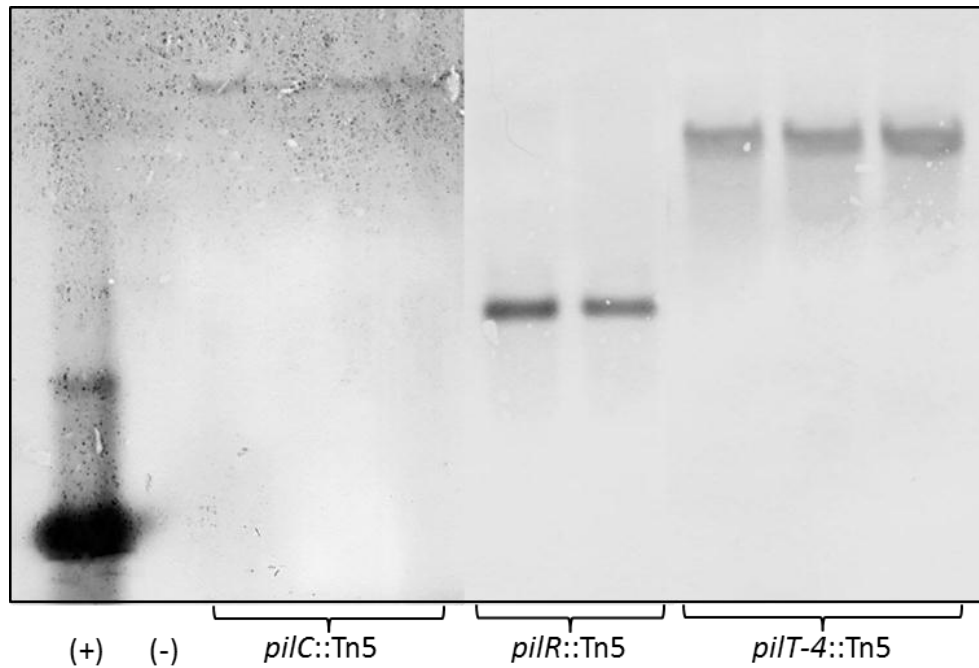


**FIGURE 4.A.3: Southern blot to confirm a single Tn5 insertion event.** A positive control of the Tn5 probe (+) and negative control (wild-type genomic DNA) (-) are shown in addition to the *pilC::Tn5*, *pilR::Tn5*, *pilT-4::Tn5* insertion mutants (2-4 clones of each).

## REFERENCES

## REFERENCES

1. **Aklujkar, M., and D. R. Lovley.** 2010. Interference with histidyl-tRNA synthetase by a CRISPR spacer sequence as a factor in the evolution of *Pelobacter carbinolicus*. *BMC Evol Biol* **10**:230.
2. **Anderson, G. G., C. C. Goller, S. Justice, S. J. Hultgren, and P. C. Seed.** Polysaccharide capsule and sialic acid-mediated regulation promote biofilm-like intracellular bacterial communities during cystitis. *Infect Immun* **78**:963-975.
3. **Anderson, R. T., H. A. Vrionis, I. Ortiz-Bernad, C. T. Resch, P. E. Long, R. Dayvault, K. Karp, S. Marutzky, D. R. Metzler, A. Peacock, D. C. White, M. Lowe, and D. R. Lovley.** 2003. Stimulating the in situ activity of *Geobacter* species to remove uranium from the groundwater of a uranium-contaminated aquifer. *Appl. Environ. Microbiol.* **69**:5884-5891.
4. **Ausubel, F. M., R. Brent, R. E. Kingston, D. D. Moore, J. G. Seidman, J. A. Smith, and K. Struhl.** 1995. *Current Protocols in Molecular Biology*, vol. 2. John Wiley & Sons, Inc.
5. **Beall, B., and C. P. Moran, Jr.** 1994. Cloning and characterization of spoVR, a gene from *Bacillus subtilis* involved in spore cortex formation. *J Bacteriol* **176**:2003-2012.
6. **Caetano-Anolles, G.** 1993. Amplifying DNA with arbitrary oligonucleotide primers. *PCR Methods Appl* **3**:85-94.
7. **Cao, B., B. Ahmed, and H. Beyenal.** 2010. Immobilization of Uranium in Groundwater Using Biofilms, p. 1-37. *In* V. Shah (ed.), *Emerging Environmental Technologies*, vol. Volume II. Springer Netherlands.
8. **Chang, B. Y., and M. Dworkin.** 1994. Isolated fibrils rescue cohesion and development in the Dsp mutant of *Myxococcus xanthus*. *J Bacteriol* **176**:7190-7196.
9. **Chiang, P., and L. L. Burrows.** 2003. Biofilm formation by hyperpiliated mutants of *Pseudomonas aeruginosa*. *J Bacteriol* **185**:2374-2378.
10. **Coates, J. D., D. J. Lonergan, H. Jenter, and D. R. Lovley.** 1996. Isolation of *Geobacter* species from diverse sedimentary environments. *Appl. Environ. Microbiol.* **62**:1531-1536.
11. **Cologgi, D. L., S. Lampa-Pastirk, A. M. Speers, S. D. Kelly, and G. Reguera.** 2011. Extracellular reduction of uranium via *Geobacter* conductive pili as a protective cellular mechanism. *Proc Natl Acad Sci U S A* **108**:15248-15252.
12. **Coppi, M. V., C. Leang, S. J. Sandler, and D. R. Lovley.** 2001. Development of a genetic system for *Geobacter sulfurreducens*. *Appl. Environ. Microbiol.* **67**:3180-3187.

13. **Costerton, J. W.** 1995. Overview of microbial biofilms. *J Ind Microbiol* **15**:137-140.
14. **Costerton, J. W., K. J. Cheng, G. G. Geesey, T. I. Ladd, J. C. Nickel, M. Dasgupta, and T. J. Marrie.** 1987. Bacterial biofilms in nature and disease. *Annu. Rev. Microbiol.* **41**:435-464.
15. **Costerton, J. W., Z. Lewandowski, D. E. Caldwell, D. R. Korber, and H. M. Lappin-Scott.** 1995. Microbial biofilms. *Annu Rev Microbiol* **49**:711-745.
16. **Davey, M. E., and M. J. Duncan.** 2006. Enhanced biofilm formation and loss of capsule synthesis: deletion of a putative glycosyltransferase in *Porphyromonas gingivalis*. *J Bacteriol* **188**:5510-5523.
17. **Davey, M. E., and A. O'Toole G.** 2000. Microbial biofilms: from ecology to molecular genetics. *Microbiol. Mol. Biol. Rev.* **64**:847-867.
18. **Davies, D. G., and G. G. Geesey.** 1995. Regulation of the alginate biosynthesis gene *algC* in *Pseudomonas aeruginosa* during biofilm development in continuous culture. *Appl Environ Microbiol* **61**:860-867.
19. **Finneran, K. T., R. T. Anderson, K. P. Nevin, and D. R. Lovley.** 2002. Potential for Bioremediation of uranium-contaminated aquifers with microbial U(VI) reduction. *Soil & Sediment Contamination* **11**:339-357.
20. **Goryshin, I. Y., J. Jendrisak, L. M. Hoffman, R. Meis, and W. S. Reznikoff.** 2000. Insertional transposon mutagenesis by electroporation of released *Tn5* transposition complexes. *Nat. Biotechnol.* **18**:97-100.
21. **Harrison, J. J., H. Ceri, and R. J. Turner.** 2007. Multimetal resistance and tolerance in microbial biofilms. *Nat. Rev. Microbiol.* **5**:928-938.
22. **Inoue, K., X. Qian, L. Morgado, B. C. Kim, T. Mester, M. Izallalen, C. A. Salgueiro, and D. R. Lovley.** 2010. Purification and characterization of OmcZ, an outer-surface, octaheme c-type cytochrome essential for optimal current production by *Geobacter sulfurreducens*. *Appl Environ Microbiol* **76**:3999-4007.
23. **Juarez, K., B. C. Kim, K. Nevin, L. Olvera, G. Reguera, D. R. Lovley, and B. A. Methe.** 2009. PilR, a transcriptional regulator for pilin and other genes required for Fe(III) reduction in *Geobacter sulfurreducens*. *J Mol Microbiol Biotechnol* **16**:146-158.
24. **Kataeva, I. A., R. D. Seidel, 3rd, A. Shah, L. T. West, X. L. Li, and L. G. Ljungdahl.** 2002. The fibronectin type 3-like repeat from the *Clostridium thermocellum* cellobiohydrolase CbhA promotes hydrolysis of cellulose by modifying its surface. *Appl Environ Microbiol* **68**:4292-4300.

25. **Kerkhof, L. J., K. H. Williams, P. E. Long, and L. R. McGuinness.** 2011. Phase Preference by Active, Acetate-Utilizing Bacteria at the Rifle, CO Integrated Field Research Challenge Site. *Environmental science & technology* **45**:1250-1256.
26. **Kirby, J. R.** 2007. In vivo mutagenesis using EZ-*Tn5*. *Methods Enzymol.* **421**:17-21.
27. **Levano-Garcia, J., S. Verjovski-Almeida, and A. C. da Silva.** 2005. Mapping transposon insertion sites by touchdown PCR and hybrid degenerate primers. *Biotechniques* **38**:225-229.
28. **Liu, Y., and D. R. Bond.** 2012. Long-Distance Electron Transfer by *G. sulfurreducens* Biofilms Results in Accumulation of Reduced c-Type Cytochromes. *ChemSusChem* **5**:1047-1053.
29. **Lovley, D. R., and S. Goodwin.** 1988. Hydrogen concentrations as an indicator of the predominant terminal electron accepting reactions in aquatic sediments. *Geochim. Cosmochim. Acta* **52**:2993-3003.
30. **Lovley, D. R., and E. J. P. Phillips.** 1988. Novel mode of microbial energy metabolism: organic carbon oxidation coupled to dissimilatory reduction of iron or manganese. *Appl. Environ. Microbiol.* **54**:1472-1480.
31. **Mack, D., M. Nedelmann, A. Krokotsch, A. Schwarzkopf, J. Heesemann, and R. Laufs.** 1994. Characterization of transposon mutants of biofilm-producing *Staphylococcus epidermidis* impaired in the accumulative phase of biofilm production: genetic identification of a hexosamine-containing polysaccharide intercellular adhesin. *Infect. Immun.* **62**:3244-3253.
32. **Mah, T. F., B. Pitts, B. Pellock, G. C. Walker, P. S. Stewart, and G. A. O'Toole.** 2003. A genetic basis for *Pseudomonas aeruginosa* biofilm antibiotic resistance. *Nature* **426**:306-310.
33. **Marsili, E., D. B. Baron, I. D. Shikhare, D. Coursolle, J. A. Gralnick, and D. R. Bond.** 2008. *Shewanella* secretes flavins that mediate extracellular electron transfer. *Proc. Natl. Acad. Sci. U S A* **105**:3968-3973.
34. **Marsili, E., J. B. Rollefson, D. B. Baron, R. M. Hozalski, and D. R. Bond.** 2008. Microbial biofilm voltammetry: direct electrochemical characterization of catalytic electrode-attached biofilms. *Appl Environ Microbiol* **74**:7329-7337.
35. **Mattick, J. S.** 2002. Type IV pili and twitching motility. *Annu. Rev. Microbiol.* **56**:289-314.
36. **Mehta, T., S. E. Childers, R. Glaven, D. R. Lovley, and T. Mester.** 2006. A putative multicopper protein secreted by an atypical type II secretion system involved in the reduction of insoluble electron acceptors in *Geobacter sulfurreducens*. *Microbiology* **152**:2257-2264.

37. **Merritt, J. H., D. E. Kadouri, and G. A. O'Toole.** 2005. Growing and analyzing static biofilms. *Curr Protoc Microbiol* **Chapter 1**:Unit 1B 1.
38. **Moyrand, F., and G. Janbon.** 2004. UGD1, encoding the *Cryptococcus neoformans* UDP-glucose dehydrogenase, is essential for growth at 37 degrees C and for capsule biosynthesis. *Eukaryotic cell* **3**:1601-1608.
39. **O'Toole, G., H. B. Kaplan, and R. Kolter.** 2000. Biofilm formation as microbial development. *Annu. Rev. Microbiol.* **54**:49-79.
40. **O'Toole, G. A., and R. Kolter.** 1998. Flagellar and twitching motility are necessary for *Pseudomonas aeruginosa* biofilm development. *Mol. Microbiol.* **30**:295-304.
41. **O'Toole, G. A., and R. Kolter.** 1998. Initiation of biofilm formation in *Pseudomonas fluorescens* WCS365 proceeds via multiple, convergent signalling pathways: a genetic analysis. *Mol. Microbiol.* **28**:449-461.
42. **O'Toole, G. A., L. A. Pratt, P. I. Watnick, D. K. Newman, V. B. Weaver, and R. Kolter.** 1999. Genetic approaches to study of biofilms. *Methods Enzymol.* **310**:91-109.
43. **Pratt, L. A., and R. Kolter.** 1998. Genetic analysis of *Escherichia coli* biofilm formation: roles of flagella, motility, chemotaxis and type I pili. *Mol. Microbiol.* **30**:285-293.
44. **Reguera, G., and R. Kolter.** 2005. Virulence and the environment: a novel role for *Vibrio cholerae* toxin-coregulated pili in biofilm formation on chitin. *J. Bacteriol.* **187**:3551-3555.
45. **Reguera, G., K. D. McCarthy, T. Mehta, J. S. Nicoll, M. T. Tuominen, and D. R. Lovley.** 2005. Extracellular electron transfer via microbial nanowires. *Nature* **435**:1098-1101.
46. **Reguera, G., K. P. Nevin, J. S. Nicoll, S. F. Covalla, T. L. Woodard, and D. R. Lovley.** 2006. Biofilm and nanowire production lead to increased current in microbial fuel cells. *Appl. Environ. Microbiol.* **72**:7345-7348.
47. **Reguera, G., R. B. Pollina, J. S. Nicoll, and D. R. Lovley.** 2007. Possible Nonconductive Role of *Geobacter sulfurreducens* Pilus Nanowires in Biofilm Formation. *J. Bacteriol.* **189**:2125-2127.
48. **Rollefson, J. B., C. E. Levar, and D. R. Bond.** 2009. Identification of genes involved in biofilm formation and respiration via mini-Himar transposon mutagenesis of *Geobacter sulfurreducens*. *J Bacteriol* **191**:4207-4217.
49. **Rollefson, J. B., C. S. Stephen, M. Tien, and D. R. Bond.** 2011. Identification of an extracellular polysaccharide network essential for cytochrome anchoring and biofilm formation in *Geobacter sulfurreducens*. *J Bacteriol* **193**:1023-1033.

50. **Sadykov, M. R., T. A. Mattes, T. T. Luong, Y. Zhu, S. R. Day, C. D. Sifri, C. Y. Lee, and G. A. Somerville.** 2010. Tricarboxylic acid cycle-dependent synthesis of *Staphylococcus aureus* Type 5 and 8 capsular polysaccharides. *J Bacteriol* **192**:1459-1462.
51. **Shelobolina, E. S., M. V. Coppi, A. A. Korenevsky, L. N. DiDonato, S. A. Sullivan, H. Konishi, H. Xu, C. Leang, J. E. Butler, B. C. Kim, and D. R. Lovley.** 2007. Importance of *c*-Type cytochromes for U(VI) reduction by *Geobacter sulfurreducens*. *BMC Microbiol.* **7**:16.
52. **Southey-Pillig, C. J., D. G. Davies, and K. Sauer.** 2005. Characterization of temporal protein production in *Pseudomonas aeruginosa* biofilms. *J Bacteriol* **187**:8114-8126.
53. **Speers, A. M., and G. Reguera.** 2012. Electron donors supporting growth and electroactivity of *Geobacter sulfurreducens* anode biofilms. *Appl Environ Microbiol* **78**:437-444.
54. **Thomas, P. E., D. Ryan, and W. Levin.** 1976. An improved staining procedure for the detection of the peroxidase activity of cytochrome P-450 on sodium dodecyl sulfate polyacrylamide gels. *Analytical biochemistry* **75**:168-176.
55. **Vimr, E., S. Steenbergen, and M. Cieslewicz.** 1995. Biosynthesis of the polysialic acid capsule in *Escherichia coli* K1. *J Ind Microbiol* **15**:352-360.
56. **Wang, L., S. Li, and Y. Li.** 2003. Isolation and sequencing of glycosyltransferase gene and UDP-glucose dehydrogenase gene that are located on a gene cluster involved in a new exopolysaccharide biosynthesis in *Streptomyces*. *DNA sequence : the journal of DNA sequencing and mapping* **14**:141-145.
57. **Wang, L. Y., S. T. Li, and Y. Li.** 2003. Identification and characterization of a new exopolysaccharide biosynthesis gene cluster from *Streptomyces*. *FEMS Microbiol Lett* **220**:21-27.
58. **Wang, X., J. F. Preston, 3rd, and T. Romeo.** 2004. The *pgaABCD* locus of *Escherichia coli* promotes the synthesis of a polysaccharide adhesin required for biofilm formation. *J Bacteriol* **186**:2724-2734.
59. **Watanabe, T., Y. Ito, T. Yamada, M. Hashimoto, S. Sekine, and H. Tanaka.** 1994. The roles of the C-terminal domain and type III domains of chitinase A1 from *Bacillus circulans* WL-12 in chitin degradation. *J Bacteriol* **176**:4465-4472.
60. **Watnick, P. I., and R. Kolter.** 1999. Steps in the development of a *Vibrio cholerae* El Tor biofilm. *Mol. Microbiol.* **34**:586-595.
61. **Wimpenny, J. W., and R. Colasanti.** 1997. A unifying hypothesis for the structure of microbial biofilms based on cellular automaton models. *FEMS Microbiol Ecol* **22**:1-16.

62. **Wolfgang, M., J. P. van Putten, S. F. Hayes, D. Dorward, and M. Koomey.** 2000. Components and dynamics of fiber formation define a ubiquitous biogenesis pathway for bacterial pili. *EMBO J* **19**:6408-6418.

## CHAPTER 5

### IDENTIFICATION AND CHARACTERIZATION OF THE RPOE SIGMA FACTOR OF *GEOBACTER SULFURREDUCTENS*

The following former members of Dr. Gemma Reguera (Michigan State University) and Dr. Derek Lovley's (University of Massachusetts, Amherst) laboratories contributed to the work presented in the chapter:

**Blair Bullard** (Michigan State University): Biofilm assays

**Dr. Evengeny Shelobolina** (University of Massachusetts, Amherst): resting cell suspensions

**Dr. Gemma Reguera** (University of Massachusetts, Amherst/Michigan State University): mutant generation, bioinformatic analyses, biofilm assays, and microarray analyses

## ABSTRACT

Metal and electrode reduction in *Geobacter* bacteria is intimately connected to the integrity and functionality of the cell envelope, yet little is known about its regulation. Here we report on the genetic identification and functional characterization of the RpoE sigma factor of *Geobacter sulfurreducens* (RpoE<sub>GSU</sub>). As reported for other RpoE sigma factors such as in *Escherichia coli*, RpoE<sub>GSU</sub> regulated growth transitions in response to nutritional shifts and during biofilm formation, and was also involved in the oxidative stress response. All of these functions ultimately depended on the role of RpoE in the regulation of cell envelope integrity and homeostasis. Despite these conserved roles, RpoE<sub>GSU</sub> was not required for growth at high temperatures or low pHs, but for growth at lower temperatures and higher pHs, thus reflecting the adaptation of *G. sulfurreducens* extracytoplasmic functions to stressors commonly found in environments inhabited by *Geobacter* bacteria. The phenotypes were also consistent with transcriptomic profiling, which identified genes in the RpoE regulon required for conserved mechanisms of RpoE response to cell envelope stress as well as specialized responses required to regulate *Geobacter* extracellular electron transfer pathways. This work highlights the functional specialization that RpoE has undergone to control the adaptive responses that enable *Geobacter* bacteria to survive in the subsurface and that are relevant for applications in bioremediation and current generation in microbial fuel cells.

## INTRODUCTION

Microorganisms in the family *Geobacteraceae* conserve energy to support growth from the reduction of Fe(III) and Mn(IV) (44) and are also recognized as important agents in the bioremediation of organic (2, 43, 65, 66, 70) or metal (3, 46, 60) contaminants, and as primary contributors to current production in microbial fuel cells harvesting electricity from the environment (4, 23, 42, 71). Key to their physiology and applications is the control of electron transfer across the cell envelope. The genome sequence of some representative species of the *Geobacteraceae* available in pure culture reveals a great number of genes potentially encoding cell envelope proteins involved in electron transfer processes as well as a complex regulatory circuitry that could be responsible for signal integration and response to environmental cues (48). Studies in the model dissimilatory Fe(III) reducer *Geobacter sulfurreducens* have shown that the expression of most genes known to be of relevance to electron transfer may be tightly regulated (15, 24, 25, 28, 31-33, 35, 49, 57, 58, 73). Some of these studies (28, 34, 57, 58, 73, 76-78) have identified a great number of genes and operons encoding proteins relevant to electron transfer and environmental survival that may be under transcriptional control by sigma factors. The expression and/or availability of sigma factors is regulated by environmental signals. As a result, sigma factors modulate the cell's transcriptional machinery and allow it to reprogram gene expression by 'turning on' those genes necessary to respond to a particular environmental signal and 'turning off' those that are no longer needed (27).

The genome of *G. sulfurreducens* contains genes encoding homologues of the sigma factors RpoD, RpoS, RpoH, RpoE and FliA of the  $\sigma^{70}$ -family (48). The RpoS ( $\sigma^S$ ) of *G. sulfurreducens* controls the expression of genes required for survival in stationary phase,

oxygen tolerance, heat shock and alkaline stress responses, and electron transfer pathways to Fe(III) (57, 58), whereas RpoH ( $\sigma^H$ ,  $\sigma^{32}$ ) controls the heat shock response (73) and FliA is predicted to function in regulating the expression of flagellar and chemotaxis-related genes (37, 72). To date, no functional characterization is available for RpoE in *G. sulfurreducens*.

RpoE is a member of the extracytoplasmic function (ECF) subfamily, which encompasses those  $\sigma^{70}$  factors that respond to extracytoplasmic stimuli such as the accumulation of misfolded proteins in the periplasmic space (RpoE) or the extracellular availability of ferric citrate (Fecl) (16, 22, 52, 62). The RpoE homologue of *G. sulfurreducens* is the only ECF sigma factor identified in its genome (48). Although annotated as a putative RpoE sigma factor, sequence analyses of the encoding gene failed to shed light on its function, and putative roles as an RpoE (57) or a Fecl (76) sigma factor have been proposed. Bioinformatics analyses using *E. coli*'s known transcription factors and transcription regulatory sites also failed to identify conserved RpoE-like regulatory elements in the genome of *G. sulfurreducens* (76). As a result, no functional confirmation is yet available for the putative RpoE sigma factor in this organism. As this is the only ECF sigma factor homologue identified in the genome of *G. sulfurreducens*, we hypothesized that the identified gene represents a functional RpoE sigma factor and major regulator of cell envelope functions such as metal reduction and survival of this organism in the subsurface. To further elucidate the role of RpoE, we investigated the genetic organization and operon structure of the *rpoE* gene. We also studied the phenotype of an *rpoE* deletion mutant under a variety of growth conditions and environmental stresses. The results demonstrate that RpoE plays a role in the maintenance of cell envelope integrity and physiological responses of

*Geobacter* spp. that are relevant to metal reduction and applications in bioremediation and microbial fuel cells.

## MATERIALS AND METHODS

**Bacterial strains and culture conditions.** *Geobacter sulfurreducens* strain ATCC 51573 (6) was obtained from the American Type Culture Collection (ATCC). The RpoE-deficient (RpoE<sup>-</sup>) mutant used in this study was generated by complete deletion of the *rpoE* gene (GSU0721) and insertion of a kanamycin resistance cassette in the same orientation of *rpoE* transcription (Gemma Reguera, personal communication). The wild-type (WT) strain and RpoE<sup>-</sup> mutant were routinely cultured in NB (10) or fresh water (FW) (9, 45) medium containing 15 mM acetate and 40 mM fumarate (NBAF or FWAF). NBAF medium was supplemented with 1 mM cysteine-HCl and 0.1% yeast extract and, when indicated, 20mM MOPS buffer. FWAF was supplemented with 0.25 mM cysteine-HCl and 0.05% yeast extract. Cultures were incubated at 30°C unless otherwise indicated. Growth curves were generated from mid-log phase cultures grown in NBAF medium and inoculated to a final OD<sub>600</sub> of 0.04 in NBAF medium. Growth was measured spectrophotometrically by periodically monitoring the optical density (OD<sub>600</sub>) of the cultures.

**Complementation.** A wild-type copy of the *rpoE* gene was PCR-amplified using primers RpoE-Comp-pRG5-F (BglII): GGAAGATCTAAGGAGAAGTGACGCTGGAT and RpoE-Comp-pRG5-R (HindIII): CCCAAGCTTTCACGCTCGTCATGTTTCAT (restriction sites are underlined) and Phusion high-fidelity DNA polymerase (New England Biolabs) according to the manufacturer's

specification. PCRs were carried out on a Mastercycler Personal (Eppendorf) using the following conditions: 98°C for 30 s, followed by 30 cycles of 98°C for 10 s, 55°C for 30 s, and 72°C for 30 s, followed by a final 10 min extension step at 72°C. The resulting PCR products were digested with BglII and HindIII (New England Biolabs), and a medium-copy plasmid, pRG5 (32), was digested with BamHI and HindIII (New England Biolabs) according to the manufacturer's recommendations. The digested products were ligated with T4 DNA ligase (Invitrogen) according to the manufacturer's recommendations. RpoE<sup>-</sup> electrocompetent cells were prepared as described previously (10), and ~1 µg of the pRG5::*rpoE* plasmid was electroporated using a Eppendorf 2510 Electroporator operated at 1470 volts. Cultures were recovered overnight and then plated on NBAF medium supplemented with 75 µg/ml spectinomycin to select for the pRG5 plasmid. Controls included non-electroporated competent cells, cells that were subjected to electroporation without the introduction of foreign DNA, and cells electroporated with the pRG5 plasmid only (no insert).

**Transcriptional analysis of the *rpoE* gene and the gene region by RT-PCR.** Reverse Transcriptase-Polymerase Chain Reaction (RT-PCR) was used to quantify the transcription of the *rpoE* gene and the downstream genes (GSU0722 and GSU0723). For these experiments, cells of the wild-type and RpoE<sup>-</sup> mutant were grown in NBAF at 25°C, 30°C, and 35°C. RNA was extracted using TRIzol reagent (Invitrogen), treated with RQ1 RNase-free DNase (Promega), and reverse transcription was performed using Superscript III Reverse Transcriptase (Invitrogen), all according to the manufacturer's recommendations. Reverse transcription and PCR amplification of *rpoE* was performed using primers RpoE-qPCR-771279F (5'-

GTGACGCTGGATACAACAGACGAA-3') and RpoE-qPCR-771430R

(5'GCGCATAGTTTCTGACAAAGCCGA-3'). The co-transcription of *rpoE* with the downstream genes (GSU0722 and GSU0723) was studied using primer combinations RpoE-qPCR-771279 with GSU0722-R (5' TCATTGGCTGCAATCAACTC 3') and GSU0723-R (5' CCGGAATCATCAGTTGACCT 3'), respectively. A constitutively-expressed control gene, *recA*, was assayed using primers *recA660f* and *recA737r* (25). Using the cDNA generated from reverse transcription, a PCR reaction was performed on a Mastercycler egradient S (Eppendorf) using the following conditions: 95°C for 5 min, followed by 30 cycles of 94°C for 30 s, 55°C for 45 s, and 72°C for 1 min, followed by a final 10 min extension step at 72°C. The resulting products were run on a 1.2% agarose gel, stained with ethidium bromide, and visualized using an AlphaImager™2200 (Cell Biosciences).

**Stress tolerance assays.** The aerotolerance of the wild-type and RpoE<sup>-</sup> mutant strains was evaluated in mid-exponential phase cultures grown in FWF medium. 2 mL aliquots were removed from the cultures and placed in sterile cuvettes capped with sterile aluminum foil and incubated at 30°C. The OD<sub>600</sub> of the cultures was monitored periodically and the aerotolerance of the strains was inferred from the decreases in the cultures' absorbance over time.

The effect of pH was assayed using an adaptation of a previously described method (57). Briefly, cultures were grown to mid-exponential phase in MOPS-buffered NBAF medium (pH 7), and then transferred (final OD<sub>600</sub> of 0.04) to fresh medium buffered at pH 6 or 9. After 48 h (pH 6) and 24 h (pH 9) of exposure, the cultures were transferred (10% (v/v) inoculum) into

anaerobic NBAF medium (pH 7) and growth ( $OD_{600}$ ) was monitored periodically. The length of the *lag* phase of the cultures was used to estimate the survival rates of the strains after exposure to suboptimal pH conditions and, therefore, their pH tolerance

**Biofilm assays.** Cells were grown to mid-late exponential phase at 30°C in NBAF medium and transferred three times prior to assaying for biofilm formation. Biofilm assays were performed using glass coverslips (18x18 mm<sup>2</sup>), as previously described (64), except that FWAf medium supplemented with 0.25 mM cysteine and 0.05% yeast extract was used as the growth medium. Planktonic growth was monitored periodically by measuring the  $OD_{600}$  of the culture. Biofilm growth was quantified every 24 h by staining the biofilm biomass on the coverslips with 0.1% crystal violet (59). The biofilm-associated dye was solubilized in 33% acetic acid and quantified by measuring the  $OD_{580}$  of the dye-acid solution. The biofilms were also washed in anaerobic PBS buffer and stained with the BacLight™ viability kit (Invitrogen) prior to examination by Confocal Laser Scanning Microscopy (CLSM) using a Zeiss 510 Meta ConfoCor 3 LSM equipped with a 40X objective.

**Transmission Electron Microscopy (TEM).** Early-stationary phase cultures grown in NBAF medium were mixed with an equal volume of reaction buffer (67). The cell suspension was adsorbed onto 300-mesh carbon-coated copper grids (Ted Pella), fixed with 1% glutaraldehyde for 5 min, washed with ddH<sub>2</sub>O for 3 x 2 min, and stained with 1% uranyl acetate for 30 s. Cells were imaged on a JEOL100CX electron microscope (Japan Electron Optic Laboratory) operated at a 100 kV accelerating voltage.

**Fe(III) reduction assays.** The ability of the wild-type and the RpoE mutant strains to reduce Fe(III) was measured in resting cell suspensions prepared as previously described (67). Briefly, *G. sulfurreducens* strains were cultured in FW medium amended with 10 mM acetate and 20 mM fumarate. Late logarithmic phase cultures were harvested by centrifugation and washed twice in wash buffer, resuspended in reaction buffer, and Fe(III)-reducing activities were quantified, as described before (67). Cells were added to the reaction buffer to give a final OD of ca. 0.06-0.08. The ability of cells to reduce Fe(III) was determined using either poorly crystalline ferric hydroxide (Fe(III) oxide) (20 mM) or ferric citrate (Fe(III) citrate) (20 mM) as the electron acceptor and 5 mM acetate as the electron donor. Fe(II) concentrations were determined hourly using a ferrozine assay as previously described (69). All Fe(III) reduction assays were performed by Evgenya Shelobolina (University of Massachusetts, Amherst).

## RESULTS AND DISCUSSION

**Genetic organization of the *rpoE* region.** ECF sigma factors are often co-transcribed with a transmembrane antisigma factor and an accessory protein, such as RseA and RseB in *E. coli*, respectively (13). The RseA antisigma factor of *E. coli*, for example, is an inner membrane protein with a periplasmic sensory domain and a cytoplasmic anti- $\sigma^E$  domain that sequesters the RpoE protein, thus controlling its cytoplasmic availability and binding to the RNA polymerase (7, 13, 51). The inhibitory function of RseA is enhanced by RseB, a periplasmic protein that binds to RseA's periplasmic domain and protects it from proteolysis (1, 13, 21, 51). Although a search for RseA and RseB homologues in the genome of *G. sulfurreducens* using *E. coli*'s amino acid sequences retrieved no matches (Gemma Reguera, personal communication),

bioinformatics analyses (76) predicted that the gene encoding RpoE in *G. sulfurreducens* (herein termed RpoE<sub>GSU</sub>) is part of a predicted operon with genes encoding a hypothetical protein (GSU0722) and a conserved hypothetical protein (GSU0723) (Fig. 5.1A).

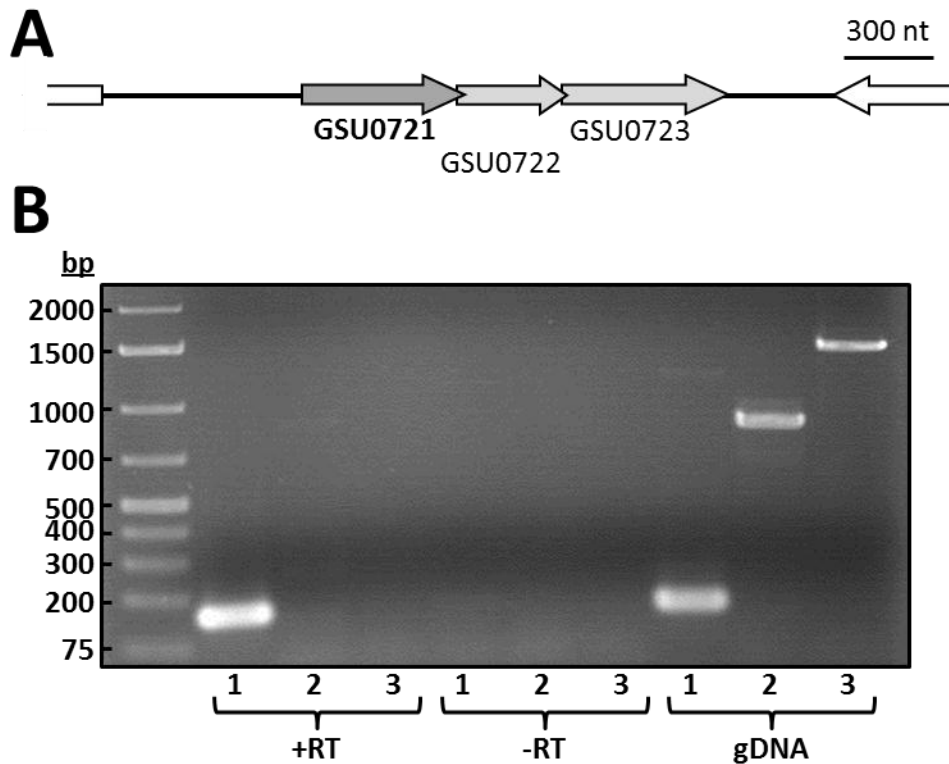


**FIGURE 5.1: Genetic arrangement of the *rpoE* region (A) and transcriptional analysis by reverse transcriptase (RT) PCR of the predicted operon (B). Controls with (+RT) or without (-RT) reverse transcriptase are shown for the *rpoE* operon transcripts, as well as controls with WT genomic DNA (gDNA). 1, GSU0721 only; 2, GSU0721+GSU0722; 3, GSU0721+GSU0722+GSU0723.**

The hypothetical protein encoded by GSU0722 contained one internal helix between amino acids 55 and 74 that could function as a transmembrane domain and had no predicted signal peptide. This is consistent with the cytoplasmic membrane localization expected for a putative antisigma factor. The conserved hypothetical protein encoded by GSU0723 contained a signal peptide with a putative cleavage site between amino acids 35 and 36 (AWG-DG) and

had no transmembrane domains, suggestive of a periplasmic localization, analogous to RseB of *E. coli*. However, transcriptional analyses of the *rpoE* gene region demonstrated that *rpoE* is not co-transcribed with the downstream genes under the conditions tested. Rather, *rpoE* is transcribed independently of the two downstream genes (Fig. 5.1B). These results can be interpreted as RpoE<sub>GSU</sub> being regulated by mechanisms that differ substantially from the canonical regulation of RpoE in *E. coli* and other bacteria, similarly to what has been proposed for several mycobacterial species (74). Interestingly, the genetic arrangement of the *rpoE* gene homologue in *G. sulfurreducens* is conserved in other *Geobacter* spp. such as *Geobacter metallireducens* and *Geobacter uraniireducens*, both containing genes downstream of the *rpoE* homologue encoding a hypothetical protein (45% identity out of 121 amino acids and 38% identity out of 118 amino acids, respectively) and a conserved hypothetical protein (55% identity out of 134 amino acids and 42% identity out of 146 amino acids, respectively) (Gemma Reguera, personal communication). This conservation in the family *Geobacteraceae* is consistent with regulatory adaptations of these organisms to their unique physiology based on extracellular electron transfer, as previously demonstrated for other sigma factors (57).

**RpoE is not essential for growth, but regulates cell envelope integrity during growth transitions.** Colonies of an RpoE<sup>-</sup> mutant strain were easily recovered in medium with acetate and fumarate with recovery efficiencies comparable to that of other mutants (10). Thus, although RpoE<sub>GSU</sub> is the only ECF sigma factor homologue identified in *G. sulfurreducens*, it was not essential for growth under these conditions. This contrasts with the essential role of RpoE in *E. coli*, which prevents the recovery of RpoE<sup>-</sup> mutants (12). However, the growth rates of the

RpoE<sup>-</sup> mutant during exponential growth in NABF medium at 30°C were 0.6-fold lower than in the wild-type strain (Fig. 5.2A).

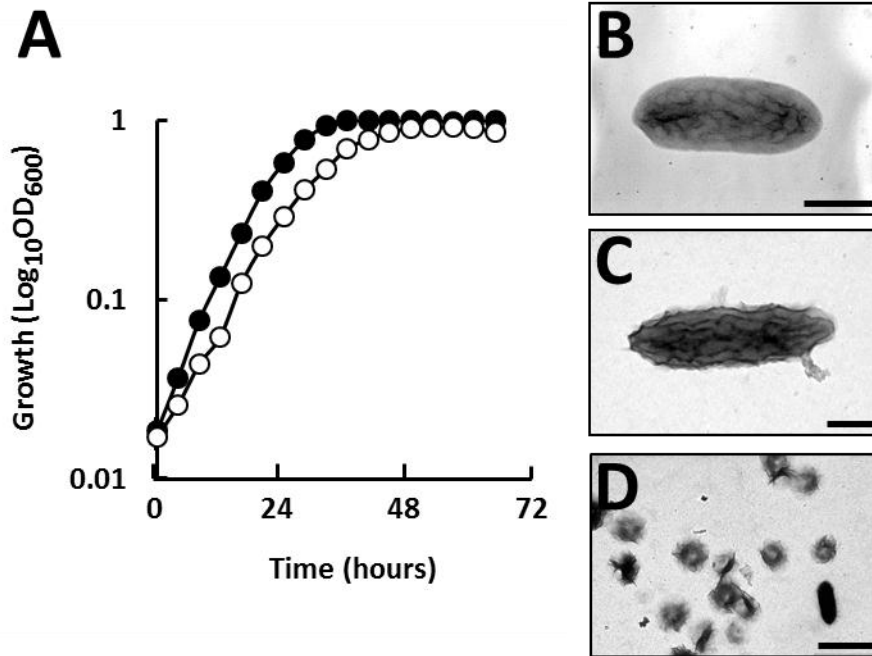


**FIGURE 5.2: RpoE<sup>-</sup> demonstrates impaired growth in NABF medium compared to WT.** (A) Growth of the WT (filled circles), and RpoE<sup>-</sup> (open circles) strains at 30°C in NABF medium. (B-D) Morphology of negatively stained cells of the wild-type (B) and RpoE<sup>-</sup> (C and D) strains by TEM. RpoE<sup>-</sup> mutant cells with cell envelope distortions and damage (C) and abundant spheroplasts (D) are shown. Bar, 500 nm (B and C), 2 μm (D).

Furthermore, while the wild type resumed exponential growth in NABF medium upon inoculation, the RpoE<sup>-</sup> mutant had a growth defect (Fig. 5.2A). Extended *lag* phases (17, 41) have been reported for RpoE-deficient mutants in other bacteria and have been correlated to an increased sensitivity of the mutant strains to adapt to even transient growth transitions. This is because of the extensive reprogramming of the cell's physiology that is required to adapt to

the new nutritional status and resume exponential growth. Such nutritional stress often leads to periplasmic shock and the activation of the RpoE-mediated response (8).

Although we did not observe any defect in the transition of the RpoE<sup>-</sup> cells from exponential to stationary phase (Fig. 5.2A), TEM micrographs of negatively-stained cells of the wild-type and RpoE<sup>-</sup> mutant were consistent with losses of cell envelope integrity in the mutant (Fig. 5.2B-D). In contrast to the smooth appearance of wild-type cells (Fig. 5.2B), mutant cells from cultures transitioning from exponential to stationary phase had outer membrane distortions and damage (Fig. 5.2C). Periplasmic shock during growth transitions can severely damage the cell envelope and result in morphological changes such as those noted for the RpoE<sup>-</sup> cells (41). Furthermore, the mutant cultures contained abundant spheroplasts (Fig. 5.2D). Depletion of periplasmic contents due to the formation of spheroplasts has been proposed to mimic the effect of misfolded proteins caused by extracytoplasmic stressors, which in *E. coli* induces the Cpx cell envelope stress response (61).

Interestingly, attempts to complement the *rpoE* mutation *in trans* using a medium-copy plasmid were unsuccessful. Control reactions demonstrated that RpoE<sup>-</sup> can survive electroporation, as both controls lacking foreign DNA grew as confluent lawns when plated. However, with the introduction of foreign DNA (pRG5 or pRG5::*rpoE*) no growth was observed. This effect was reproducible, as the same result was repeated using several preparations of fresh competent cells, and numerous electroporation attempts. Thus, we concluded that

electrocompetent RpoE<sup>-</sup> cells are unable to recover after the introduction of foreign DNA, likely due to the lack of cell envelope integrity, as described above.

Another growth transition that *Geobacter* spp. encounter in the environment and that is of interest for applications in bioremediation and microbial fuel cells is the transition from the planktonic to the biofilm mode of growth. Biofilm formation requires proper functioning of the bacterial cell envelope to ensure surface colonization as well as adaptation to growth on the surface. To study a potential role for RpoE during biofilm formation in *G. sulfurreducens*, we compared the biofilm-forming abilities of the wild-type and RpoE<sup>-</sup> mutant strains on glass surfaces under conditions in which the wild type predominately grows as a planktonic culture (Fig. 5.3A). In contrast to the wild type, the RpoE<sup>-</sup> mutant predominantly grew as a biofilm.

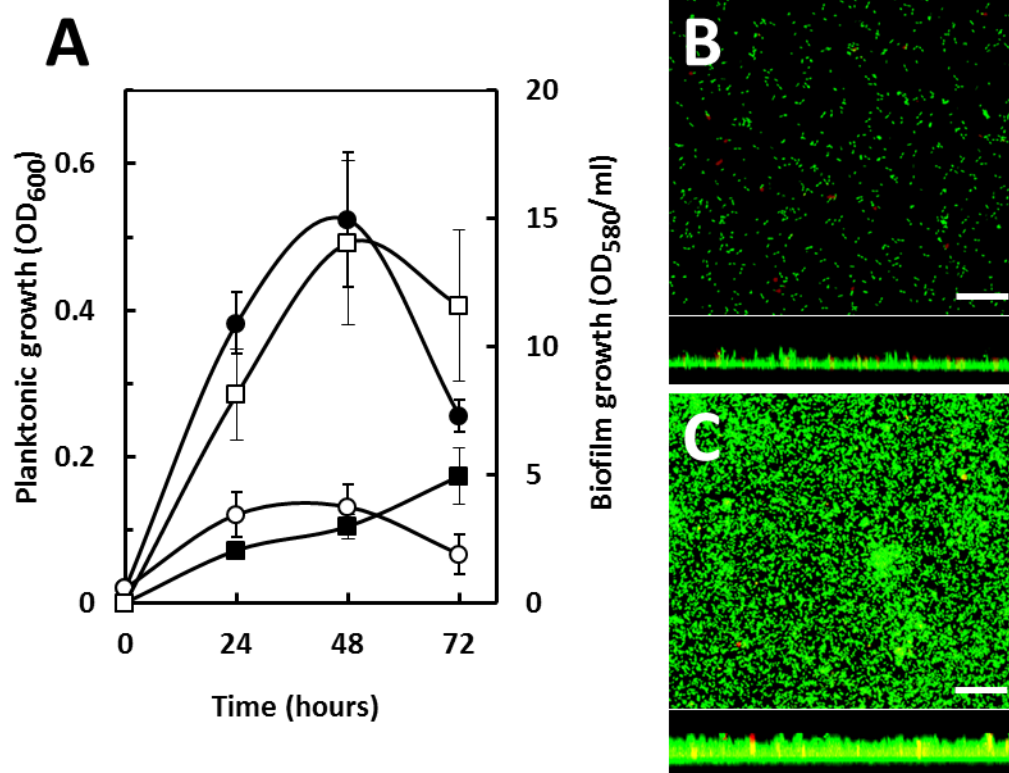


**FIGURE 5.3: Regulation of biofilm formation by RpoE.** (A) Planktonic (circles) and biofilm (squares) growth of the wild-type (solid symbols) and RpoE<sup>-</sup> mutant (open symbols) strains. (B and C) CSLM micrographs showing top (top panels) and side (bottom panels) projections of 48 h biofilms of the wild-type (B) and RpoE<sup>-</sup> (C) strains on glass coverslips. Cells were stained with the BacLight viability dyes (green, live cells; red, dead cells). Bar, 20  $\mu$ m.

After 48 h, when the wild-type biofilms were still thin and unstructured (Fig. 5.3B), the RpoE<sup>-</sup> biofilms had the highest levels of biofilm biomass (Fig. 5.3C). Thus, although inactivation of RpoE in other bacteria impairs biofilm growth (75) the RpoE<sup>-</sup> mutant of *G. sulfurreducens* promotes it. It is interesting to note that the biofilm physiology is thought to be analogous to that of cells entering stationary phase (19). The morphological changes noted for the RpoE<sup>-</sup> cells of *G. sulfurreducens* in early stationary phase (Fig. 5.2C) are likely to change the physical

and chemical properties of the cell surface in a way that could promote adhesion to glass surfaces. Increased viability in stationary phase has also been reported for RpoE-deficient mutants in other bacteria (30, 56). In *E. coli*, for example, the expression of the *rpoE* gene promotes cell lysis in early stationary phase but not in exponential phase (30). Hence, RpoE<sub>GSU</sub> could mediate similar functions and prevent cell lysis during biofilm formation, thus promoting biofilm growth.

**RpoE is required for stress tolerance.** In *E. coli*, the RpoE transcriptional cascade plays a major role in responding to stressful environmental conditions that are caused by any internal or external parameter that affects protein folding and stability in the cell envelope, and increases the accumulation of misfolded or unfolded proteins in the periplasm (50, 52). RpoE then activates the genes that are required to degrade and/or repair the misfolded proteins and synthesize new ones, when appropriate. Protein misfolding in the bacterial periplasm is counteracted by the activation by RpoE of genes encoding periplasmic protein-folding catalysts and degradation factors as well as secretion of newly synthesized proteins to replace those damaged. Consistent with this repair mechanism, genes involved in the degradation and repair of proteins, protein export via the Sec apparatus, amino acid transport, and protein synthesis were found to be activated by RpoE<sub>GSU</sub> (Gemma Reguera, personal communication). Similarly, genes involved in the synthesis of cell envelope components, such as lipoproteins, membrane proteins, and fatty acid and phospholipids metabolism, as well as genes involved in gluconeogenesis, biosynthesis and anaplerosis, were also activated by RpoE<sub>GSU</sub> (Gemma

Reguera, personal communication), also indicating a role for RpoE<sub>GSU</sub> in the repair mechanisms that restore and replace damaged components of the cell envelope.

Hence, we investigated the effect of extracytoplasmic stressors commonly found in environments inhabited by *Geobacter* bacteria such as O<sub>2</sub> intrusions, pH, and temperature shifts on the growth of the RpoE<sup>-</sup> mutant in comparison with the wild type (Fig. 5.4).

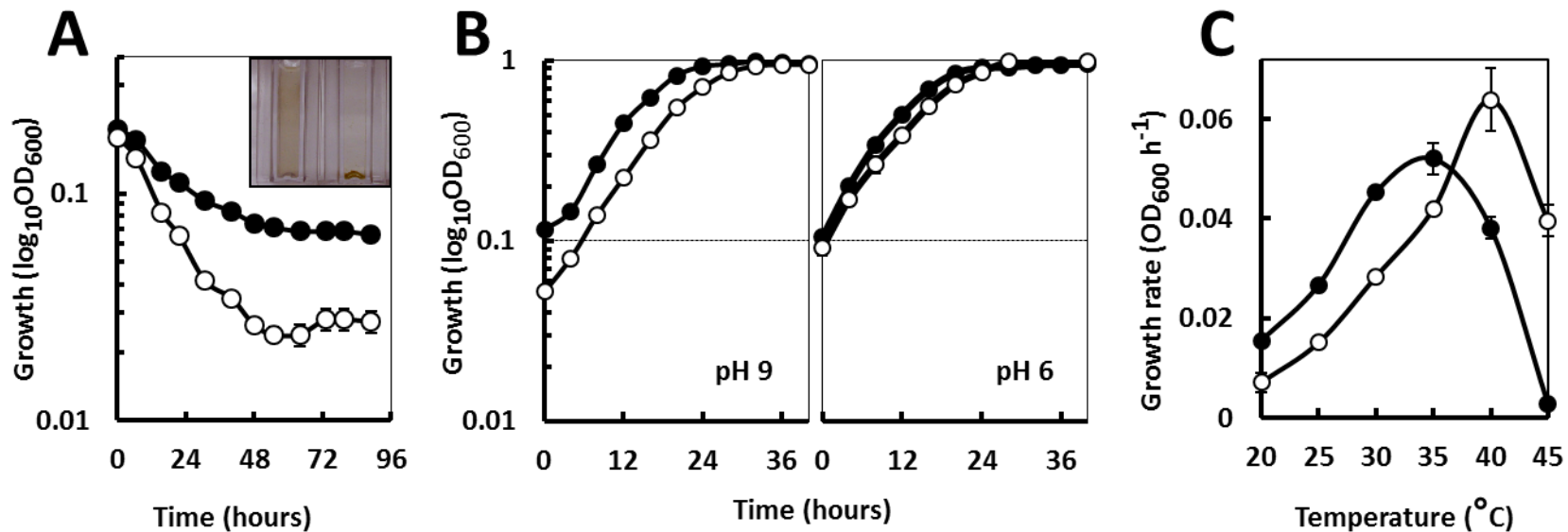


**FIGURE 5.4: The effect of environmental stressors on the growth of the wild-type (solid symbols) and the *RpoE*<sup>-</sup> mutant (open symbols) strains.** Stressors include O<sub>2</sub> exposure (A), pH (B) and temperature (C). Each data point represents the result of triplicate biological replicates. Inset in (A) shows cuvettes of WT (left) and *RpoE*<sup>-</sup> (right) following exposure to oxygen.

Oxygen intrusions are common in the subsurface environments inhabited by *Geobacter* bacteria. Not surprisingly, *G. sulfurreducens*, though first described as a strict anaerobe (6), can tolerate long-term exposure to O<sub>2</sub> and grow with O<sub>2</sub> under microaerophilic conditions for limited periods of time (39). Survival in the presence of O<sub>2</sub> was significantly inhibited in the RpoE<sup>-</sup> mutant compared to the wild type and cell lysis was apparent after just 24 h of exposure to air (Fig. 5.4A, inset). This is consistent with a role of RpoE<sub>GSU</sub> in the oxidative stress response in *G. sulfurreducens*. Previous studies (57) also demonstrated a role for the stationary-phase sigma factor RpoS, which also controls the expression of RpoE, in aerotolerance in *G. sulfurreducens*. Thus, RpoE and RpoS likely cooperate to regulate the response to oxidative stress in this organism. Two stress responses that are not mediated by RpoS<sub>GSU</sub> are resistance to acidic pH (pH 6 for 60 min) and high temperature (45°C for 7 days) (57). Similarly, RpoE<sub>GSU</sub> had no apparent function in resistance to acidic pH (pH 6 for 48 h). However, it was involved in growth survival after exposure for 24 h to basic pH (pH 9) (Fig. 5.3B). Inasmuch as *Geobacter* spp. use acids as electron donors (e.g., acetate) or acceptors (e.g., fumarate), this result is consistent with an environmental adaptation to the low pHs inhabited by these organisms.

The RpoE<sup>-</sup> mutant was also sensitive to low, suboptimal growth temperatures, yet tolerated high temperatures better than the wild type, having optimal growth temperatures at 40°C rather than 35°C (Fig. 5.4C). This heat-tolerant phenotype can be explained by three cytoplasmic small heat shock proteins (Hsp20-family) that are normally repressed by RpoE<sub>GSU</sub>,

but are overexpressed in the RpoE<sup>-</sup> mutant (Gemma Reguera, personal communication). Small heat shock proteins associate with cytoplasmic denatured proteins and protein aggregates, which are produced during exposure to stressors, and facilitate chaperone-mediated disaggregation and refolding (14, 18, 38, 53, 54). The activation of genes encoding cytoplasmic small heat shock proteins thus serves as an indicator of the cytoplasmic stress level in the cells. Their negative regulation by RpoE<sub>Gsu</sub> is in agreement with a shift of the stress response to the cell envelope, as well as the observed heat-tolerant phenotype of the RpoE<sup>-</sup> mutant. Analyses of *rpoE* transcripts by RT-PCR confirmed the inverse correlation between *rpoE* expression and temperature (Fig. 5.5), thereby supporting the involvement of RpoE in growth at low suboptimal temperatures that are relevant to the environmental survival of *Geobacter* bacteria in the subsurface.

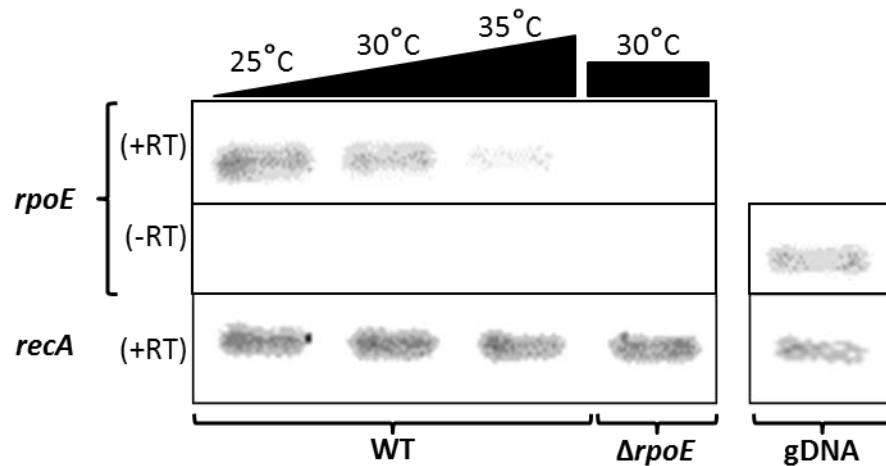


**FIGURE 5.5: Reverse Transcriptase (RT)-PCR of *rpoE* and *recA* transcripts.** Transcripts from WT cells grown at 25°C, 30°C or 35°C or RpoE<sup>-</sup> cells grown at 30°C are included. Controls with (+RT) or without (-RT) reverse transcriptase are shown for the *rpoE* transcripts as well as controls with WT gDNA.

Thus, the mechanisms for coping with cell envelope damage by stressors commonly found in environments inhabited by *Geobacter* bacteria are, at least partially, RpoE-dependent.

**RpoE regulates electron transfer at the cell envelope.** As the integrity of the cell envelope is required for extracellular transfer reactions and cell viability in *G. sulfurreducens* (9), we investigated the ability of resting cell suspensions of the wild-type and RpoE-deficient mutant strains to catalyze the reduction of soluble (Fe(III) citrate) and insoluble (Fe(III) oxides) forms of Fe(III) as electron acceptors with acetate or H<sub>2</sub> serving as electron donors and (Fig. 5.6).

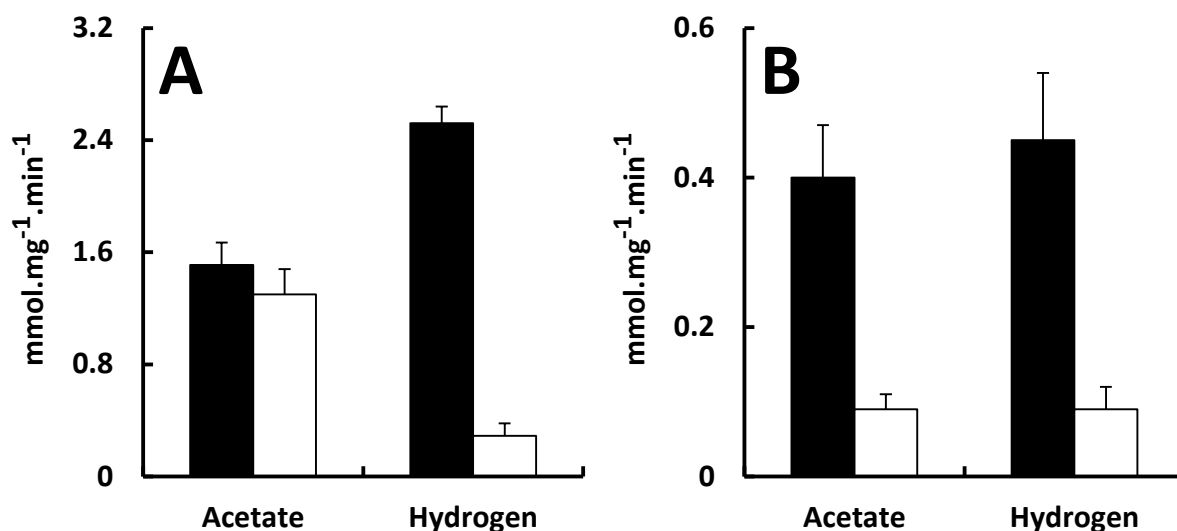


**FIGURE 5.6: Fe(III) reductase activity of resting cell suspensions.** WT (filled blocks) and RpoE<sup>-</sup> (open blocks) strains were tested using soluble (Fe(III) citrate) (A) or insoluble (poorly crystalline Fe(III) hydroxide) (B) as electron acceptors.

As shown in Fig. 5.6A, the reduction of Fe(III) citrate was similar in the two strains when acetate was the electron donor. However, the Fe(III) citrate reduction activity of the RpoE<sup>-</sup> cells

was only 12% ( $\pm$  4%) of wild-type activity when H<sub>2</sub> was used as an electron donor (Fig. 5.6A).

Acetate is oxidized in the cytoplasm, whereas H<sub>2</sub> is oxidized in the periplasm. Thus, the defects in the reduction of Fe(III) citrate when H<sub>2</sub> was the electron donor are consistent with a reduced activity in H<sub>2</sub> oxidation. In support of this, microarray analyses of the RpoE<sup>-</sup> mutant in reference to the wild-type strain revealed a decrease in transcription of genes in the *hybSABLP* operon in the mutant (Gemma Reguera, personal communication), which encodes the respiratory hydrogenase of *G. sulfurreducens* (11). The Hyb hydrogenase is essential for H<sub>2</sub>-dependent growth in *G. sulfurreducens* (11) and, as a result, the diminished transcript levels for the *hyb* genes in the RpoE<sup>-</sup> mutant also correlate with reduced uptake hydrogenase activity in the RpoE<sup>-</sup> mutant (51% ( $\pm$  3%)) of the activity measured in resting cell suspensions of the wild-type cells (Gemma Reguera, personal communication).

By contrast, the RpoE<sup>-</sup> mutant was defective at the reduction of insoluble Fe(III) oxides with both acetate and H<sub>2</sub> (23  $\pm$  5% and 20  $\pm$  7% of wild-type activities with acetate and H<sub>2</sub>, respectively) (Fig. 5.6B). Although acetate oxidation takes place in the cytoplasm, the electrons generated in this intracellular reaction must be transferred to periplasmic and then to outer membrane *c*-cytochromes (5, 32, 33, 36, 40, 47) and conductive pili (63) to reduce the insoluble Fe(III) oxides present outside the cell. Transcript levels for numerous *c*-type cytochromes were diminished or up-regulated in the RpoE-deficient mutant (Gemma Reguera, personal communication). *C*-cytochromes are key components of the electron transport chain that takes

the electrons across the periplasmic space and to the outer membrane in *Geobacter* cells (20, 32, 33, 36, 40, 68). Among the *c*-cytochrome genes that were activated by RpoE were those encoding three outer-membrane cytochromes important for Fe(III) reduction, such as OmcS, OmcD, and OmcG, and genes encoding proteins required for *c*-cytochrome biogenesis. OmcS is required for the reduction of insoluble Fe(III) oxides (47) and electrodes (24) by *G. sulfurreducens* while OmcD has been proposed to play a compensatory role during adaptation to electron transfer disruption (35). Defects in OmcG have been linked to decreased rates of Fe(III) reduction through an indirect effect on the levels of key *c*-cytochromes such as OmcB (33). Protein misfolding in the periplasm also affects the integrity of proteins involved in the assembly of extracellular appendages spanning the bacterial envelope such as pili (26, 29, 55). . In fact, genes required for type IV pilus biogenesis (GSU2030 and GSU2031) were down-regulated in the RpoE<sup>-</sup> mutant (Gemma Reguera, personal communication). The pili of *G. sulfurreducens* are conductive protein appendages that function as nanowires to transfer electrons from the cell envelope to insoluble Fe(III) oxides, their natural electron acceptor for growth (63), and to uranium (9). Thus, stresses affecting the integrity of the cell envelope also are likely to affect the assembly of *G. sulfurreducens* pilus nanowires and their ability to function as electronic conduits to extracellular electron acceptors.

**Implications.** This first study of RpoE in a member of the *Geobacteraceae* demonstrates the functional conservation of a global master regulator for cell envelope integrity and homeostasis and highlights specific adaptations to the natural environments inhabited by these bacteria. As in other bacteria, RpoE responded to extracytoplasmic stressors that lead to cell envelope damage and protein misfolding in the periplasm and used conserved stress response

mechanisms of repair to cope with cell envelope damage. However, the response was specific to signals relevant to the survival of *Geobacter* bacteria in the subsurface such as O<sub>2</sub> intrusions, higher pHs and low, suboptimal temperatures. Interestingly, all these stressors lead to slow growth in *G. sulfurreducens*, similarly to the slow growth that occurs during the reduction of *Geobacter's* insoluble electron acceptors such as Fe(III) oxides or electrodes. Furthermore, genes required for these reductive processes are part of the RpoE regulon. The adaptation of the RpoE-mediated response to control processes relevant to survival in the subsurface, bioremediation of toxic metals and microbial fuel cell performance thus helps explain why *G. sulfurreducens* and related organisms function so effectively in Fe(III)-reducing subsurface environments and in applications that harness their unique reductive activities.

## REFERENCES

## REFERENCES

1. **Ades, S. E., L. E. Connolly, B. M. Alba, and C. A. Gross.** 1999. The *Escherichia coli* sigma(E)-dependent extracytoplasmic stress response is controlled by the regulated proteolysis of an anti-sigma factor. *Genes Dev.* **13**:2449-2461.
2. **Anderson, R. T., and D. R. Lovley.** 1999. Naphthalene and benzene degradation under Fe(III)-reducing conditions in petroleum-contaminated aquifers. *Bioremediation J* **3**:121-135.
3. **Andrews, S. C., A. K. Robinson, and F. Rodriguez-Quinones.** 2003. Bacterial iron homeostasis. *FEMS Microbiol Rev* **27**:215-237.
4. **Bond, D. R., D. E. Holmes, L. M. Tender, and D. R. Lovley.** 2002. Electrode-reducing microorganisms that harvest energy from marine sediments. *Science* **295**:483-485.
5. **Butler, J. E., F. Kaufmann, M. V. Coppi, C. Nunez, and D. R. Lovley.** 2004. MacA, a diheme c-type cytochrome involved in Fe(III) reduction by *Geobacter sulfurreducens*. *J. Bacteriol.* **186**:4042-4045.
6. **Caccavo, F., Jr., D. J. Lonergan, D. R. Lovley, M. Davis, J. F. Stolz, and M. J. McInerney.** 1994. *Geobacter sulfurreducens* sp. nov., a hydrogen- and acetate-oxidizing dissimilatory metal-reducing microorganism. *Appl. Environ. Microbiol.* **60**:3752-3759.
7. **Campbell, E. A., J. L. Tupy, T. M. Gruber, S. Wang, M. M. Sharp, C. A. Gross, and S. A. Darst.** 2003. Crystal structure of *Escherichia coli* sigmaE with the cytoplasmic domain of its anti-sigma RseA. *Mol. Cell* **11**:1067-1078.
8. **Chang, D. E., D. J. Smalley, and T. Conway.** 2002. Gene expression profiling of *Escherichia coli* growth transitions: an expanded stringent response model. *Mol. Microbiol.* **45**:289-306.
9. **Cologgi, D. L., S. Lampa-Pastirk, A. M. Speers, S. D. Kelly, and G. Reguera.** 2011. Extracellular reduction of uranium via *Geobacter* conductive pili as a protective cellular mechanism. *Proc Natl Acad Sci U S A* **108**:15248-15252.
10. **Coppi, M. V., C. Leang, S. J. Sandler, and D. R. Lovley.** 2001. Development of a genetic system for *Geobacter sulfurreducens*. *Appl. Environ. Microbiol.* **67**:3180-3187.
11. **Coppi, M. V., R. A. O'Neil, and D. R. Lovley.** 2004. Identification of an uptake hydrogenase required for hydrogen-dependent reduction of Fe(III) and other electron acceptors by *Geobacter sulfurreducens*. *J. Bacteriol.* **186**:3022-3028.
12. **De Las Penas, A., L. Connolly, and C. A. Gross.** 1997. Sigma-E is an essential sigma factor in *Escherichia coli*. *J. Bacteriol.* **179**:6862-6864.

13. **De Las Penas, A., L. Connolly, and C. A. Gross.** 1997. The sigmaE-mediated response to extracytoplasmic stress in *Escherichia coli* is transduced by RseA and RseB, two negative regulators of sigmaE. *Mol. Microbiol.* **24**:373-385.
14. **Deuerling, E., H. Patzelt, S. Vorderwulbecke, T. Rauch, G. Kramer, E. Schaffitzel, A. Mogk, A. Schulze-Specking, H. Langen, and B. Bukau.** 2003. Trigger Factor and DnaK possess overlapping substrate pools and binding specificities. *Mol Microbiol* **47**:1317-1328.
15. **DiDonato, L. N., S. A. Sullivan, B. A. Methe, K. P. Nevin, R. England, and D. R. Lovley.** 2006. Role of RelGsu in stress response and Fe(III) reduction in *Geobacter sulfurreducens*. *J. Bacteriol.* **188**:8469-8478.
16. **Duguay, A. R., and T. J. Silhavy.** 2004. Quality control in the bacterial periplasm. *Biochim. Biophys. Acta* **1694**:121-134.
17. **Egler, M., C. Grosse, G. Grass, and D. H. Nies.** 2005. Role of the extracytoplasmic function protein family sigma factor RpoE in metal resistance of *Escherichia coli*. *J. Bacteriol.* **187**:2297-2307.
18. **Ehrnsperger, M., S. Graber, M. Gaestel, and J. Buchner.** 1997. Binding of non-native protein to Hsp25 during heat shock creates a reservoir of folding intermediates for reactivation. *Embo J.* **16**:221-229.
19. **Folsom, J. P., L. Richards, B. Pitts, F. Roe, G. D. Ehrlich, A. Parker, A. Mazurie, and P. S. Stewart.** 2010. Physiology of *Pseudomonas aeruginosa* in biofilms as revealed by transcriptome analysis. *BMC Microbiol.* **10**:294.
20. **Giometti, C. S.** 2006. Tale of two metal reducers: comparative proteome analysis of *Geobacter sulfurreducens* PCA and *Shewanella oneidensis* MR-1. *Methods Biochem. Anal.* **49**:97-111.
21. **Grigorova, I. L., R. Chaba, H. J. Zhong, B. M. Alba, V. Rhodius, C. Herman, and C. A. Gross.** 2004. Fine-tuning of the *Escherichia coli* sigmaE envelope stress response relies on multiple mechanisms to inhibit signal-independent proteolysis of the transmembrane anti-sigma factor, RseA. *Genes Dev.* **18**:2686-2697.
22. **Helmann, J. D.** 2002. The extracytoplasmic function (ECF) sigma factors. *Adv. Microb. Physiol.* **46**:47-110.
23. **Holmes, D. E., D. R. Bond, R. A. O'Neil, C. E. Reimers, L. R. Tender, and D. R. Lovley.** 2004. Microbial communities associated with electrodes harvesting electricity from a variety of aquatic sediments. *Microb. Ecol.* **48**:178-190.
24. **Holmes, D. E., S. K. Chaudhuri, K. P. Nevin, T. Mehta, B. A. Methe, A. Liu, J. E. Ward, T. L. Woodard, J. Webster, and D. R. Lovley.** 2006. Microarray and genetic analysis of

- electron transfer to electrodes in *Geobacter sulfurreducens*. Environ. Microbiol. **8**:1805-1815.
25. **Holmes, D. E., K. P. Nevin, and D. R. Lovley.** 2004. Comparison of 16S rRNA, *nifD*, *recA*, *gyrB*, *rpoB* and *fusA* genes within the family *Geobacteraceae* fam. nov. Int. J. Syst. Evol. Microbiol. **54**:1591-1599.
  26. **Hung, D. L., T. L. Raivio, C. H. Jones, T. J. Silhavy, and S. J. Hultgren.** 2001. Cpx signaling pathway monitors biogenesis and affects assembly and expression of P pili. Embo J. **20**:1508-1518.
  27. **Ishihama, A.** 2000. Functional modulation of *Escherichia coli* RNA polymerase. Annu. Rev. Microbiol. **54**:499-518.
  28. **Juarez, K., B. C. Kim, K. Nevin, L. Olvera, G. Reguera, D. R. Lovley, and B. A. Methe.** 2009. PilR, a transcriptional regulator for pilin and other genes required for Fe(III) reduction in *Geobacter sulfurreducens*. J. Mol. Microbiol. Biotechnol. **16**:146-158.
  29. **Jubelin, G., A. Vianney, C. Beloin, J. M. Ghigo, J. C. Lazzaroni, P. Lejeune, and C. Dorel.** 2005. CpxR/OmpR interplay regulates curli gene expression in response to osmolarity in *Escherichia coli*. J. Bacteriol. **187**:2038-2049.
  30. **Kabir, M. S., D. Yamashita, S. Koyama, T. Oshima, K. Kurokawa, M. Maeda, R. Tsunedomi, M. Murata, C. Wada, H. Mori, and M. Yamada.** 2005. Cell lysis directed by sigmaE in early stationary phase and effect of induction of the *rpoE* gene on global gene expression in *Escherichia coli*. Microbiology **151**:2721-2735.
  31. **Khare, T., A. Esteve-Nunez, K. P. Nevin, W. Zhu, J. R. Yates, 3rd, D. Lovley, and C. S. Giometti.** 2006. Differential protein expression in the metal-reducing bacterium *Geobacter sulfurreducens* strain PCA grown with fumarate or ferric citrate. Proteomics **6**:632-640.
  32. **Kim, B. C., C. Leang, Y. H. Ding, R. H. Glaven, M. V. Coppi, and D. R. Lovley.** 2005. OmcF, a putative c-Type monoheme outer membrane cytochrome required for the expression of other outer membrane cytochromes in *Geobacter sulfurreducens*. J. Bacteriol. **187**:4505-4513.
  33. **Kim, B. C., X. Qian, C. Leang, M. V. Coppi, and D. R. Lovley.** 2006. Two putative c-type multiheme cytochromes required for the expression of OmcB, an outer membrane protein essential for optimal Fe(III) reduction in *Geobacter sulfurreducens*. J. Bacteriol. **188**:3138-3142.
  34. **Krushkal, J., B. Yan, L. N. DiDonato, M. Puljic, K. P. Nevin, T. L. Woodard, R. M. Adkins, B. A. Methe, and D. R. Lovley.** 2007. Genome-wide expression profiling in *Geobacter sulfurreducens*: identification of Fur and RpoS transcription regulatory sites in a relGsu mutant. Funct. Integr. Genomics **7**:229-255.

35. **Leang, C., L. A. Adams, K. J. Chin, K. P. Nevin, B. A. Methe, J. Webster, M. L. Sharma, and D. R. Lovley.** 2005. Adaptation to disruption of the electron transfer pathway for Fe(III) reduction in *Geobacter sulfurreducens*. *J. Bacteriol.* **187**:5918-5926.
36. **Leang, C., M. V. Coppi, and D. R. Lovley.** 2003. OmcB, a c-type polyheme cytochrome, involved in Fe(III) reduction in *Geobacter sulfurreducens*. *J. Bacteriol.* **185**:2096-2103.
37. **Leang, C., J. Krushkal, T. Ueki, M. Puljic, J. Sun, K. Juarez, C. Nunez, G. Reguera, R. DiDonato, B. Postier, R. M. Adkins, and D. R. Lovley.** 2009. Genome-wide analysis of the RpoN regulon in *Geobacter sulfurreducens*. *BMC genomics* **10**:331.
38. **Lee, G. J., A. M. Roseman, H. R. Saibil, and E. Vierling.** 1997. A small heat shock protein stably binds heat-denatured model substrates and can maintain a substrate in a folding-competent state. *Embo J.* **16**:659-671.
39. **Lin, W. C., M. V. Coppi, and D. R. Lovley.** 2004. *Geobacter sulfurreducens* can grow with oxygen as a terminal electron acceptor. *Appl. Environ. Microbiol.* **70**:2525-2528.
40. **Lloyd, J. R., C. Leang, A. L. Hodges Myerson, M. V. Coppi, S. Cuifo, B. Methe, S. J. Sandler, and D. R. Lovley.** 2003. Biochemical and genetic characterization of PpcA, a periplasmic c-type cytochrome in *Geobacter sulfurreducens*. *Biochem. J.* **369**:153-161.
41. **Lopez de Saro, F. J., N. Yoshikawa, and J. D. Helmann.** 1999. Expression, abundance, and RNA polymerase binding properties of the delta factor of *Bacillus subtilis*. *J. Biol. Chem.* **274**:15953-15958.
42. **Lovley, D. R.** 2006. Bug juice: harvesting electricity with microorganisms. *Nat. Rev. Microbiol.* **4**:497-508.
43. **Lovley, D. R., M. J. Baedeker, D. J. Lonergan, I. M. Cozzarelli, E. J. P. Phillips, and D. I. Siegel.** 1989. Oxidation of aromatic contaminants coupled to microbial iron reduction. *Nature* **339**:297-299.
44. **Lovley, D. R., D. E. Holmes, and K. P. Nevin.** 2004. Dissimilatory Fe(III) and Mn(IV) reduction, p. 219-286. *In* R. K. Poole (ed.), *Adv. Microb. Physiol.*, vol. 49. Elsevier Academic Press, London.
45. **Lovley, D. R., and E. J. P. Phillips.** 1988. Novel mode of microbial energy metabolism: organic carbon oxidation coupled to dissimilatory reduction of iron or manganese. *Appl. Environ. Microbiol.* **54**:1472-1480.
46. **Lovley, D. R., E. J. P. Phillips, Y. A. Gorby, and E. R. Landa.** 1991. Microbial reduction of uranium. *Nature* **350**:413-416.

47. **Mehta, T., M. V. Coppi, S. E. Childers, and D. R. Lovley.** 2005. Outer membrane c-type cytochromes required for Fe(III) and Mn(IV) oxide reduction in *Geobacter sulfurreducens*. *Appl. Environ. Microbiol.* **71**:8634-8641.
48. **Méthé, B. A., K. E. Nelson, J. A. Eisen, I. T. Paulsen, W. Nelson, J. F. Heidelberg, D. Wu, M. Wu, N. Ward, M. J. Beanan, R. J. Dodson, R. Madupu, L. M. Brinkac, S. C. Daugherty, R. T. DeBoy, A. S. Durkin, M. Gwinn, J. F. Kolonay, S. A. Sullivan, D. H. Haft, J. Selengut, T. M. Davidsen, N. Zafar, O. White, B. Tran, C. Romero, H. A. Forberger, J. Weidman, H. Khouri, T. V. Feldblyum, T. R. Utterback, S. E. Van Aken, D. R. Lovley, and C. M. Fraser.** 2003. Genome of *Geobacter sulfurreducens*: metal reduction in subsurface environments. *Science* **302**:1967-1969.
49. **Méthé, B. A., J. Webster, K. Nevin, J. Butler, and D. R. Lovley.** 2005. DNA Microarray Analysis of Nitrogen Fixation and Fe(III) Reduction in *Geobacter sulfurreducens*. *Appl. Environ. Microbiol.* **71**:2530-2538.
50. **Missiakas, D., J. M. Betton, and S. Raina.** 1996. New components of protein folding in extracytoplasmic compartments of *Escherichia coli* SurA, FkpA and Skp/OmpH. *Mol. Microbiol.* **21**:871-884.
51. **Missiakas, D., M. P. Mayer, M. Lemaire, C. Georgopoulos, and S. Raina.** 1997. Modulation of the *Escherichia coli* sigmaE (RpoE) heat-shock transcription-factor activity by the RseA, RseB and RseC proteins. *Mol. Microbiol.* **24**:355-371.
52. **Missiakas, D., and S. Raina.** 1998. The extracytoplasmic function sigma factors: role and regulation. *Mol. Microbiol.* **28**:1059-1066.
53. **Mogk, A., E. Deuerling, S. Vorderwulbecke, E. Vierling, and B. Bukau.** 2003. Small heat shock proteins, ClpB and the DnaK system form a functional triade in reversing protein aggregation. *Mol. Microbiol.* **50**:585-595.
54. **Mogk, A., C. Schlieker, K. L. Friedrich, H. J. Schonfeld, E. Vierling, and B. Bukau.** 2003. Refolding of substrates bound to small Hsps relies on a disaggregation reaction mediated most efficiently by ClpB/DnaK. *J. Biol. Chem.* **278**:31033-31042.
55. **Nevesinjac, A. Z., and T. L. Raivio.** 2005. The Cpx envelope stress response affects expression of the type IV bundle-forming pili of enteropathogenic *Escherichia coli*. *J. Bacteriol.* **187**:672-686.
56. **Nitta, T., H. Nagamitsu, M. Murata, H. Izu, and M. Yamada.** 2000. Function of the sigma(E) regulon in dead-cell lysis in stationary-phase *Escherichia coli*. *J. Bacteriol.* **182**:5231-5237.
57. **Núñez, C., L. Adams, S. Childers, and D. R. Lovley.** 2004. The RpoS sigma factor in the dissimilatory Fe(III)-reducing bacterium *Geobacter sulfurreducens*. *J. Bacteriol.* **186**:5543-5546.

58. **Núñez, C., A. Esteve-Nunez, C. Giometti, S. Tollaksen, T. Khare, W. Lin, D. R. Lovley, and B. A. Methe.** 2006. DNA microarray and proteomic analyses of the RpoS regulon in *Geobacter sulfurreducens*. *J. Bacteriol.* **188**:2792-2800.
59. **O'Toole, G. A., and R. Kolter.** 1998. Initiation of biofilm formation in *Pseudomonas fluorescens* WCS365 proceeds via multiple, convergent signalling pathways: a genetic analysis. *Mol. Microbiol.* **28**:449-461.
60. **Ortiz-Bernad, I., R. T. Anderson, H. A. Vrionis, and D. R. Lovley.** 2004. Vanadium respiration by *Geobacter metallireducens*: novel strategy for in situ removal of vanadium from groundwater. *Appl Environ Microbiol* **70**:3091-3095.
61. **Raivio, T. L., M. W. Laird, J. C. Joly, and T. J. Silhavy.** 2000. Tethering of CpxP to the inner membrane prevents spheroplast induction of the *cpx* envelope stress response. *Mol. Microbiol.* **37**:1186-1197.
62. **Raivio, T. L., and T. J. Silhavy.** 2001. Periplasmic stress and ECF sigma factors. *Annu. Rev. Microbiol.* **55**:591-624.
63. **Reguera, G., K. D. McCarthy, T. Mehta, J. S. Nicoll, M. T. Tuominen, and D. R. Lovley.** 2005. Extracellular electron transfer via microbial nanowires. *Nature* **435**:1098-1101.
64. **Reguera, G., R. B. Pollina, J. S. Nicoll, and D. R. Lovley.** 2007. Possible Nonconductive Role of *Geobacter sulfurreducens* Pilus Nanowires in Biofilm Formation. *J. Bacteriol.* **189**:2125-2127.
65. **Roling, W. F., B. M. van Breukelen, M. Braster, B. Lin, and H. W. van Verseveld.** 2001. Relationships between microbial community structure and hydrochemistry in a landfill leachate-polluted aquifer. *Appl Environ Microbiol* **67**:4619-4629.
66. **Rooney-Varga, J. N., R. T. Anderson, J. L. Fraga, D. Ringelberg, and D. R. Lovley.** 1999. Microbial communities associated with anaerobic benzene degradation in a petroleum-contaminated aquifer. *Appl Environ Microbiol* **65**:3056-3063.
67. **Shelobolina, E. S., M. V. Coppi, A. A. Korenevsky, L. N. DiDonato, S. A. Sullivan, H. Konishi, H. Xu, C. Leang, J. E. Butler, B. C. Kim, and D. R. Lovley.** 2007. Importance of *c*-Type cytochromes for U(VI) reduction by *Geobacter sulfurreducens*. *BMC Microbiol.* **7**:16.
68. **Shi, L., T. C. Squier, J. M. Zachara, and J. K. Fredrickson.** 2007. Respiration of metal (hydr)oxides by *Shewanella* and *Geobacter*: a key role for multihaem *c*-type cytochromes. *Mol. Microbiol.* **65**:12-20.
69. **Stookey, L. L.** 1970. Ferrozine: a new spectrophotometric reagent for iron. *Anal. Chem.* **42**:779-781.

70. **Sung, Y., K. F. Fletcher, K. M. Ritalaliti, R. P. Apkarian, N. Ramos-Hernandez, R. A. Sanford, N. M. Mesbah, and F. E. Löffler.** 2006. *Geobacter lovleyi* sp nov strain SZ, a novel metal-reducing and tetrachloroethene-dechlorinating bacterium. Applied and Environmental Microbiology **72**:2775-2782.
71. **Tender, L. M., C. E. Reimers, H. A. Stecher, 3rd, D. E. Holmes, D. R. Bond, D. A. Lowy, K. Pilobello, S. J. Fertig, and D. R. Lovley.** 2002. Harnessing microbially generated power on the seafloor. Nat. Biotechnol. **20**:821-825.
72. **Tran, H. T., J. Krushkal, F. M. Antommattei, D. R. Lovley, and R. M. Weis.** 2008. Comparative genomics of *Geobacter* chemotaxis genes reveals diverse signaling function. BMC genomics **9**:471.
73. **Ueki, T., and D. R. Lovley.** 2007. Heat-shock sigma factor RpoH from *Geobacter sulfurreducens*. Microbiology **153**:838-846.
74. **Wu, Q. L., D. Kong, K. Lam, and R. N. Husson.** 1997. A mycobacterial extracytoplasmic function sigma factor involved in survival following stress. J Bacteriol **179**:2922-2929.
75. **Xue, X., J. Tomasch, H. Sztajer, and I. Wagner-Dobler.** 2010. The delta subunit of RNA polymerase, RpoE, is a global modulator of *Streptococcus mutans* environmental adaptation. J Bacteriol **192**:5081-5092.
76. **Yan, B., D. R. Lovley, and J. Krushkal.** 2007. Genome-wide similarity search for transcription factors and their binding sites in a metal-reducing prokaryote *Geobacter sulfurreducens*. Biosystems **90**:421-441.
77. **Yan, B., B. A. Methe, D. R. Lovley, and J. Krushkal.** 2004. Computational prediction of conserved operons and phylogenetic footprinting of transcription regulatory elements in the metal-reducing bacterial family *Geobacteraceae*. J. Theor. Biol. **230**:133-144.
78. **Yan, B., C. Nunez, T. Ueki, A. Esteve-Nunez, M. Puljic, R. M. Adkins, B. A. Methe, D. R. Lovley, and J. Krushkal.** 2006. Computational prediction of RpoS and RpoD regulatory sites in *Geobacter sulfurreducens* using sequence and gene expression information. Gene **384**:73-95.

## **CHAPTER 6**

### **CONCLUSIONS AND FUTURE DIRECTIONS**

The overall objective of this dissertation has been to further the understanding of bacterial U reduction mechanisms by *G. sulfurreducens*. In the long-term, this knowledge is critical to harness microbial U reduction processes so as to develop improved or novel bioremediation schemes in subsurface environments. In this dissertation I have demonstrated a novel role for pilus nanowires in U reduction in *G. sulfurreducens*. Furthermore, the conductive pili were the primary U reductase in planktonic cells (which is relevant to the physiology of cells in the groundwater environment) and critical catalytic components in biofilms (a physiological state relevant to the sediment environment). Additionally, I demonstrated that the U reductive abilities of the biofilms depended on their stage of development, with maximum reduction occurring only in the later stages of biofilm development due to the increased production of pili and redox biofilm matrix as the biofilms grow and mature. Furthermore, I also screened a library of transposon-insertion mutants for defects in biofilm formation and identified mutants arrested at various stages of biofilm development and, therefore, defective in attachment, microcolony formation, and biofilm maturation. Based on the genes that were interrupted by the transposon in each mutant, I was able to group the mutants in functional categories, thus enabling the genetic analysis of biofilm development in *G. sulfurreducens*. Most mutants carried the transposon insertion in genes annotated in the cell envelope biosynthesis and function category as well as in electron transport, which is mostly located in the cell envelope. To gain insights the regulation of the cell envelope in *G. sulfurreducens*, I characterized a mutant deficient in the extracytoplasmic function (ECF) sigma factor, RpoE. The results indicate that this sigma factor is, at least in part, responsible for maintaining the integrity of the cell envelope in response to environmental stressors such as temperature and oxidative stress.

Taken together, the results presented in this dissertation provide novel insights into both the mechanisms of uranium reduction by *Geobacter* bacteria, and the cellular components required for biofilm formation and survival in the subsurface. This knowledge will aid in the development of bioremediation schemes, including the use of biofilms as bioreactive barriers to immobilize and prevent the spread of U contamination.

Future directions for the work presented in this dissertation include further analysis of the biofilm-deficient transposon-insertion mutants. Genetic complementation of the pili-biogenesis mutants described in chapter 4 has been carried out by introducing a constitutively-expressed WT copy of the interrupted gene in *trans*. The biofilm formation phenotype of the complemented strains will allow us to confirm the role of the pili-biogenesis proteins in biofilm development. Also of special interest is the role that other electron transport proteins identified in our mutant screen (such as hydrogenases and cytochromes) play in the biofilms. Future work will include the phenotypic characterization, as well as complementation of these mutants. Once mutants of interest are characterized in the lab, and selected as potential molecular markers for biofilm development and/or U reduction in the subsurface, we would like to take this project to the field to determine the environmental relevance of our genes. The Zhou lab at the University of Oklahoma has developed functional gene arrays, or “GeoChips”, which contain probes that target genes involved in a specific process of interest (1). Examples include genes involved in biogeochemical cycling of organic and inorganic substances, biodegradation of contaminants, stress response, and antibiotic resistance (1). *Geobacter*-, pili-, and biofilm-specific probes could be incorporated in the GeoChip to monitor the activity and physiological state of *Geobacter* bacteria in the subsurface during active *in situ* bioremediation.

Thus, genes encoding proteins involved in U reduction, such as components of the pilus apparatus, or those expressed during biofilm development could provide molecular markers to assess the effectiveness of the bioremediation scheme and enable long-term monitoring. This will provide valuable information essential to the development of successful *in situ* bioremediation schemes.

Additionally, the identification of specific cellular components responsible for U reduction in *Geobacter* bacteria will enable the manipulation of their expression or activity to promote increased removal and reduction of U. One possibility would be to increase the biological expression of the pilus nanowires. This could be accomplished using genetic engineering to develop hyperpilated strains that also constitutively express the nanowires. Alternatively, and to avoid limitations related to the introduction of genetically engineered strains into the environment, adaptive evolution could be used to isolate hyperpilated strains. The evolution experiments could involve serial transfers of cultures grown under the pressure to produce pili such as suboptimal temperatures (2), growth with Fe(III) oxides as sole electron acceptor (2), and biofilm formation (3). These strains could be used to bioremediate environments where *Geobacter* bacteria are not present or where metal reduction cannot be stimulated *in situ*. Furthermore, the pilus nanowires could also be mass-produced and assembled *in vitro* to develop man-made devices for the bioremediation of U in environments that prevent the growth of microorganisms, such as high-radiation environments. Such biomimetic interfaces could integrate not only the pilus nanowires but also other U reductase components identified in my work, such as outer membrane cytochromes, which could also be produced *in vitro* and immobilized on the surface of an electrode. This would create a synthetic

and biodegradable mimic of the *Geobacter* cell envelope that could be used to safely remove and precipitate U in environments inhospitable to microbial growth. It could also easily be removed from the subsurface, thereby also removing the U and preventing further contamination, while not requiring large-scale excavation of the site. Our lab is currently involved in the development of these devices in collaboration with Dr. Mark Worden's lab in Chemical Engineering (Michigan State University).

In addition to the manipulation of pili production in planktonic cells described above, similar methods could be used for the development of biofilm biobarriers with increased pili and biomass so as to enhanced U reductase activity and enable the prolonged reduction of U and tolerance to higher concentrations of the contaminants. Additionally, we can use the molecular markers we have identified to monitor the U reductase activity of the biofilms, which would allow us to better predict the fate of U in the environment, and contribute to the long-term stewardship of contaminated sites.

## REFERENCES

## REFERENCES

1. **He, Z., J. D. Van Nostrand, and J. Zhou.** 2012. Applications of functional gene microarrays for profiling microbial communities. *Current opinion in biotechnology* **23**:460-466.
2. **Reguera, G., K. D. McCarthy, T. Mehta, J. S. Nicoll, M. T. Tuominen, and D. R. Lovley.** 2005. Extracellular electron transfer via microbial nanowires. *Nature* **435**:1098-1101.
3. **Reguera, G., R. B. Pollina, J. S. Nicoll, and D. R. Lovley.** 2007. Possible Nonconductive Role of *Geobacter sulfurreducens* Pilus Nanowires in Biofilm Formation. *J. Bacteriol.* **189**:2125-2127.